Applications of hybrid continuous and discrete-variable entanglement of light

Adrien Cavaillès, Tom Darras, Giovanni Guccione, Hanna Le Jeannic, Jérémy Raskop, Kun Huang, Olivier Morin and Julien Laurat

Quantum Networks Team

Laboratoire Kastler Brossel

SORBONNE UNIVERSITÉ
CRÉATEURS DE FUTURS DEPUIS 1257

The Quantum Networks Group

Laboratoire Kastler Brossel
Physique quantique et applications

Distribution, Processing and Storage of Quantum Information

Nanofiber Lab

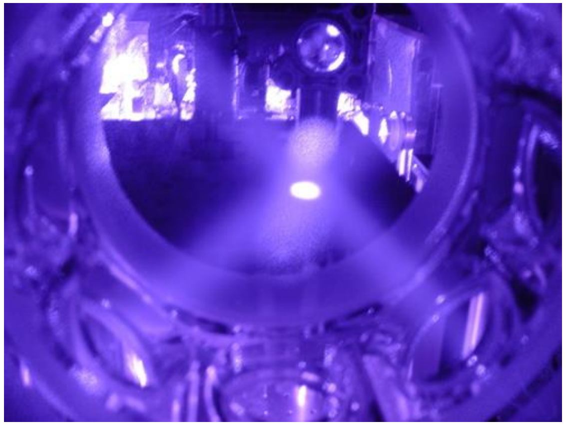

Free-Space Lab

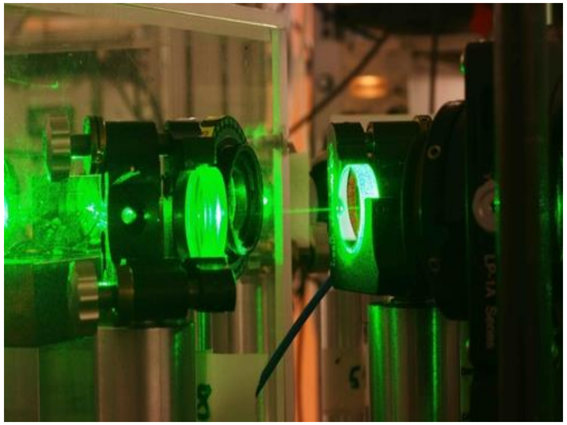

Hybrid Photonics Lab

The Quantum Networks Group

Laboratoire Kastler Brossel
Physique quantique et applications

Distribution, Processing and Storage of Quantum Information


Nanofiber Lab

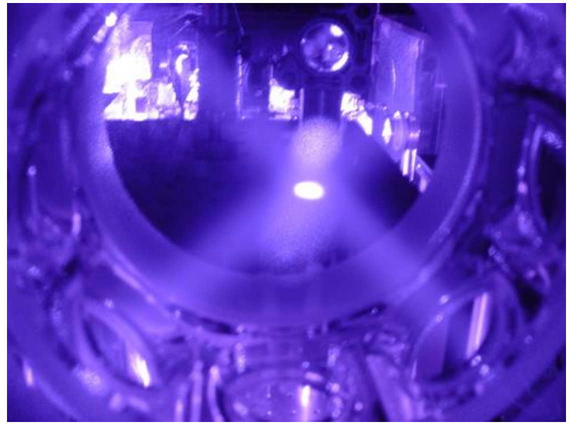
Free-Space Lab

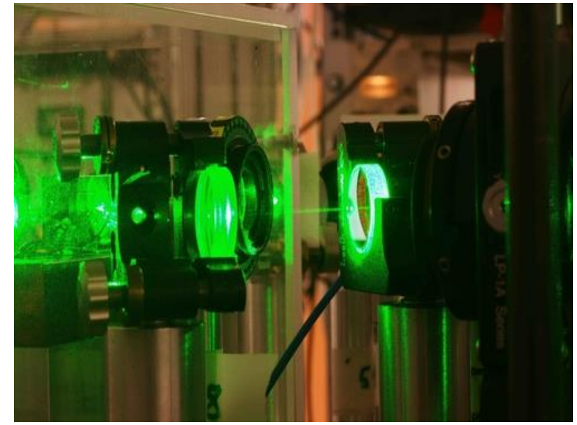
Hybrid Photonics Lab

Combining 1D nanoscale waveguide and cold atoms

All-fibered light-matter interface

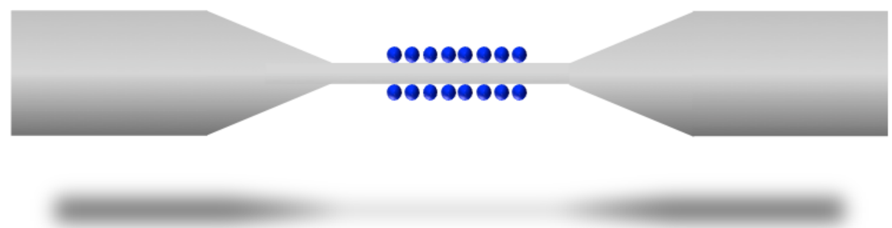

Demonstration of a memory for tightly guided light in an optical nanofiber
PRL 114, 180503 (2015): first demonstration of a memory in evanescent field
Large Bragg reflection from 1D chains of trapped atoms near a nanoscale waveguide
PRL 117, 133603 (2016): 75% reflectance with only 2000 atoms

The Quantum Networks Group

Laboratoire Kastler Brossel
Physique quantique et applications

Distribution, Processing and Storage of Quantum Information

Nanofiber Lab

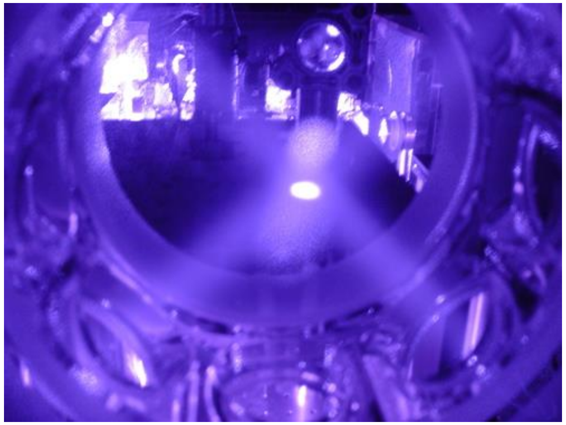

Free-Space Lab

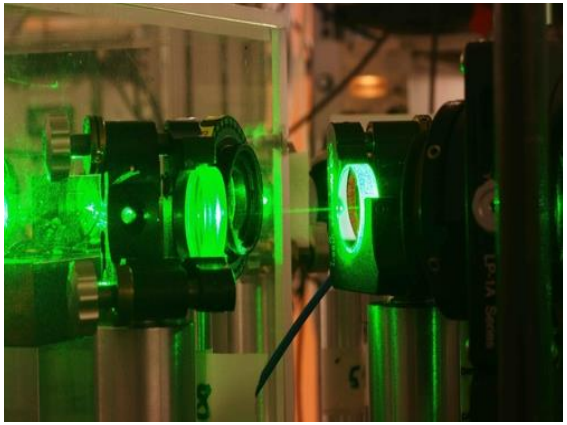

Hybrid Photonics Lab

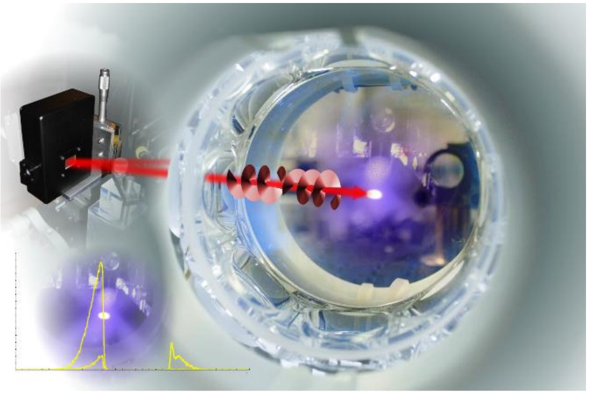

Spatial and Polarization multiplexing

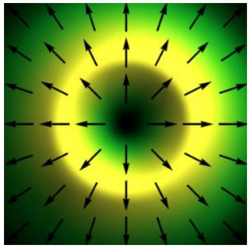

Adding complexity in free space:
Multiple degree-of-freedom memory

A quantum memory for orbital angular momentum qubits, Nature Photonics 8, 234 (2014)

Storage of vector beams in a multiple-degree-of-freedom quantum memory, Nature Communications 6, 7706 (2015)

The Quantum Networks Group

Laboratoire Kastler Brossel
Physique quantique et applications

Distribution, Processing and Storage of Quantum Information


Nanofiber Lab

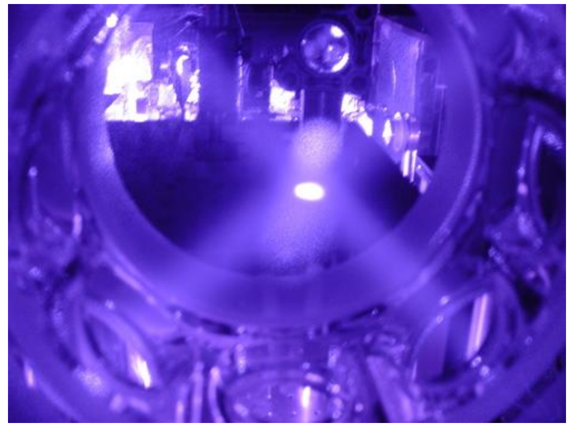
Free-Space Lab

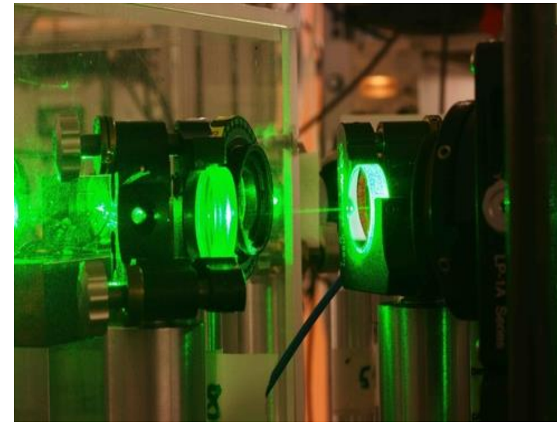
Hybrid Photonics Lab

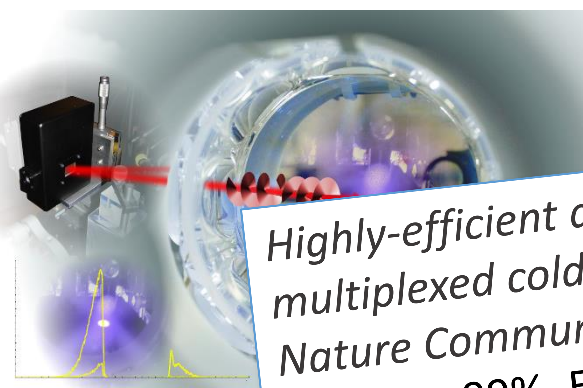

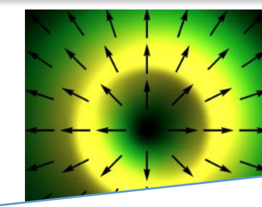

Spatial and Po
multiplexing

Addi...

ory

...quantum

...ations 6, 7706 (2015)

Highly-efficient quantum memory for polarization qubits in a spatially-multiplexed cold atomic ensemble,
Nature Communications 9, 363 (2018)
(Fidelity>99%, Efficiency >60%)

The Quantum Networks Group

Laboratoire Kastler Brossel
Physique quantique et applications

Distribution, Processing and Storage of Quantum Information

Nanofiber Lab

Free-Space Lab

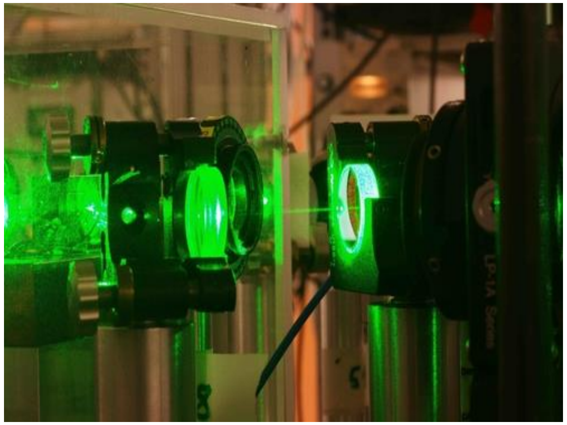

Hybrid Photonics Lab

Sculpting the quantum light

Combination of CV-DV toolboxes:
"Optical Hybrid Quantum Information"
based on optical parametric oscillators

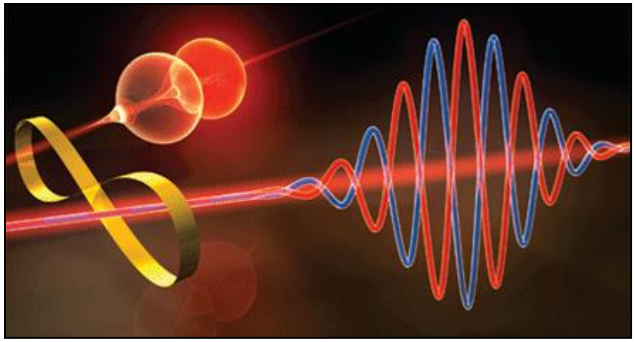

Witnessing single-photon entanglement with local homodyne measurements
PRL 110, 130401 (2013) ; NJP 16, 103035 (2014): up to 80 km
Remote generation of hybrid entanglement between particle-like and wave-like qubits
Nature Photonics 8, 570 (2014): at a distance, 80 km

The Quantum Networks Group

Laboratoire Kastler Brossel
Physique quantique et applications

Distribution, Processing and Storage of Quantum Information


Nanofiber Lab


Free-Space Lab

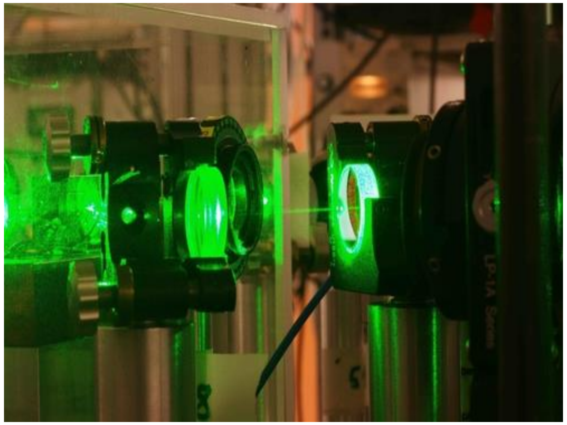
Hybrid Photonics Lab

Sculpting the quantum light

Combin…

“Optical…

based o…

- Optical Synthesis of Large-Amplitude Squeezed Coherent-State Superpositions with Minimal Resources
  Phys. Rev. Lett. **115**, 023602 (2015)
- Slowing Quantum Decoherence by Squeezing in Phase Space
  Phys. Rev. Lett. **120**, 073603 (2018)

Witnessing …
PRL 110, 13…
Remote gene… particle-like and wave-like qubits
Nature Phot… (2014). at a distance, 80 km

Outline

I	Optical quantum state engineering
II	Hybrid entanglement of light
III	Remote state preparation of arbitrary CV qu-modes
IV	Experimental demonstration of EPR steering
V	Towards quantum teleportation from DV to CV

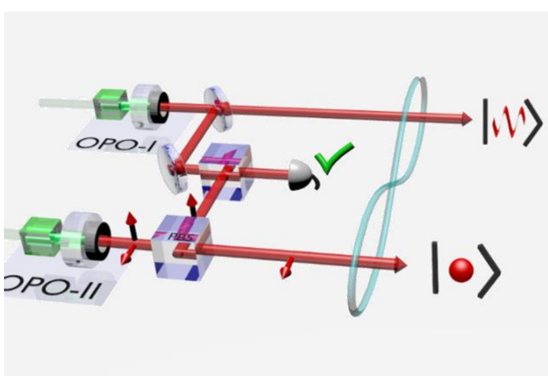

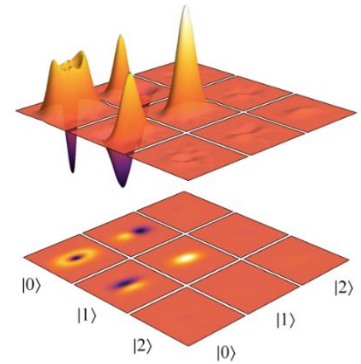

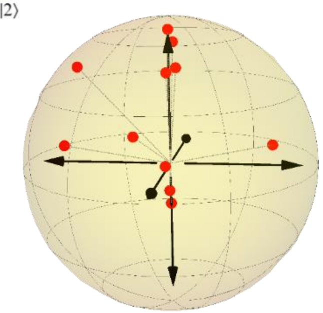

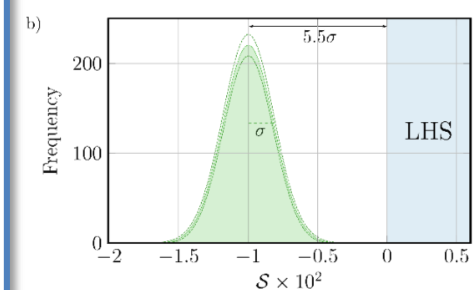

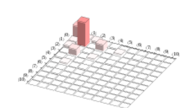

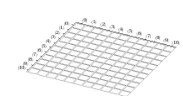

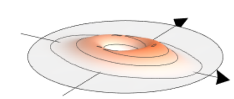

Discrete Variable encoding (DV)

→ Number of photons

Fock states: $|0\rangle,\ |1\rangle,\ |2\rangle \ldots$

Qu-bits: $c_0\,|0\rangle + c_1\,|1\rangle$

$$|\pm\rangle = |0\rangle \pm |1\rangle$$

Hilbert space of finite dimension

Photon counters: APD, SNSPD…

$$|0\rangle - |1\rangle$$

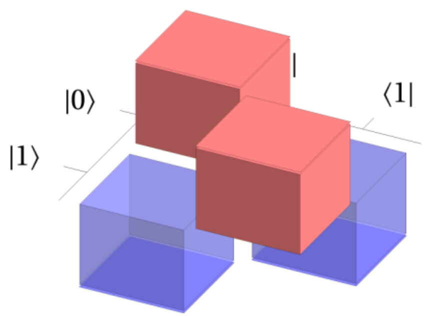

Density matrix

Optical hybrid quantum information processing

Laboratoire Kastler Brossel
Physique quantique et applications

Discrete Variable encoding (DV)

→ Number of photons

Fock states: $|0\rangle,\ |1\rangle,\ |2\rangle\ldots$

Qu-bits: $c_0\,|0\rangle + c_1\,|1\rangle$

$$|\pm\rangle = |0\rangle \pm |1\rangle$$

Hilbert space of finite dimension

Photon counters: APD, SNSPD…

Continuous Variable encoding (CV)

→ Field quadratures x and p

Coherent states: $|\alpha\rangle,\ |-\alpha\rangle$

Qu-modes: $c_\alpha\,|\alpha\rangle + c_{-\alpha}\,|-\alpha\rangle$

$$|cat\pm\rangle = |\alpha\rangle \pm |-\alpha\rangle$$

Hilbert space of infinite dimension

Homodyne detection

$$|0\rangle - |1\rangle$$

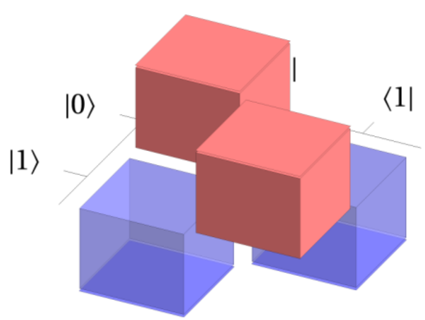

Density matrix

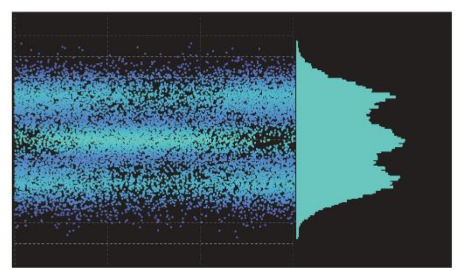

Homodyne signal

$$|\alpha\rangle + |-\alpha\rangle$$

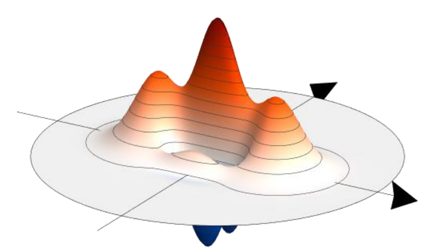

Wigner function

Optical hybrid quantum information processing

Discrete Variable encoding (DV)

→ Number of photons

Fock states: $|0\rangle,\ |1\rangle,\ |2\rangle\ldots$

Qu-bits: $c_0\,|0\rangle + c_1\,|1\rangle$

$$|\pm\rangle = |0\rangle \pm |1\rangle$$

Hilbert space of finite dimension

Photon counters: APD, SNSPD…

Continuous Variable encoding (CV)

→ Field quadratures x and p

Coherent states: $|\alpha\rangle,\ |-\alpha\rangle$

Qu-modes: $c_\alpha\,|\alpha\rangle + c_{-\alpha}\,|-\alpha\rangle$

$$|cat\pm\rangle = |\alpha\rangle \pm |-\alpha\rangle$$

Hilbert space of infinite dimension

Homodyne detection

$|1\rangle$

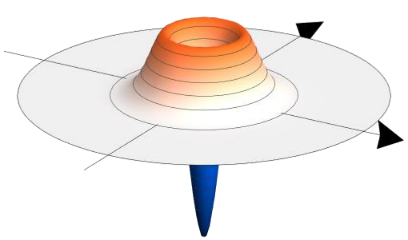

Wigner function

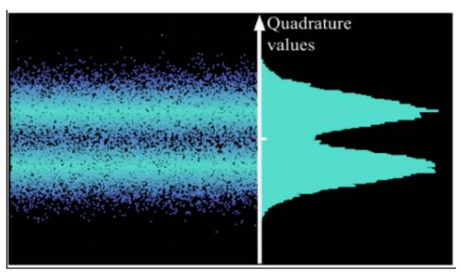

Homodyne signal

$|\alpha\rangle + |-\alpha\rangle$

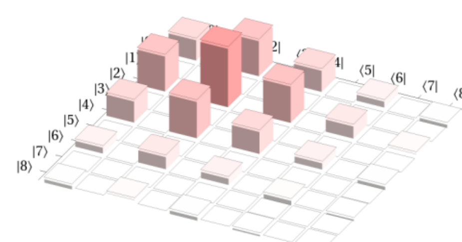

Density matrix

Optical hybrid quantum information processing

Laboratoire Kastler Brossel
Physique quantique et applications

Discrete Variable encoding (DV)

→ Number of photons

Fock states: $|0\rangle,\ |1\rangle,\ |2\rangle\ldots$

Qu-bits: $c_0\,|0\rangle + c_1\,|1\rangle$

$$|\pm\rangle = |0\rangle \pm |1\rangle$$

Hilbert space of finite dimension

Photon counters: APD, SNSPD

&

Continuous Variable encoding (CV)

→ Field quadratures x and p

Coherent states: $|\alpha\rangle,\ |-\alpha\rangle$

Qu-modes: $c_\alpha\,|\alpha\rangle + c_{-\alpha}\,|-\alpha\rangle$

$$|cat\pm\rangle = |\alpha\rangle \pm |-\alpha\rangle$$

Hilbert space of infinite dimension

dyne detection

HYBRID

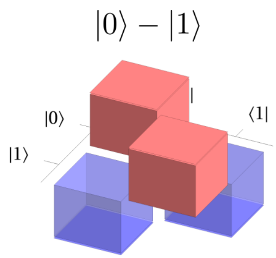

DV

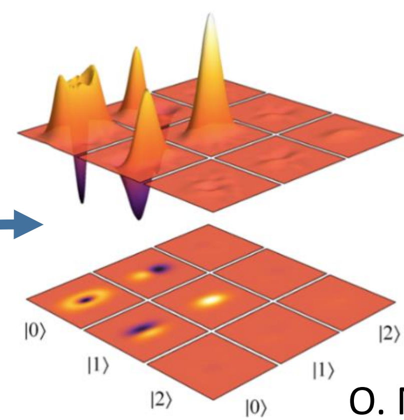

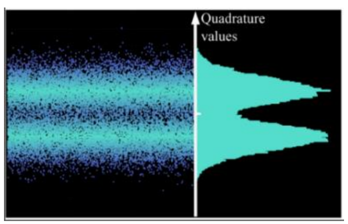

CV

O. Morin et al, Nat. Phot. **8**, 570-574 (2014)

U. L. Andersen et. al., Nature Physics **11**, 713–719 (2015)
P. Van Loock, Laser & Photonics Review s **5**, 167-200 (2011)

Optical parametric oscillators as a resource

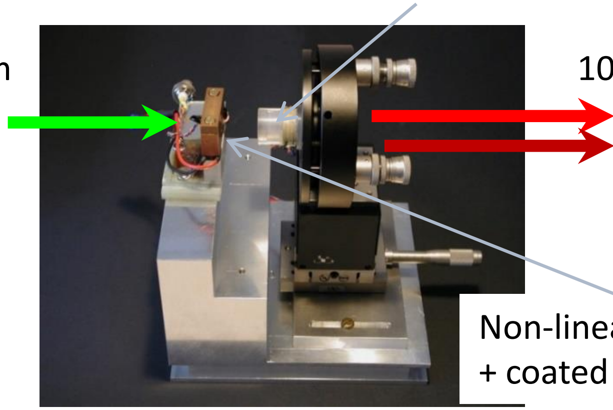

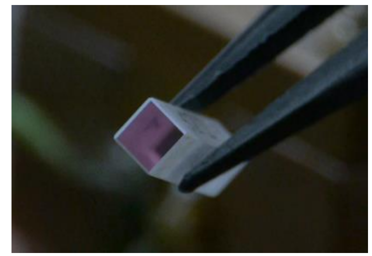

PPKTP crystal

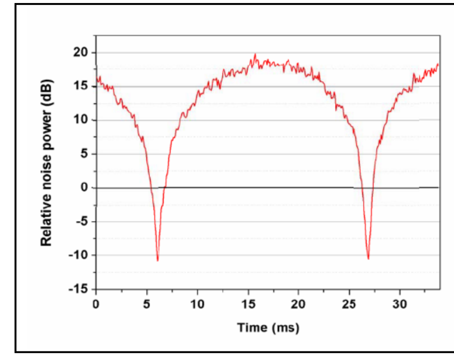

10.dB of Squeezing

Type I: **o** $\leftrightarrow$ **e + e**

$$|Sq\rangle = (1-\lambda^2)^{1/4} \sum_n \binom{2n}{n}^{1/2} (\lambda/2)^n \, |2n\rangle$$

- PPKTP crystal
- Pumping halfway to threshold
- Doubly resonant (signal + idler and pump)
- Up to 10.5dB of squeezing

Type II: **e** $\leftrightarrow$ **o + e**

$$|EPR\rangle = (1-\lambda^2)^{1/4} \sum_n \lambda^n \, |n\rangle_o \, |n\rangle_e$$

- KTP crystal
- Pumping well below threshold
- Triply resonant (signal, idler and pump)

DV states generation: Single photons

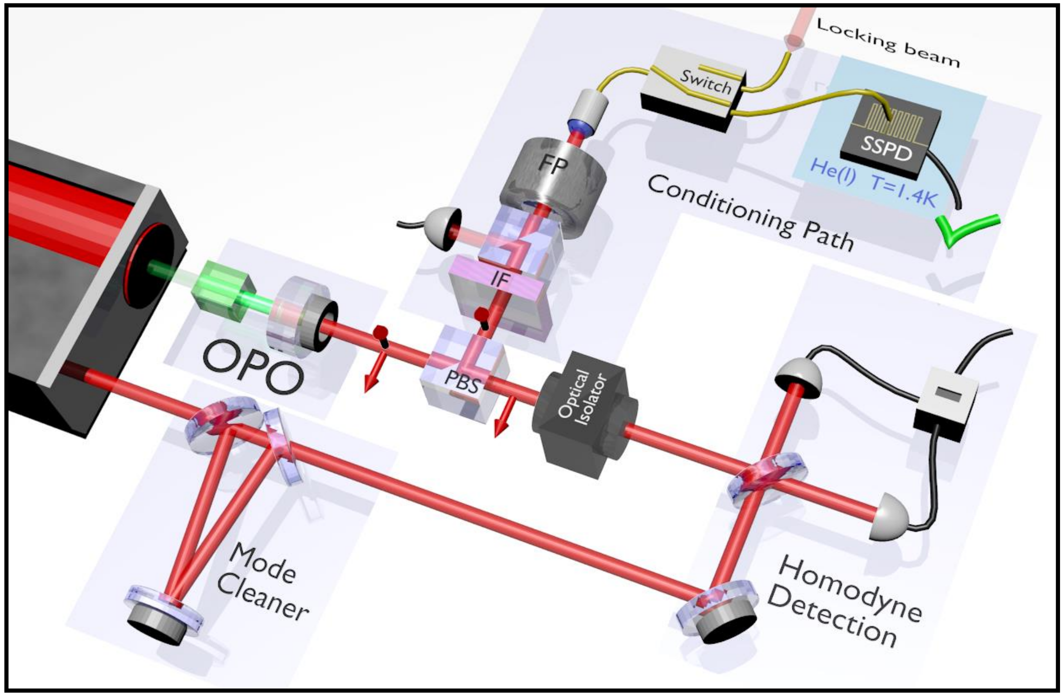

OPO II pumped at 1% of threshold

Output: $|0\rangle_H |0\rangle_V + \lambda |1\rangle_H |1\rangle_V$ with $\lambda \ll 1$

Heralded generation of single photon

DV states generation: Single photons

Laboratoire Kastler Brossel
Physique quantique et applications

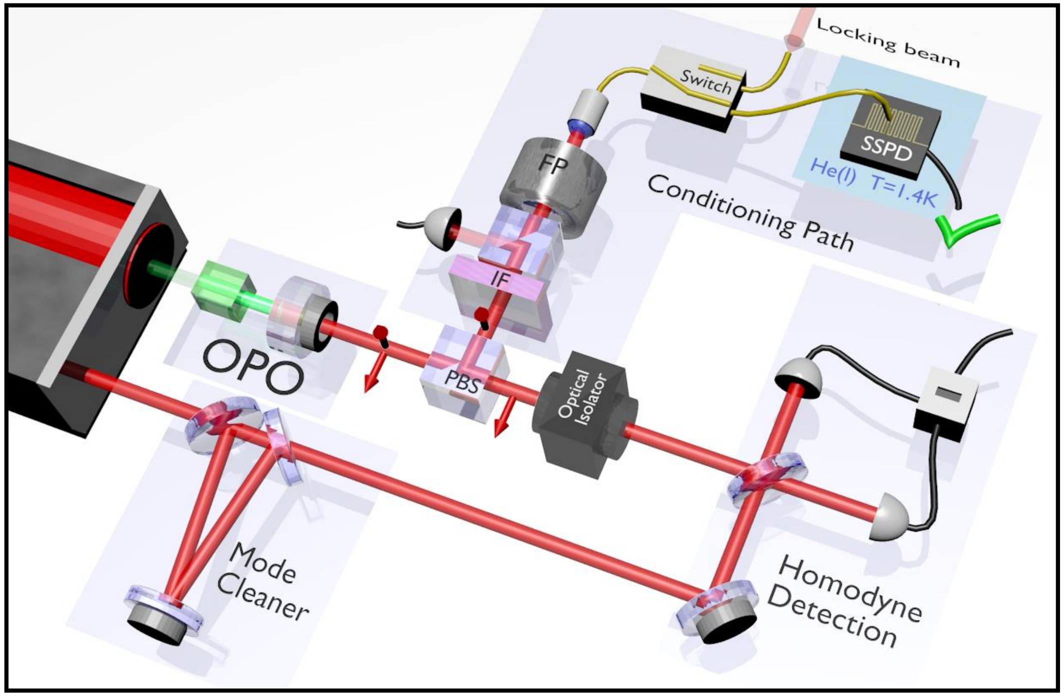

OPO II pumped at 1% of threshold

Output: $|0\rangle_H |0\rangle_V + \lambda |1\rangle_H |1\rangle_V$ with $\lambda \ll 1$

Heralded generation of single photon

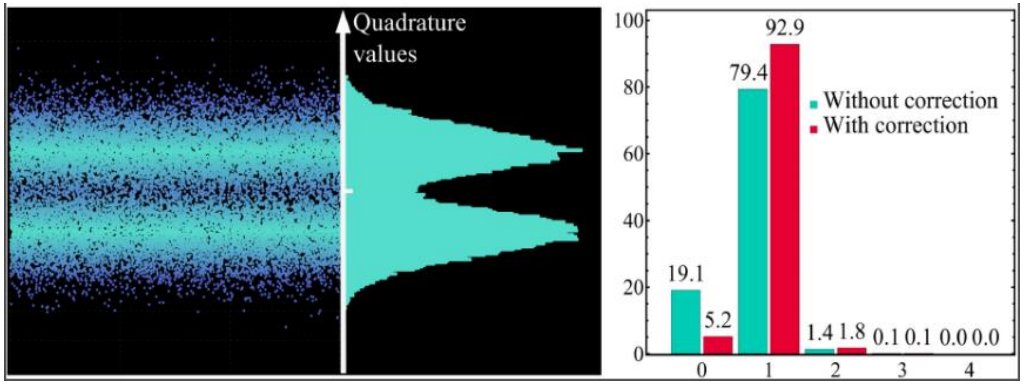

O. Morin et al, Optics letters 37,3738 (2012)
O. Morin et al, Phys. Rev. Lett. 111,213602 (2013)
H. Le Jeannic et al, *Optics letters 41,005341 (2016)*

DV states generation: Single photons

Laboratoire Kastler Brossel
Physique quantique et applications

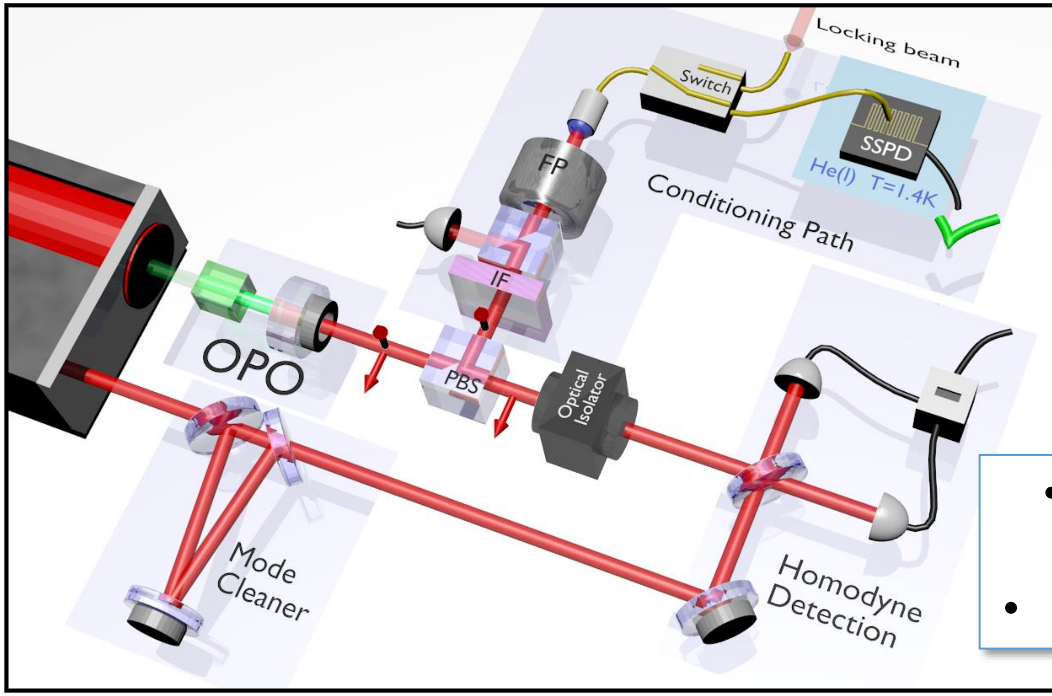

OPO II pumped at 1% of threshold

Output: $|0\rangle_H |0\rangle_V + \lambda |1\rangle_H |1\rangle_V$ with $\lambda \ll 1$

Heralded generation of single photon

- Above 90% heralding efficiency
- g(2)<0,1
- 200kHz up to 1Mhz generation rate

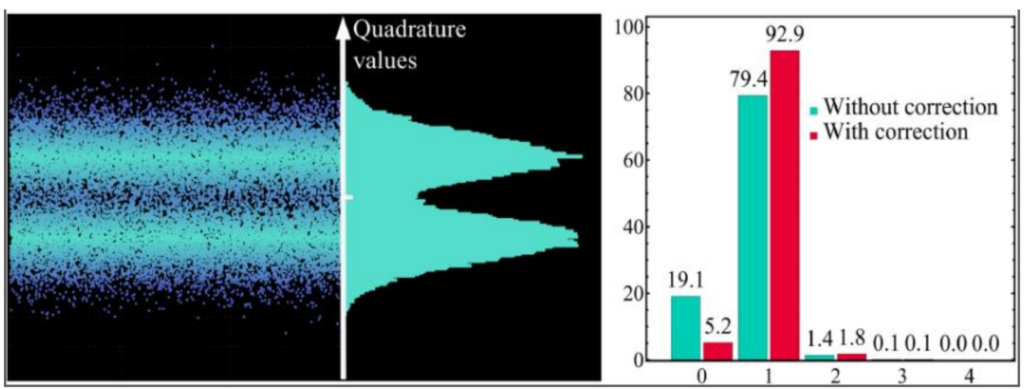

O. Morin et al, Optics letters 37,3738 (2012)
O. Morin et al, Phys. Rev. Lett. 111,213602 (2013)
H. Le Jeannic et al, *Optics letters 41,005341 (2016)*

DV states generation: Two-photon state

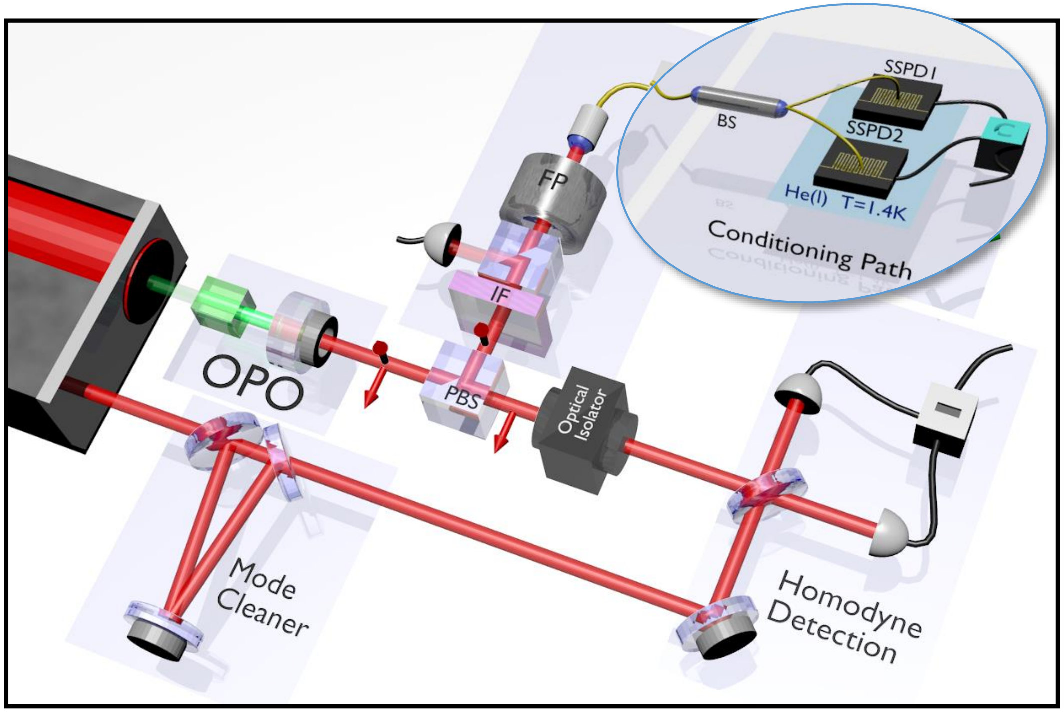

OPO II pumped at 1% of threshold

Output: $|0\rangle_H |0\rangle_V + \lambda |1\rangle_H |1\rangle_V + \lambda^2 |2\rangle_H |2\rangle_V$

Heralded generation of two-photon state

DV states generation: Two-photon state

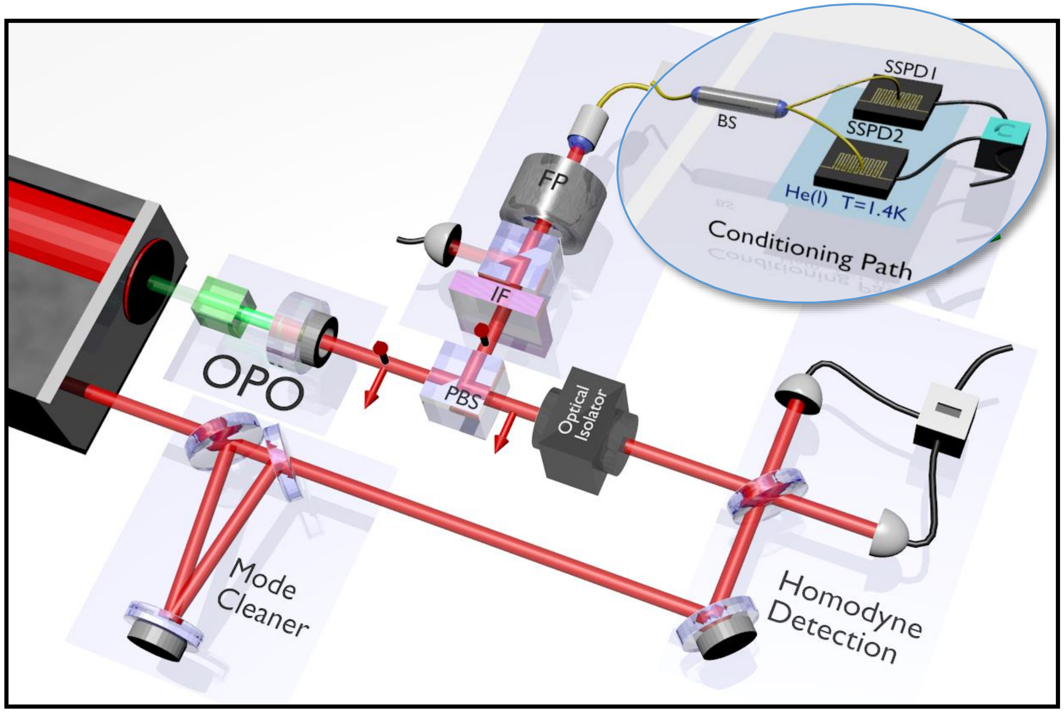

OPO II pumped at 1% of threshold

Output: $|0\rangle_H |0\rangle_V + \lambda |1\rangle_H |1\rangle_V + \lambda^2 |2\rangle_H |2\rangle_V$

Heralded generation of two-photon state

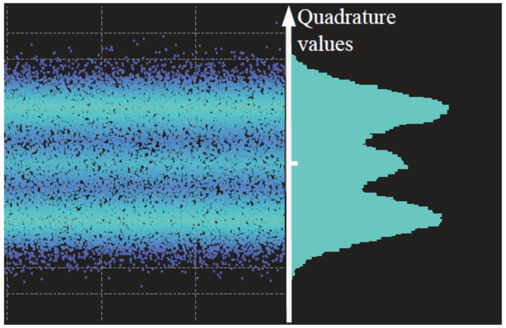

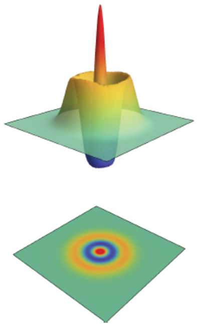

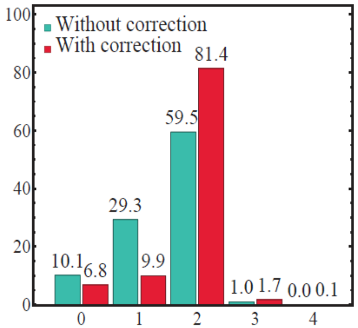

DV states generation: Two-photon state

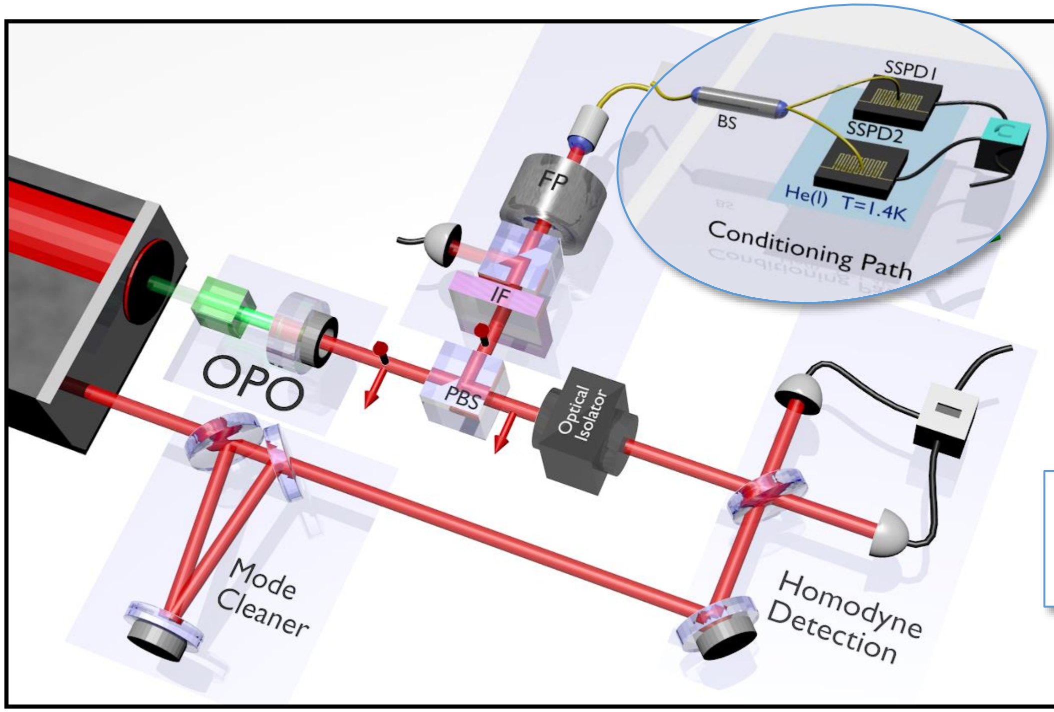

OPO II pumped at 1% of threshold

Output: $|0\rangle_H |0\rangle_V + \lambda |1\rangle_H |1\rangle_V + \lambda^2 |2\rangle_H |2\rangle_V$

Heralded generation of two-photon state

- 60% two-photon component
- >200Hz generation rate

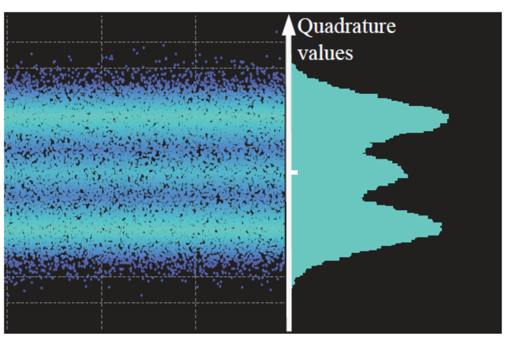

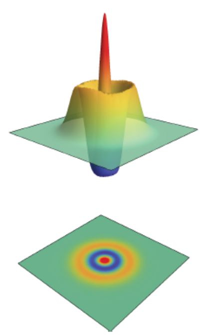

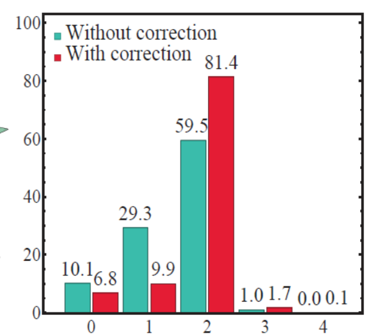

Photon subtraction using SNSPDs

- Detection efficiency > 90% (1064nm)
- Operating at 1.6K
- Dark noise <1Hz

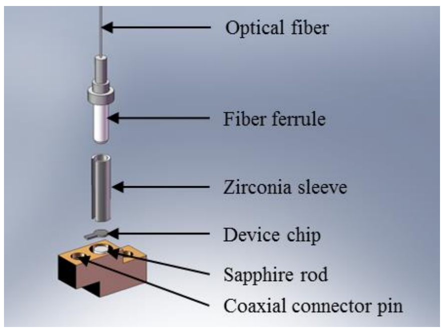

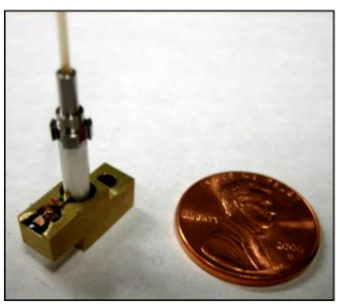

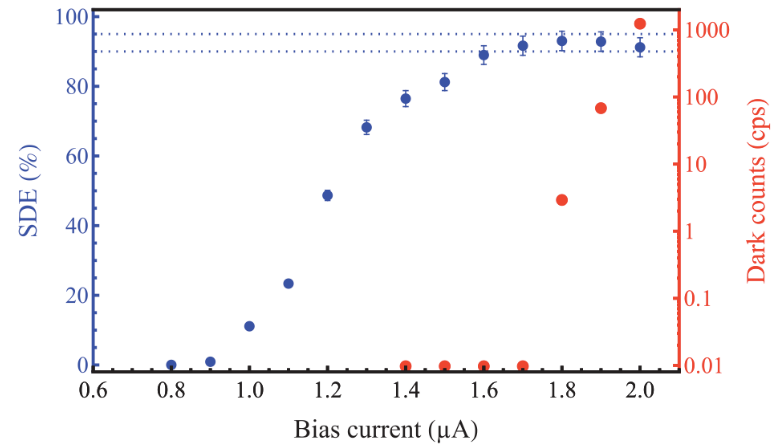

H. Le Jeannic et al, *Optics letters 41,005341 (2016)*

A collaboration with:

- NIST (S. Woo Nam, V. Verma)
- JPL (F. Marsili, M. D. Shaw)

CV states generation: Schrödinger kittens

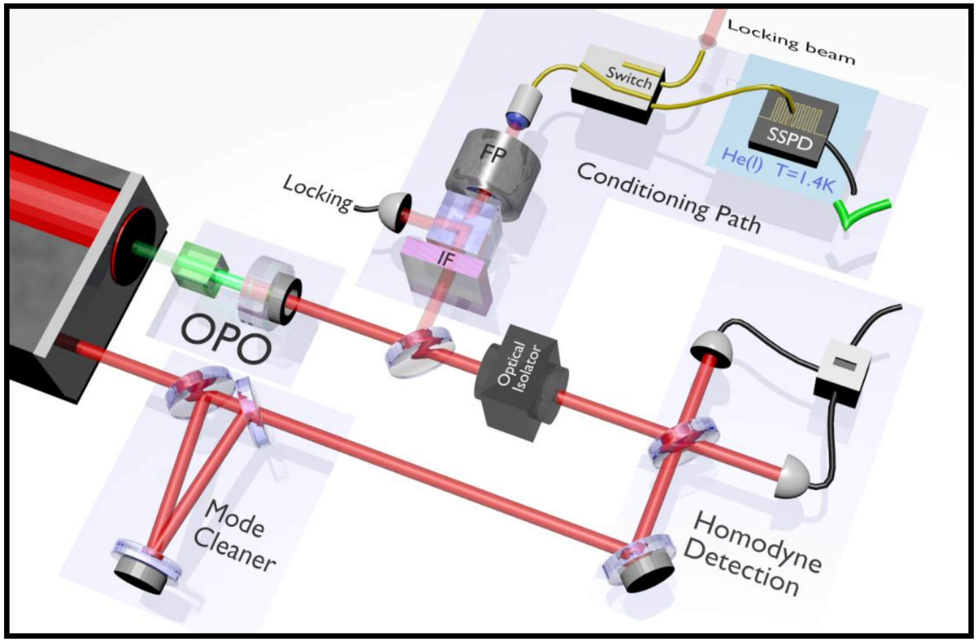

- OPO I pumped at 50% of threshold
- High transmission beam splitter

Heralded generation of Schrödinger kitten

$$\hat{a}\hat{S}\left|0\right\rangle \approx \left|cat-\right\rangle$$

CV states generation: Schrödinger kittens

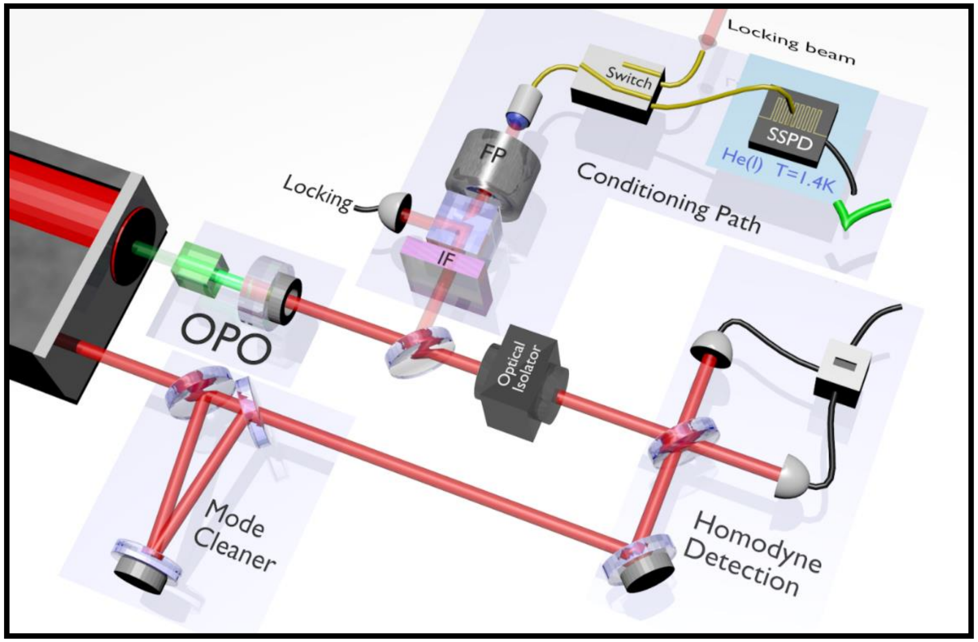

- OPO I pumped at 50% of threshold
- High transmission beam splitter

Heralded generation of Schrödinger kitten

$$\hat{a}\hat{S}\,|0\rangle \approx |cat-\rangle$$

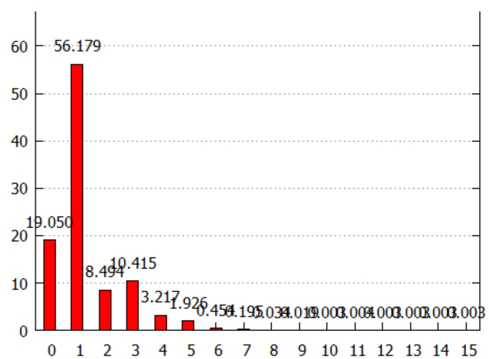

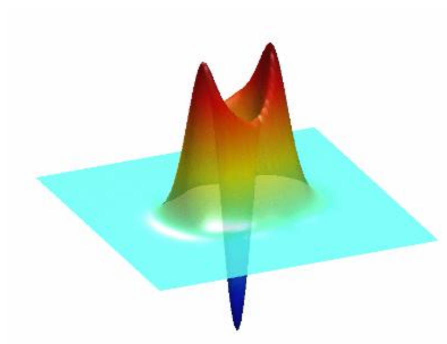

O. Morin et al, J. Vis. Exp. 87, e51224 (2014)

CV states generation: Schrödinger kittens

Laboratoire Kastler Brossel
Physique quantique et applications

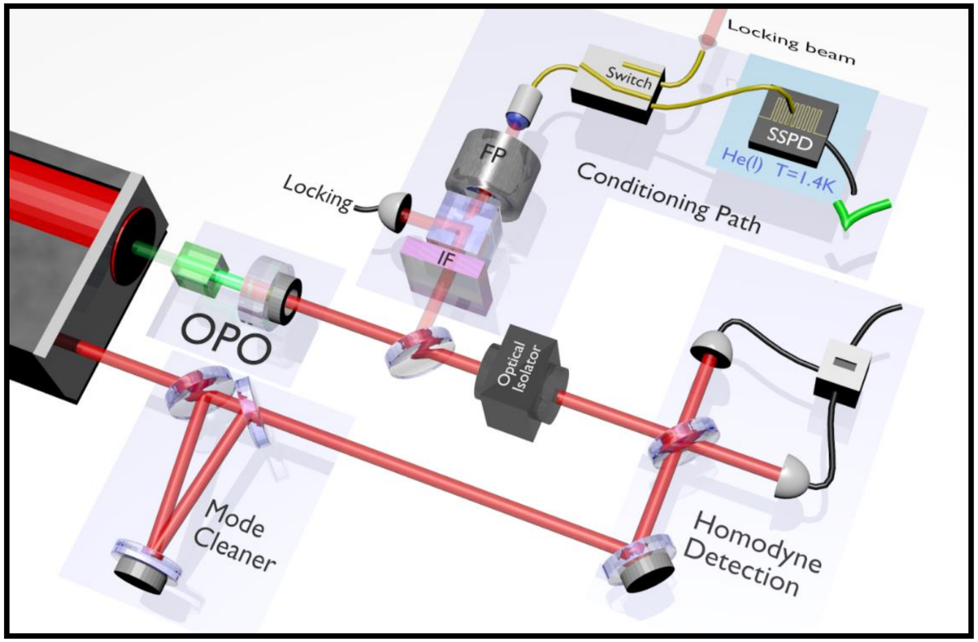

- OPO I pumped at 50% of threshold
- High transmission beam splitter

Heralded generation of Schrödinger kitten

$$\hat{a}\hat{S}\,|0\rangle \approx |cat-\rangle$$

- Close to unity purity
- 500kHz generation rate

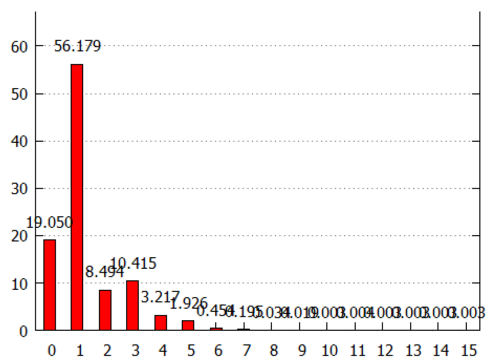

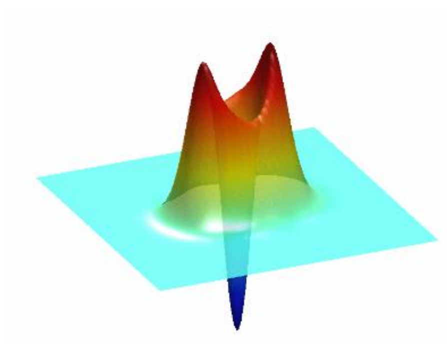

O. Morin et al, J. Vis. Exp. 87, e51224 (2014)

Outline

I	Optical quantum state engineering	☑
II	Hybrid entanglement of light	
III	Remote state preparation of arbitrary CV qu-modes	
IV	Experimental demonstration of EPR steering	
V	Towards quantum teleportation from DV to CV	

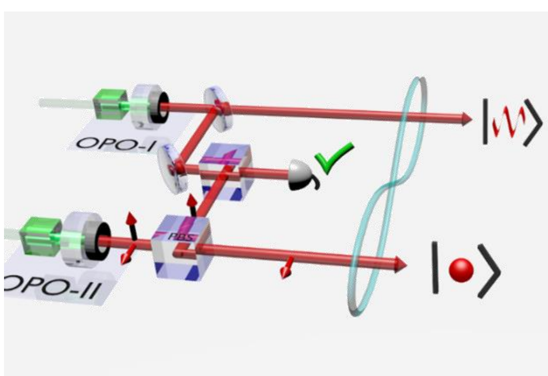

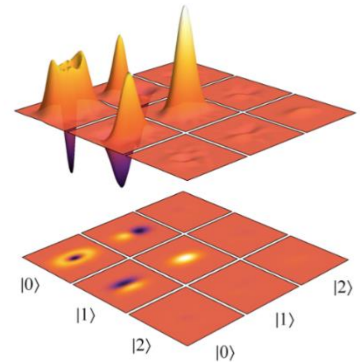

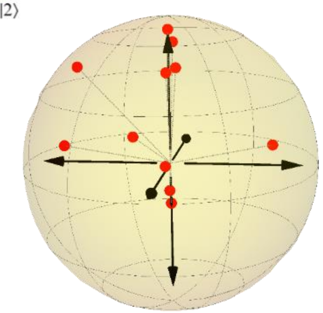

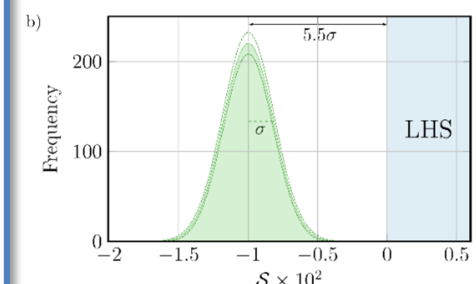

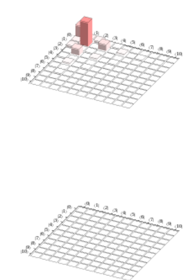

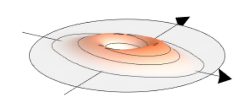

Optical hybrid entanglement

Laboratoire Kastler Brossel
Physique quantique et applications

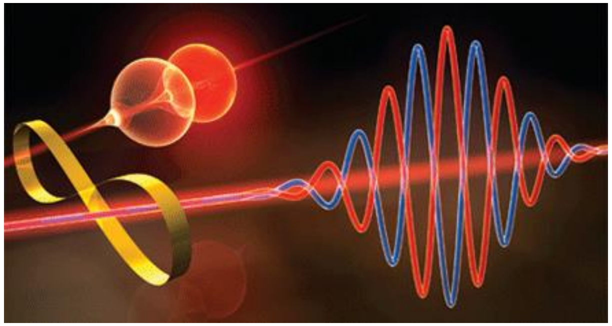

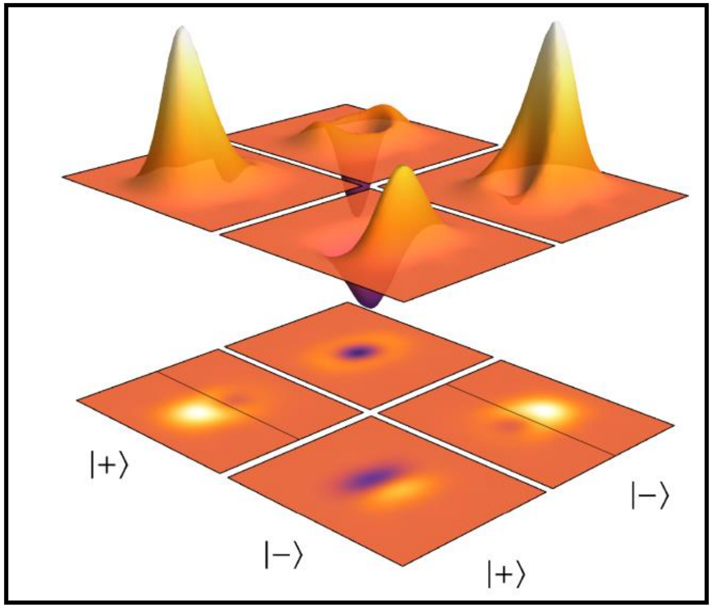

$$\frac{1}{\sqrt{2}}\left(|\alpha\rangle\,|+\rangle+|-\alpha\rangle\,|-\rangle\right)$$

Remote creation of hybrid entanglement between particle-like and wave-like optical qubits

O. Morin et al, Nat. Phot. **8**, 570-574 (2014)

Hybrid state generation

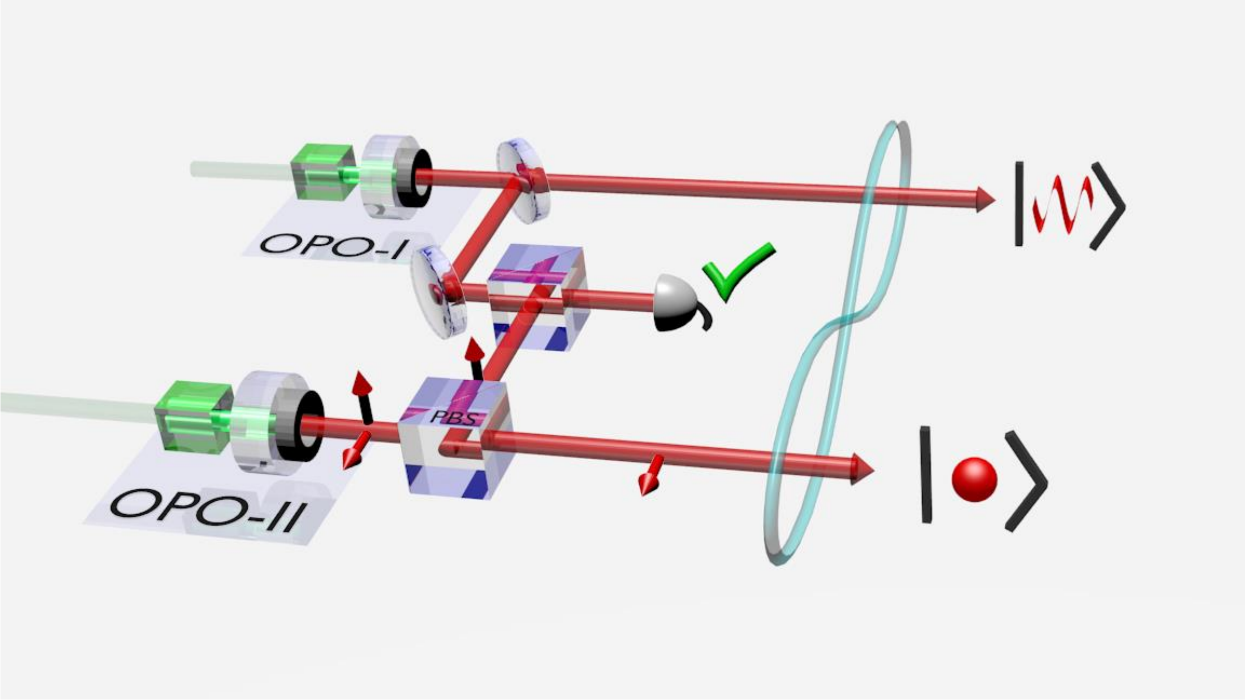

Hybrid state generation

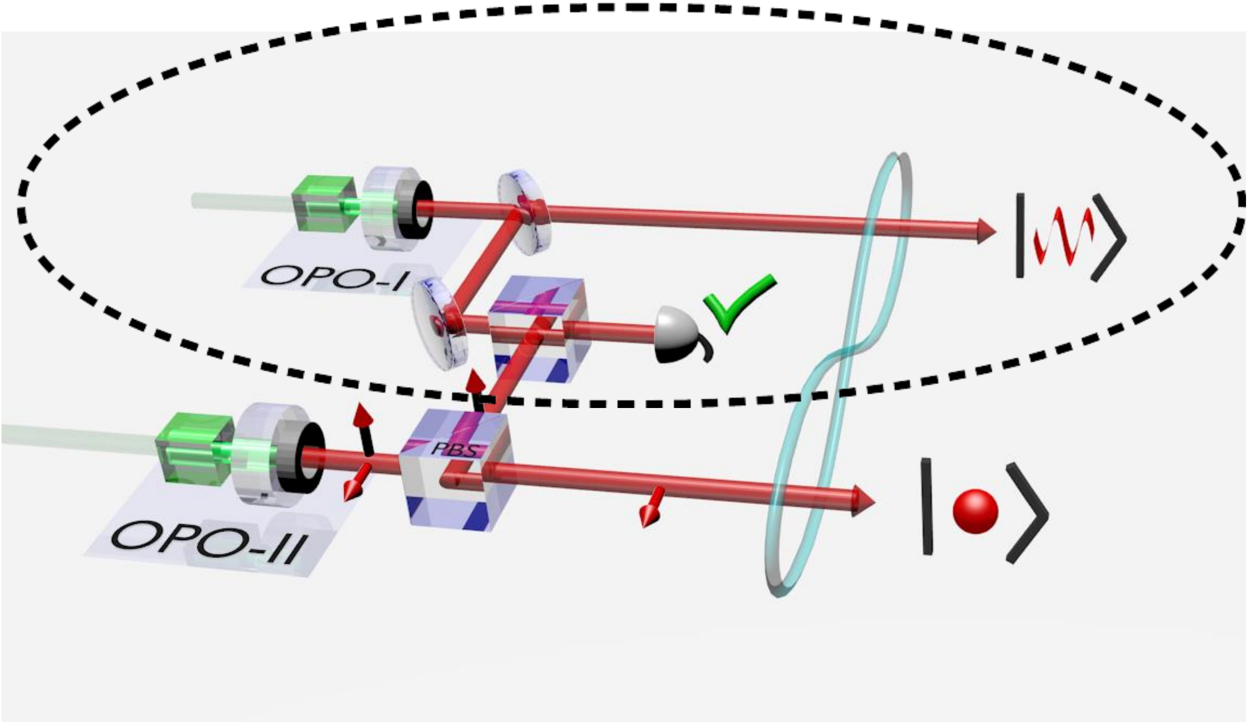

Click!

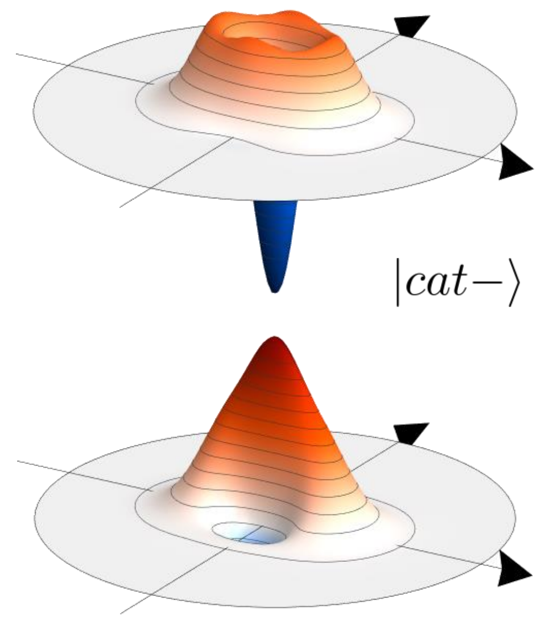

No click

$|cat+\rangle$

Hybrid state generation

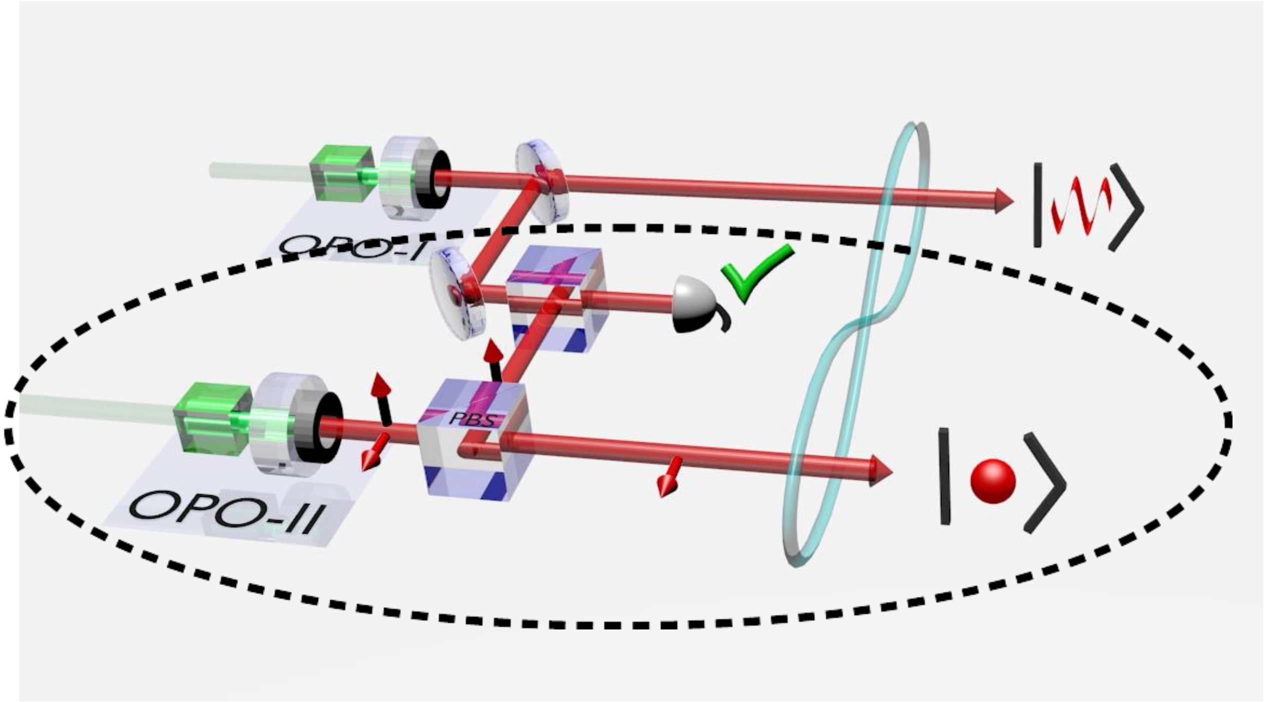

Click!

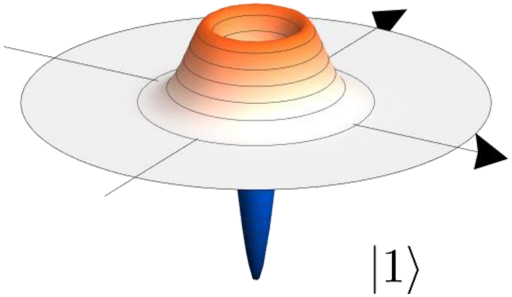

$|1\rangle$

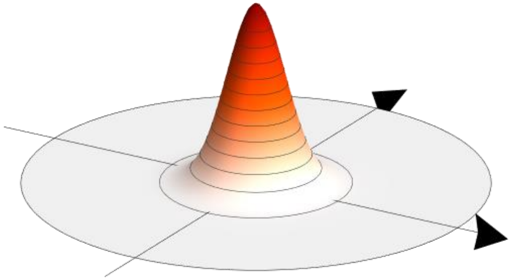

No click

$|0\rangle$

Hybrid state generation

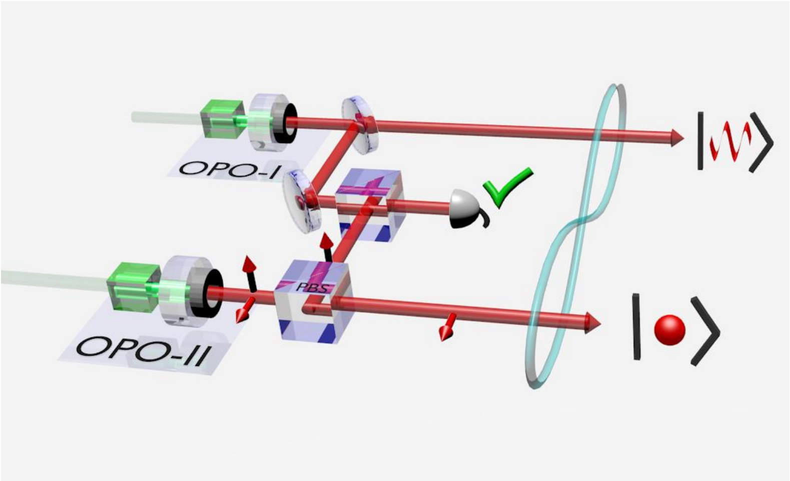

$$\frac{1}{\sqrt{2}}(|cat-\rangle\,|0\rangle + |cat+\rangle\,|1\rangle)$$

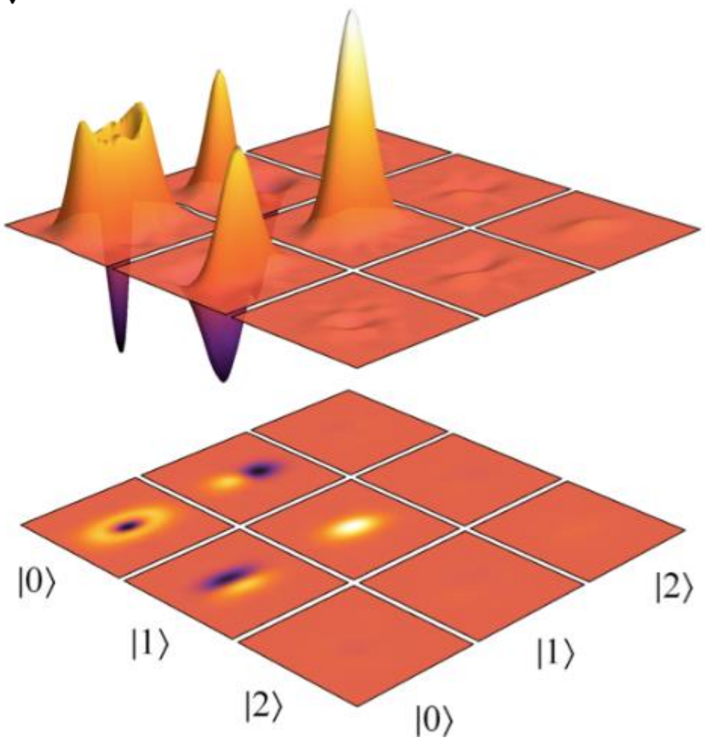

- Fidelity of 77% for $|\alpha|^2$=0.9
- Less than 2% outside of qubit subspace on DV side

O. Morin et al, *Nat. Phot.* 8, 570 (2014)

Hybrid state generation

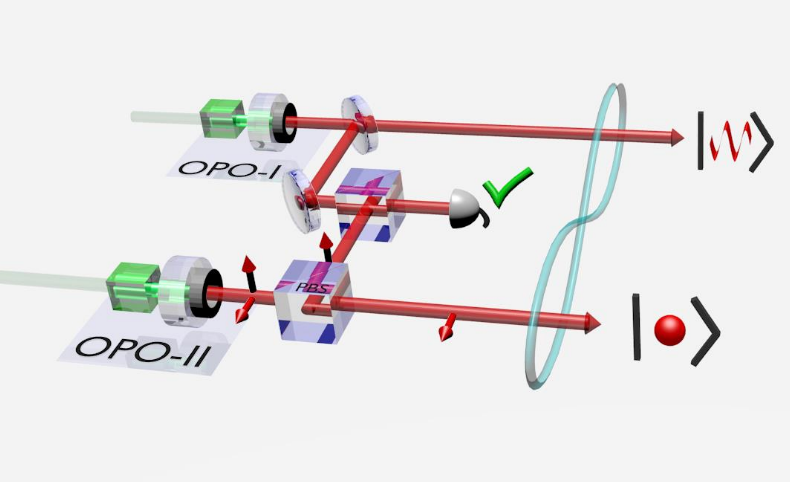

Changing the ratio between the two paths
transition from separable to maximally entangled

$$\mathcal{N} = \left(||\rho^{T_A}||_1 - 1\right)/2$$

Maximal value: $\mathcal{N}$ = 0.5

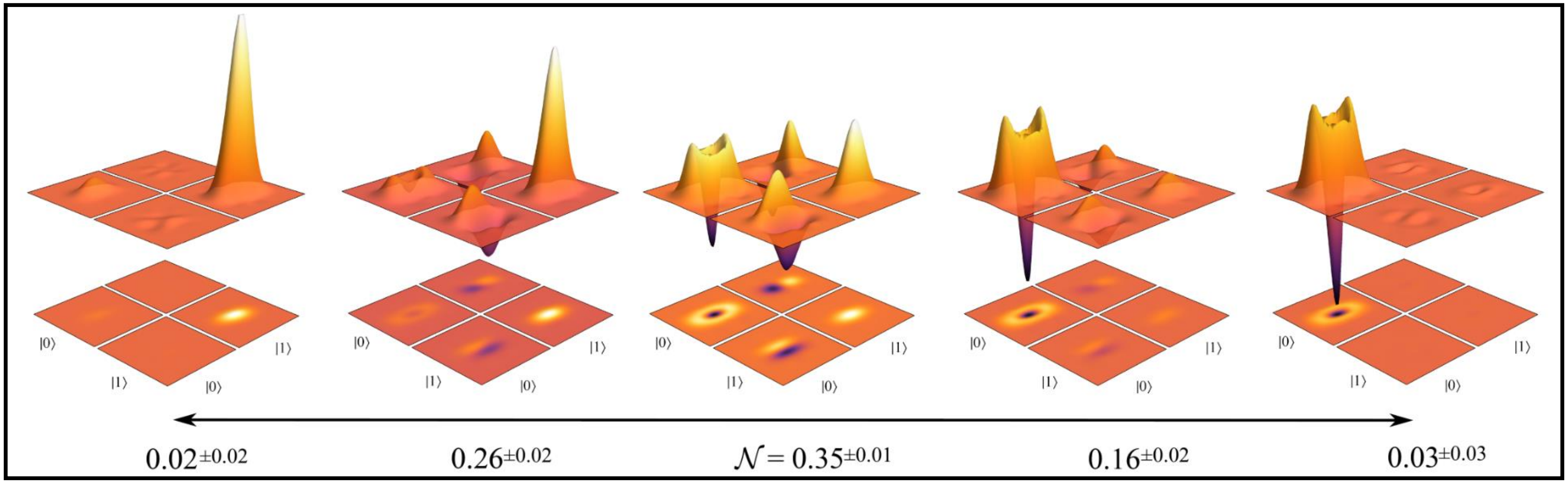

Outline

I	Optical quantum state engineering	☑
II	Hybrid entanglement of light	☑
III	Remote state preparation of arbitrary CV qu-modes	
IV	Experimental demonstration of EPR steering	
V	Towards quantum teleportation from DV to CV	

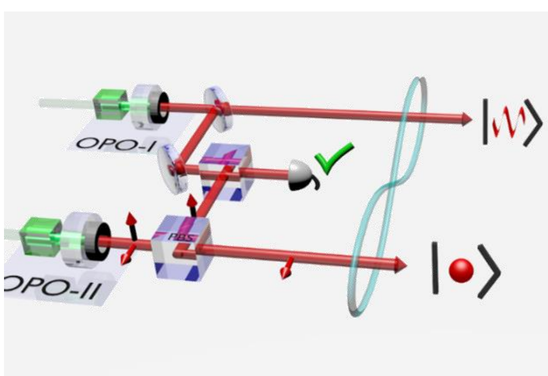

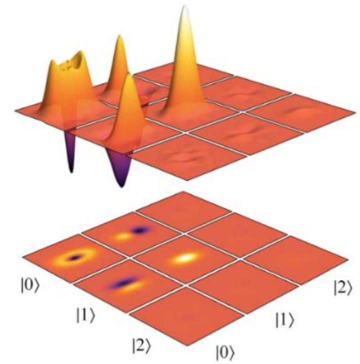

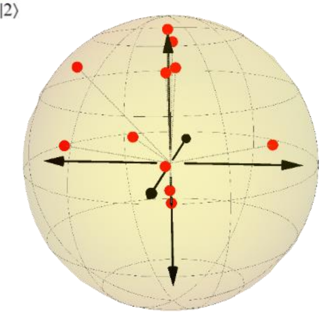

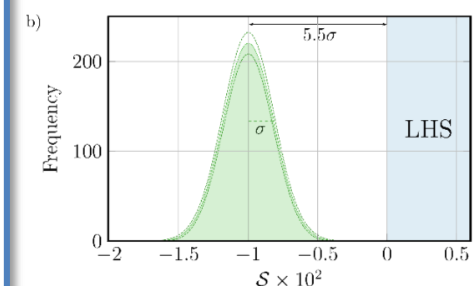

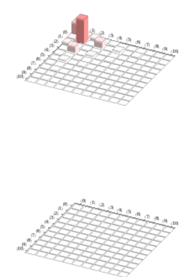

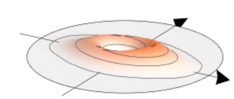

Remote State Preparation: Principle

Goal: Remotely prepare any qu-mode $c_\alpha \left|\alpha\right\rangle + e^{i\phi} c_{-\alpha} \left|-\alpha\right\rangle$

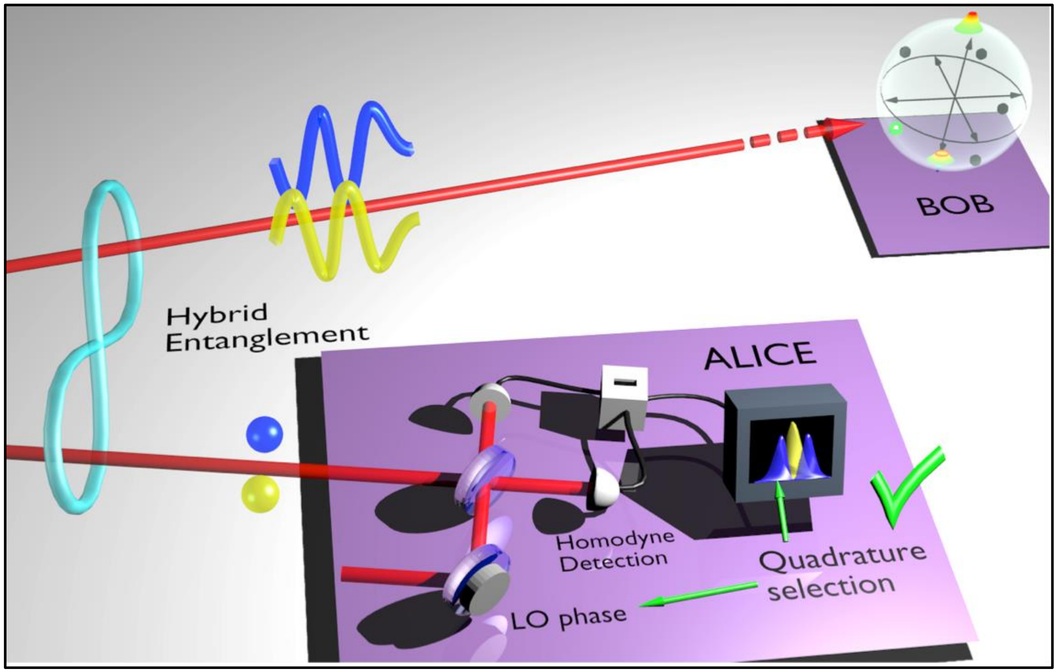

$$\frac{1}{\sqrt{2}}(\left|cat-\right\rangle \left|0\right\rangle + \left|cat+\right\rangle \left|1\right\rangle)$$

Remote State Preparation: Theory

Goal: Remotely prepare any qu-mode $c_\alpha |\alpha\rangle + e^{i\phi} c_{-\alpha} |-\alpha\rangle$

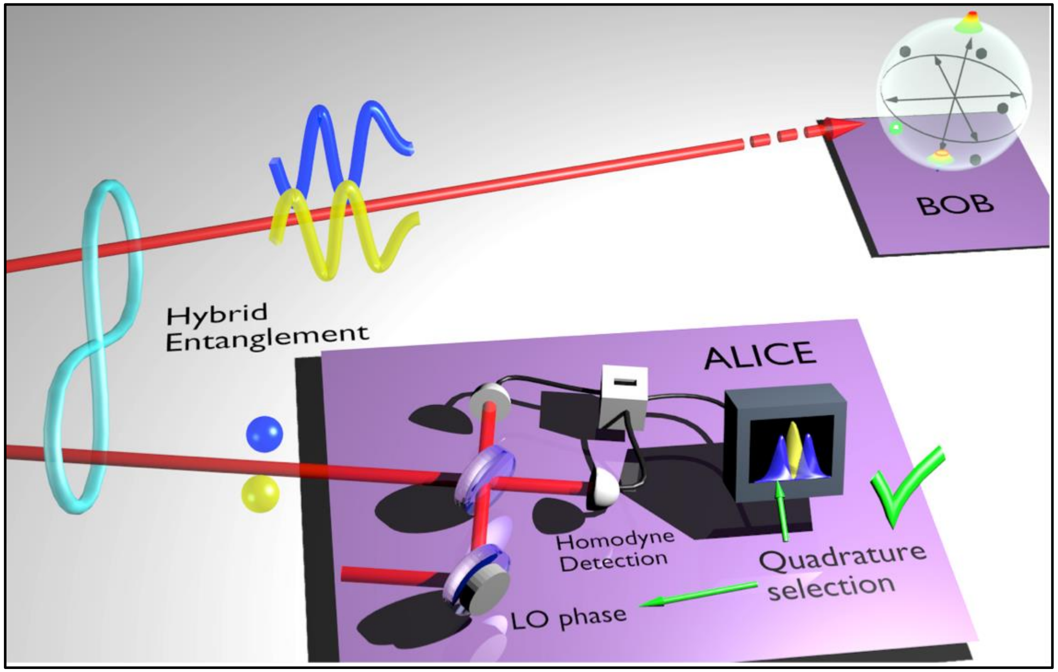

$$\frac{1}{\sqrt{2}}(|cat-\rangle |0\rangle + |cat+\rangle |1\rangle)$$

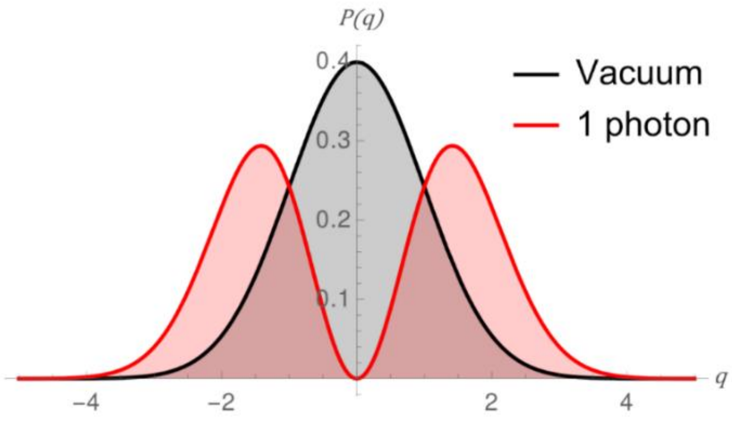

Remote State Preparation: Theory

Goal: Remotely prepare any qu-mode $c_\alpha |\alpha\rangle + e^{i\phi} c_{-\alpha} |-\alpha\rangle$

$$\frac{1}{\sqrt{2}}\left(|cat-\rangle|0\rangle + |cat+\rangle|1\rangle\right)$$

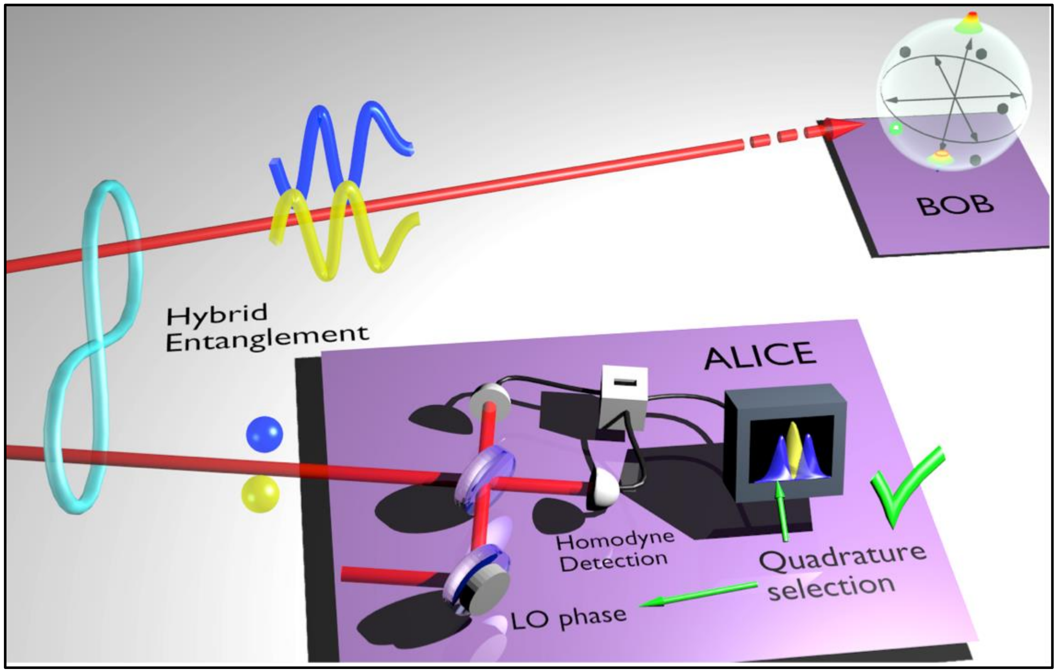

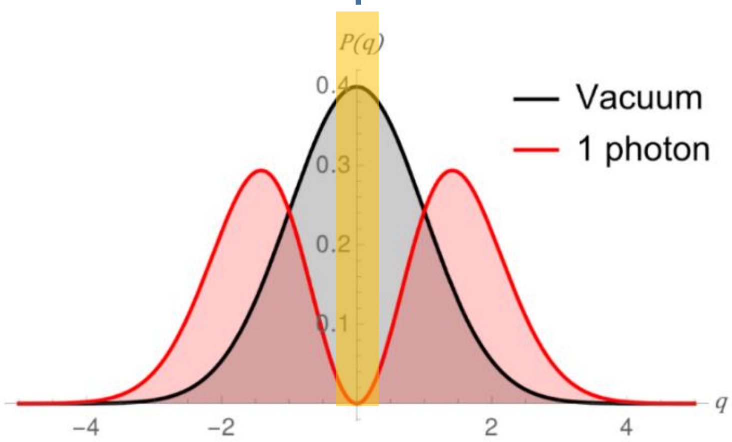

- P(q) is directly accessible through homodyne detection.
- The DV subspace is of dimension 2.

Remote State Preparation: Theory

Goal: Remotely prepare any qu-mode $c_\alpha \left|\alpha\right\rangle + e^{i\phi} c_{-\alpha} \left|-\alpha\right\rangle$

$$\frac{1}{\sqrt{2}}(\left|cat-\right\rangle\left|0\right\rangle + \left|cat+\right\rangle\left|1\right\rangle)$$

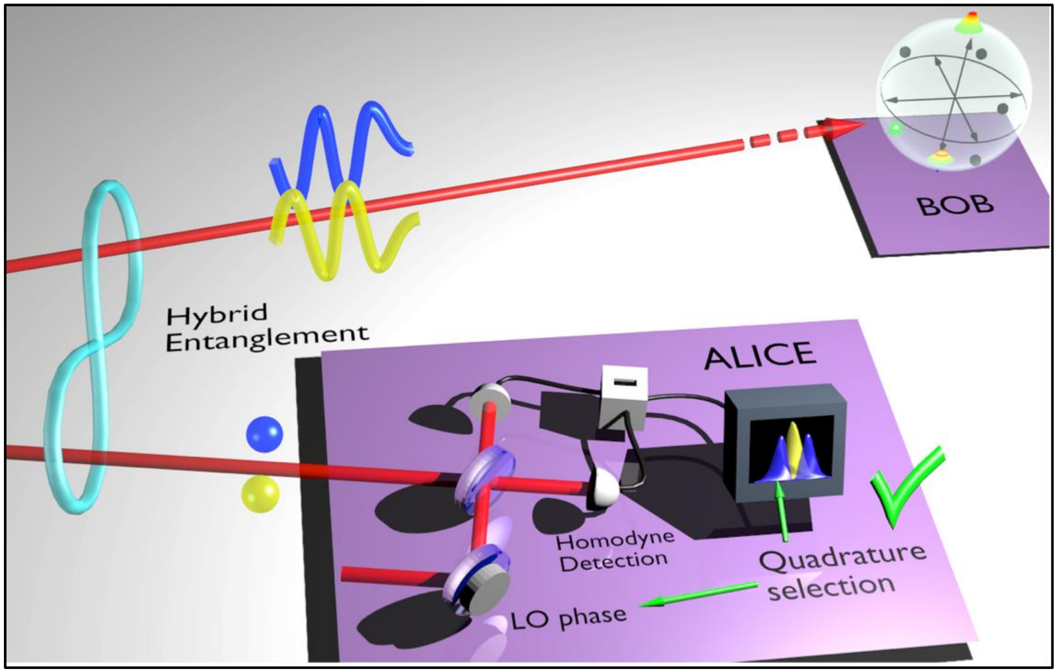

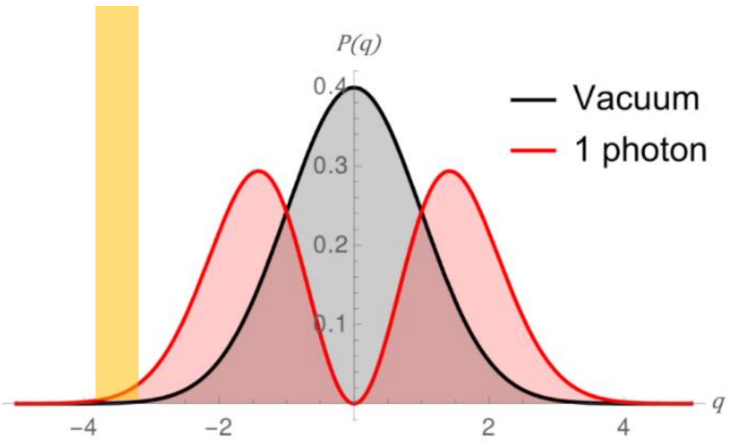

- P(q) is directly accessible through homodyne detection.
- The DV subspace is of dimension 2.

Remote State Preparation: Theory

Conditioning on homodyne measurement on DV side → Chosen state on CV side

With equal weight: $\boxed{\frac{1}{\sqrt{2}}(|cat-\rangle + |cat+\rangle)}$

$$\frac{1}{\sqrt{2}}(|cat-\rangle|0\rangle + |cat+\rangle|1\rangle)$$

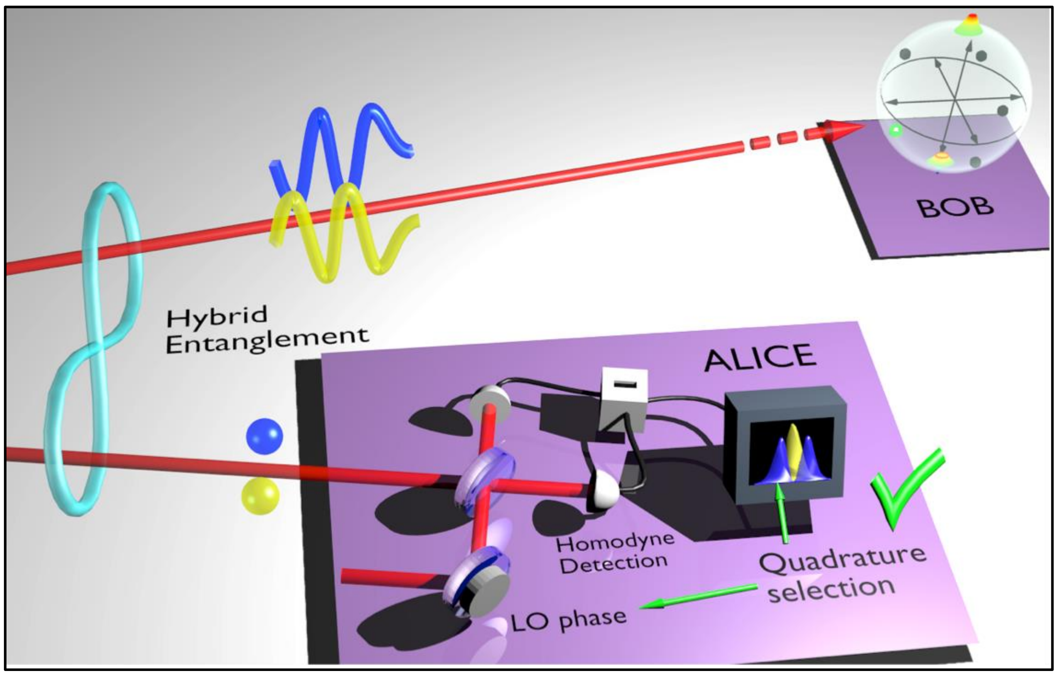

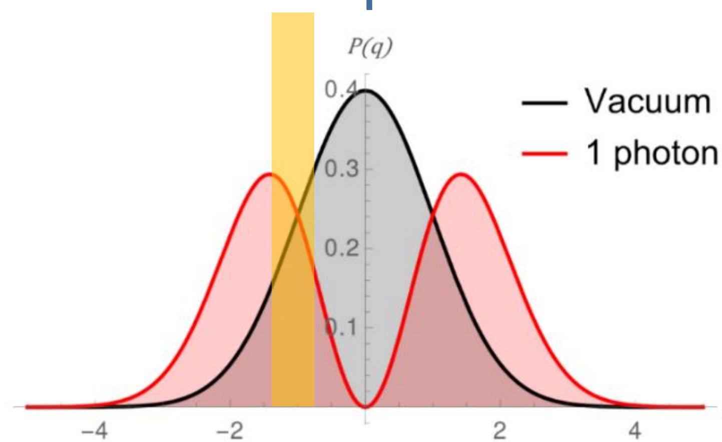

- P(q) is directly accessible through homodyne detection.
- The DV subspace is of dimension 2.

Remote State Preparation

Choosing the phase of the local oscillator ϕ and keeping only quadrature values q_ϕ

→ Any qu-mode is accessible!

Choice on DV side:

$$(\phi, q_\phi)$$

Resulting state on CV side:

$$\langle q_\phi|\psi\rangle = |cat-\rangle + q_\phi e^{i\phi}\,|cat+\rangle$$

$$\Updownarrow$$

$$c_\alpha\,|\alpha\rangle + e^{i\phi}c_{-\alpha}\,|-\alpha\rangle$$

Remote State Preparation: Results

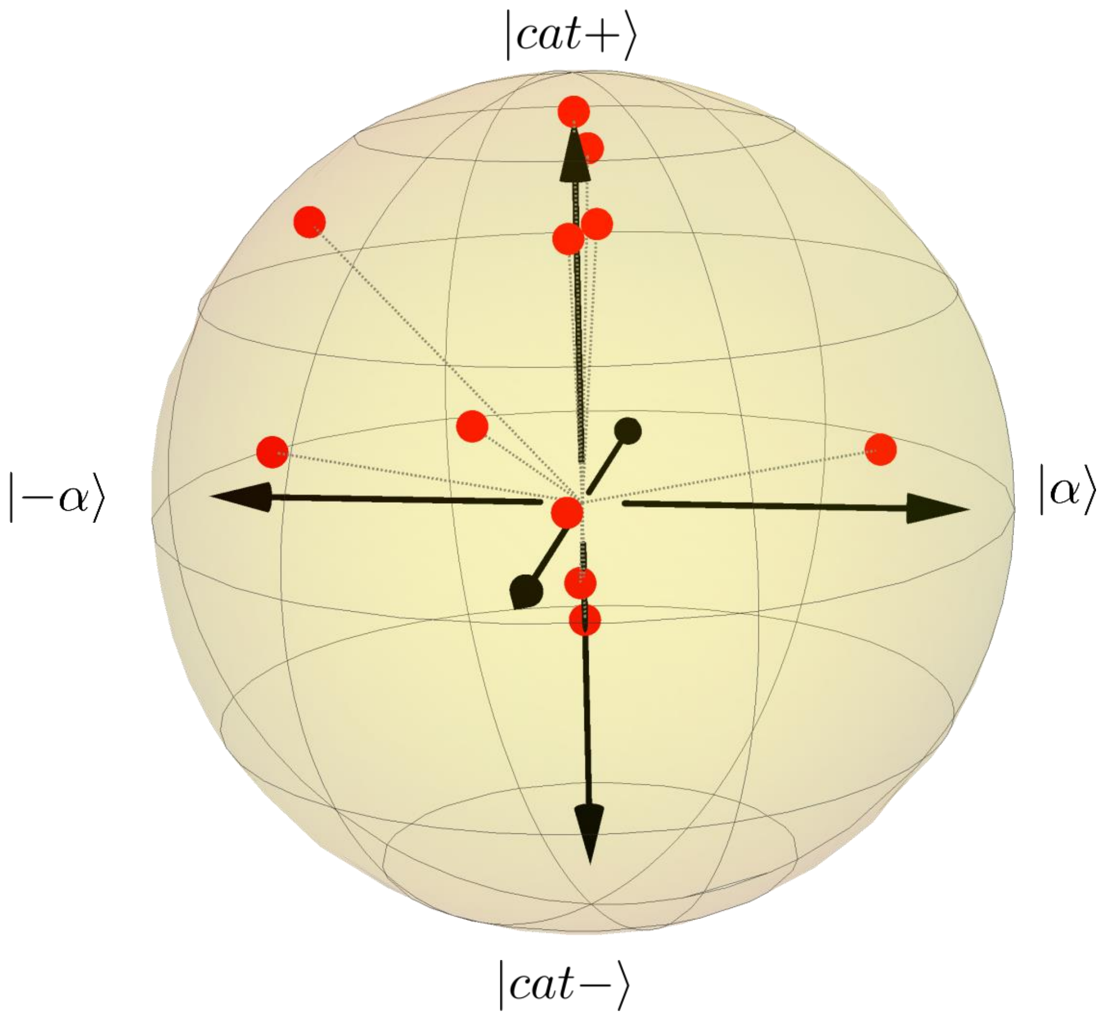

$$\frac{1}{\sqrt{N}}\left(|cat-\rangle + \color{red}{q_\phi} \color{black} e^{\color{red}{i\phi}} |cat+\rangle\right)$$

Remote State Preparation: Results

$2.2 < q_\phi$

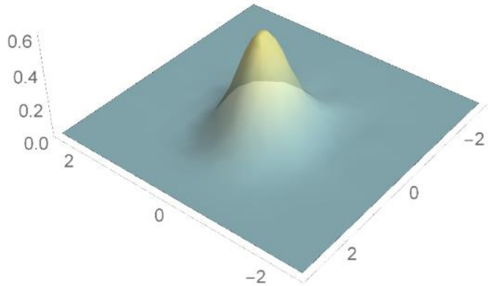

85,0%

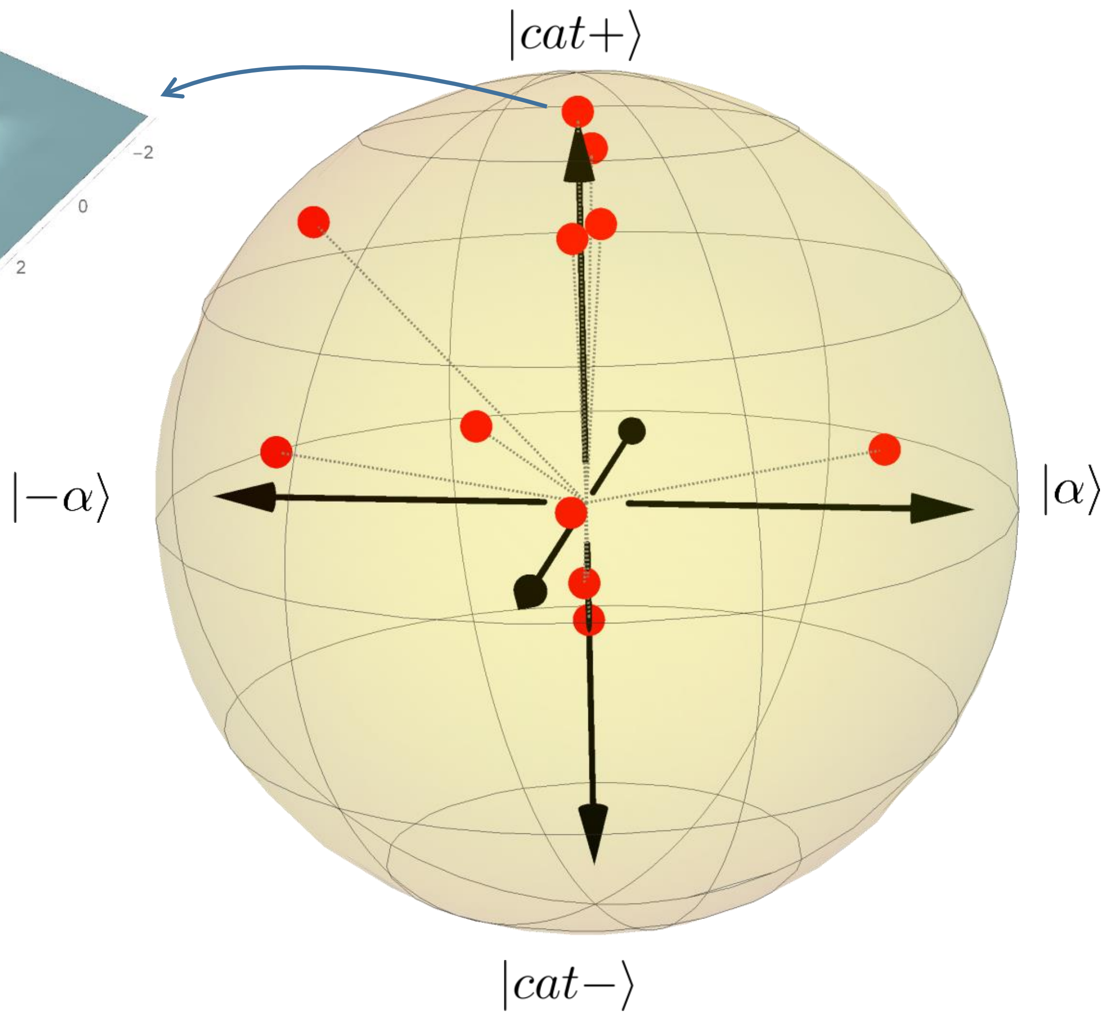

$$\frac{1}{\sqrt{N}}\left(|cat-\rangle + q_\phi e^{i\phi}\,|cat+\rangle\right)$$

Remote State Preparation: Results

$2.2 < q_\phi$

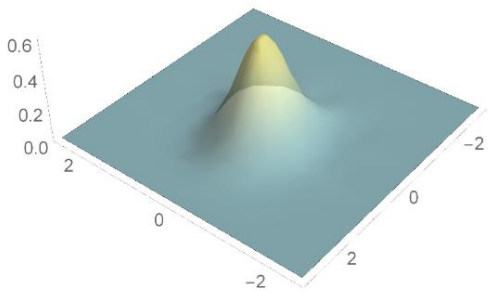

85,0%

$|cat+\rangle$

$|-\alpha\rangle$

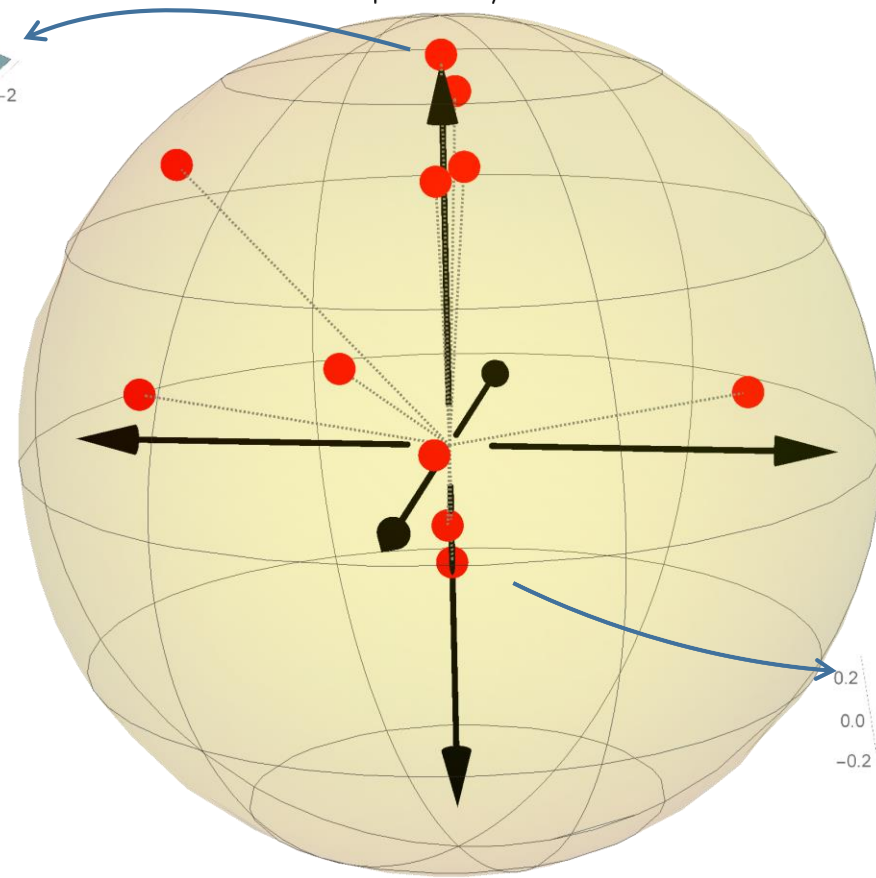

$|\alpha\rangle$

$-0.1 < q_\phi < 0.1$

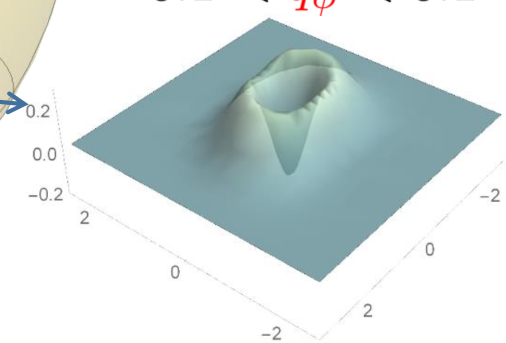

68,0%

$|cat-\rangle$

$$\frac{1}{\sqrt{N}}\left(|cat-\rangle + q_\phi e^{i\phi}\,|cat+\rangle\right)$$

Remote State Preparation: Results

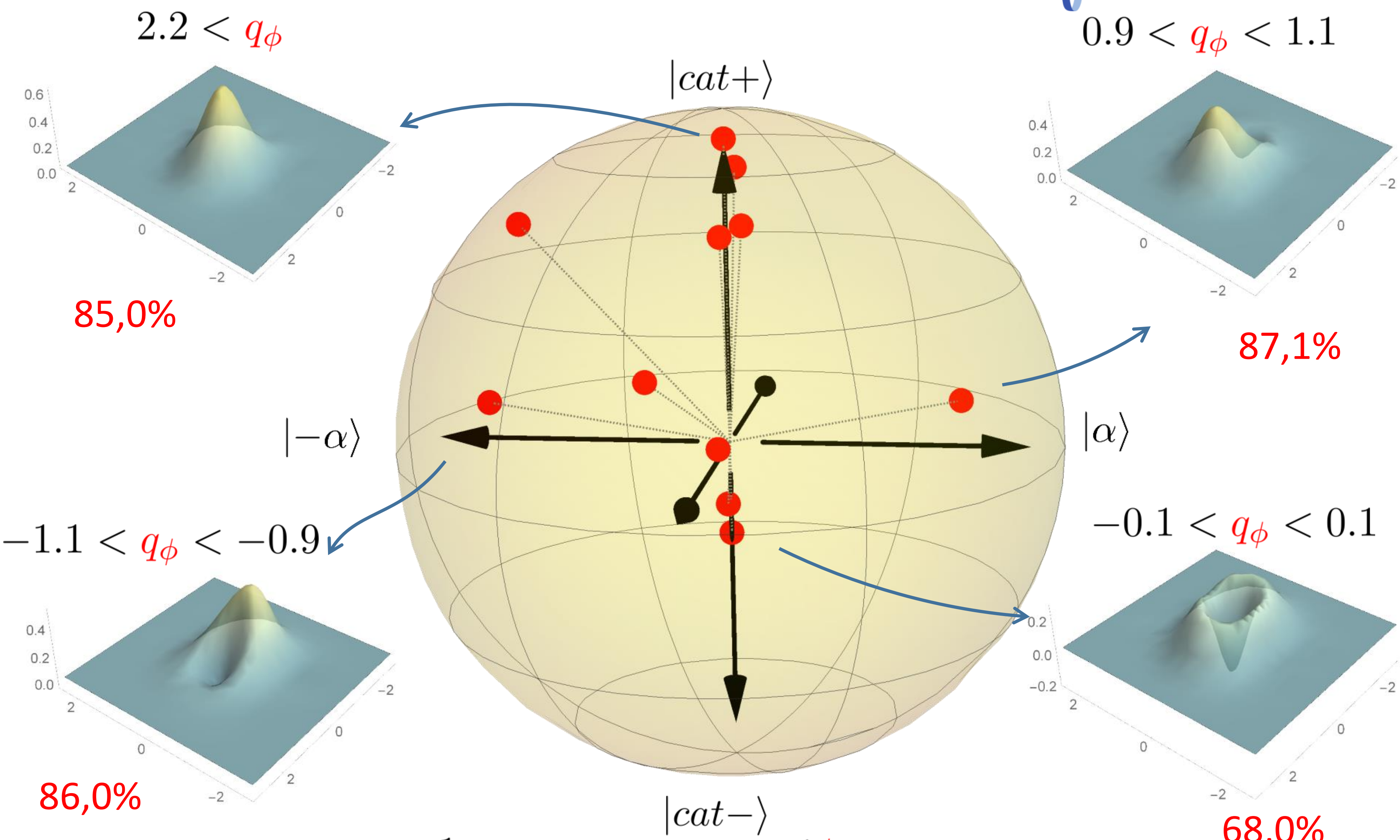

$$\frac{1}{\sqrt{N}}\left(|cat-\rangle + q_\phi e^{i\phi}\,|cat+\rangle\right)$$

H. Le Jeannic et.al. *In reviewing process*

Outline

I	Optical quantum state engineering	☑
II	Hybrid entanglement of light	☑
III	Remote state preparation of arbitrary CV qu-modes	☑
IV	Experimental demonstration of EPR steering	
V	Towards quantum teleportation from DV to CV	

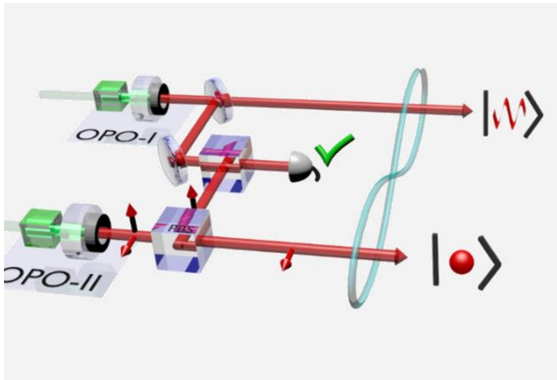

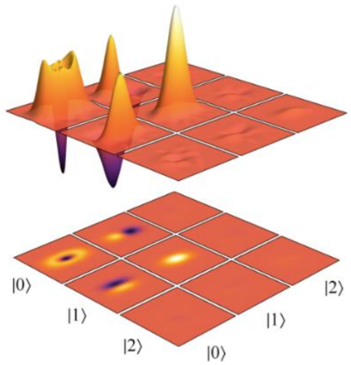

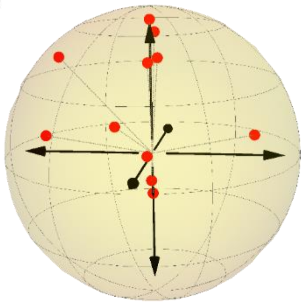

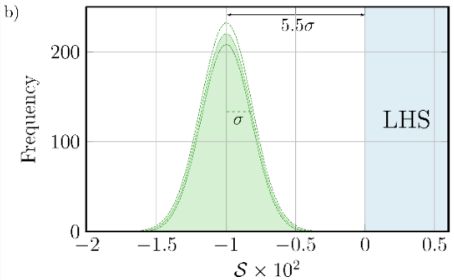

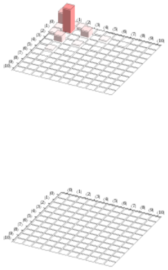

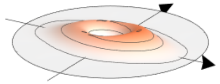

Einstein-Podolsky-Rosen Steering

- Bipartite scenario where local measurements on one party can change the state of the other party.

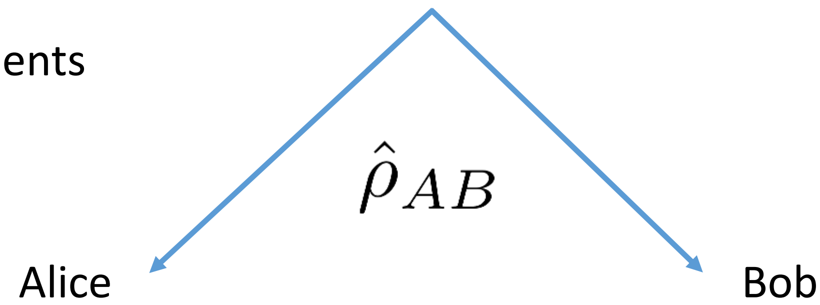

Detection of quantum entanglement when one of the parties performs uncharacterised measurements.

$$\{\text{Entangled}\} \supset \{\text{Violates steering inequality}\} \supset \{\text{Violates Bell inequality}\}$$

Fundamentally: Gives new insights on quantum separability.
Practically: Necessary to prove security of one-sided device independent protocols.

EPR Steering setup and settings

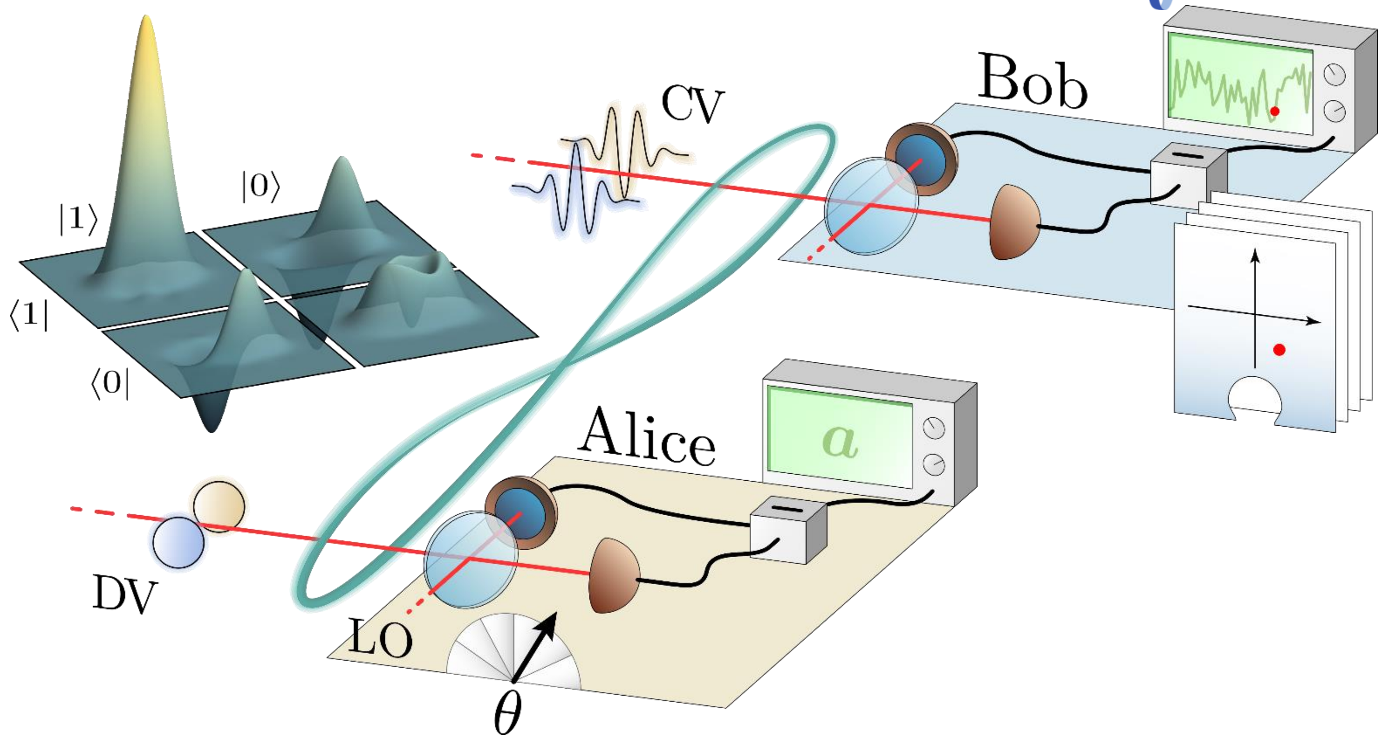

EPR Steering setup and settings

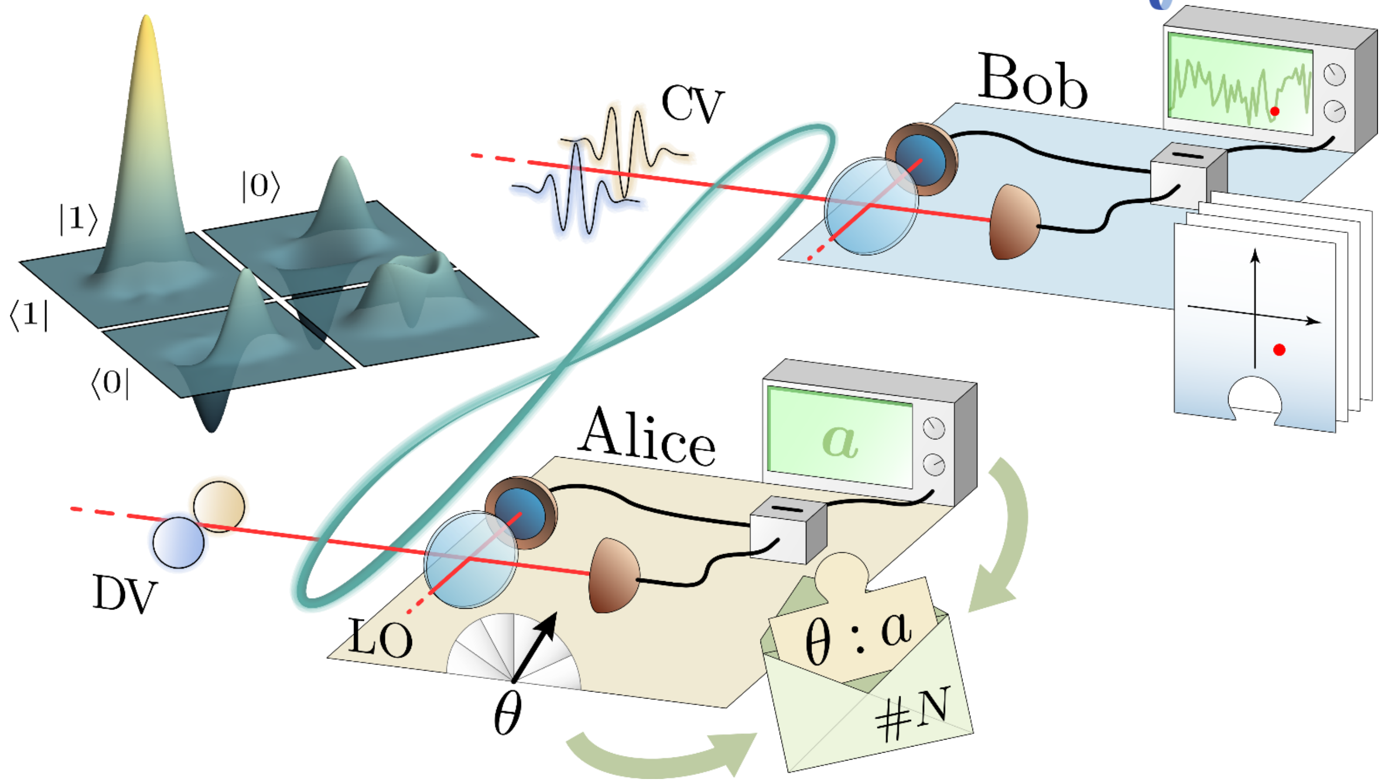

EPR Steering setup and settings

Laboratoire Kastler Brossel
Physique quantique et applications

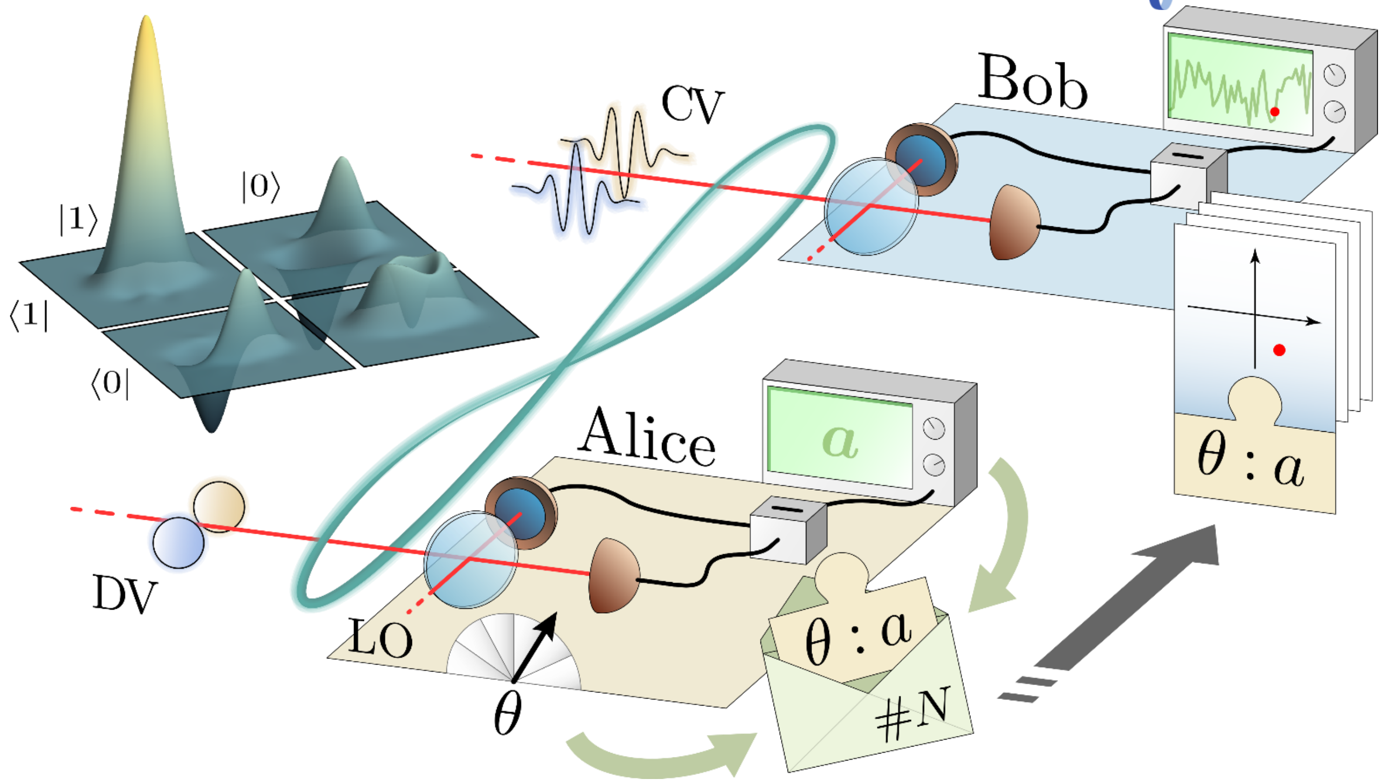

EPR Steering setup and settings

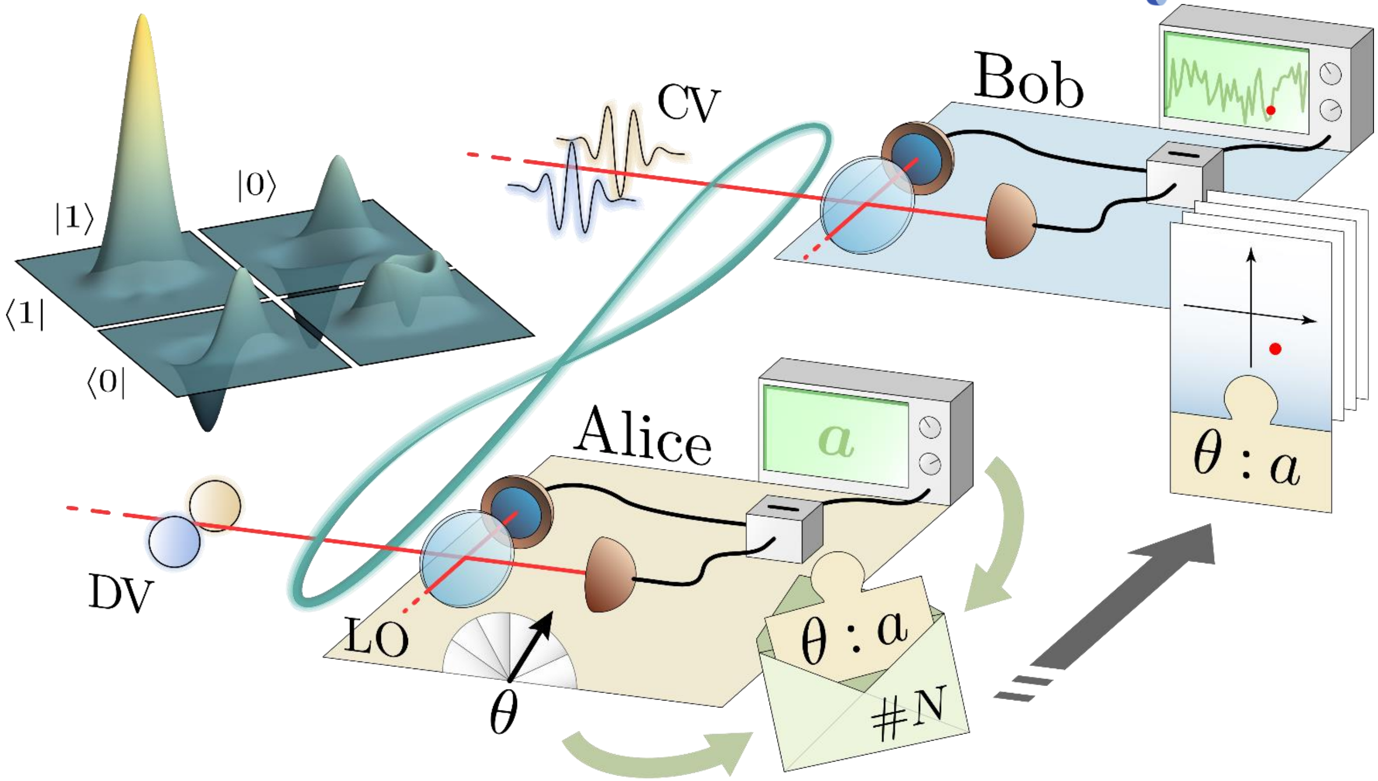

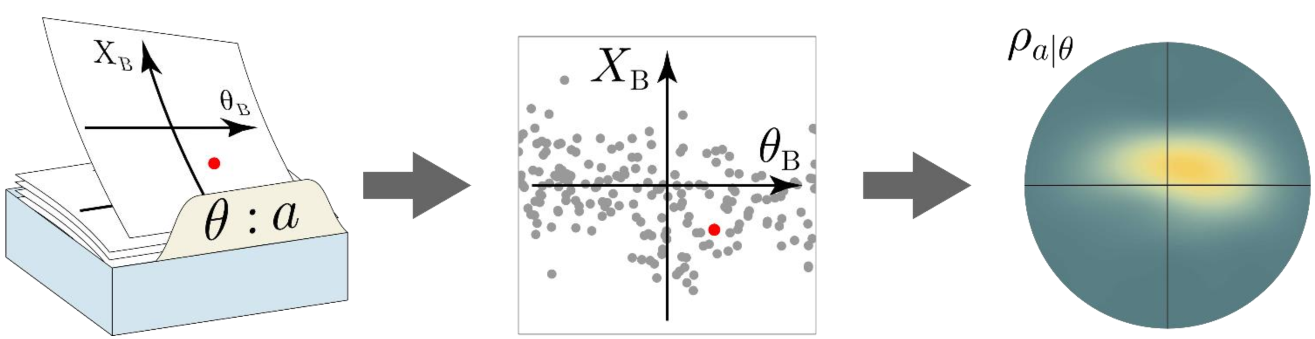

State measured on Bob's mode

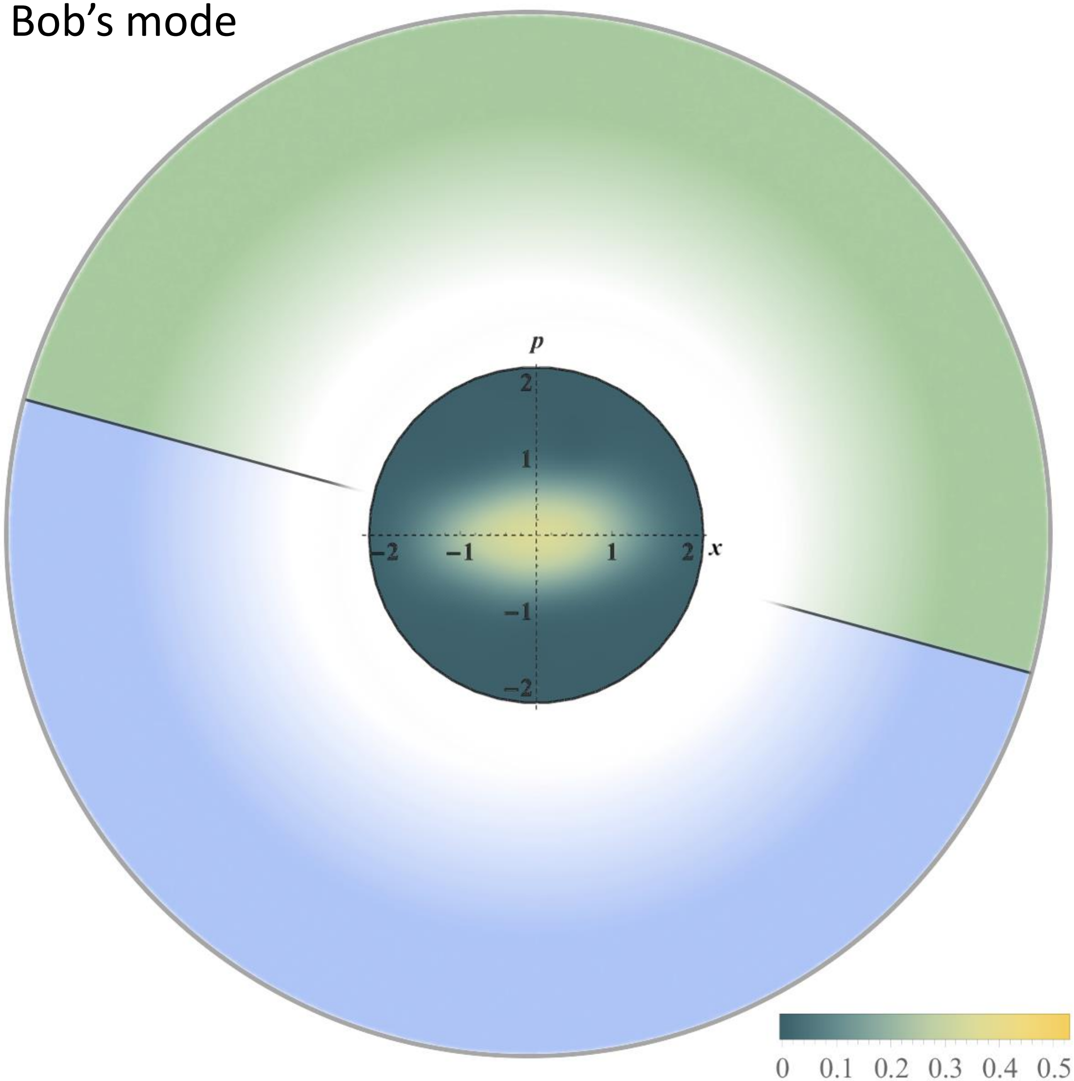

Einstein-Podolsky-Rosen Steering: Results

State measured on Bob's mode

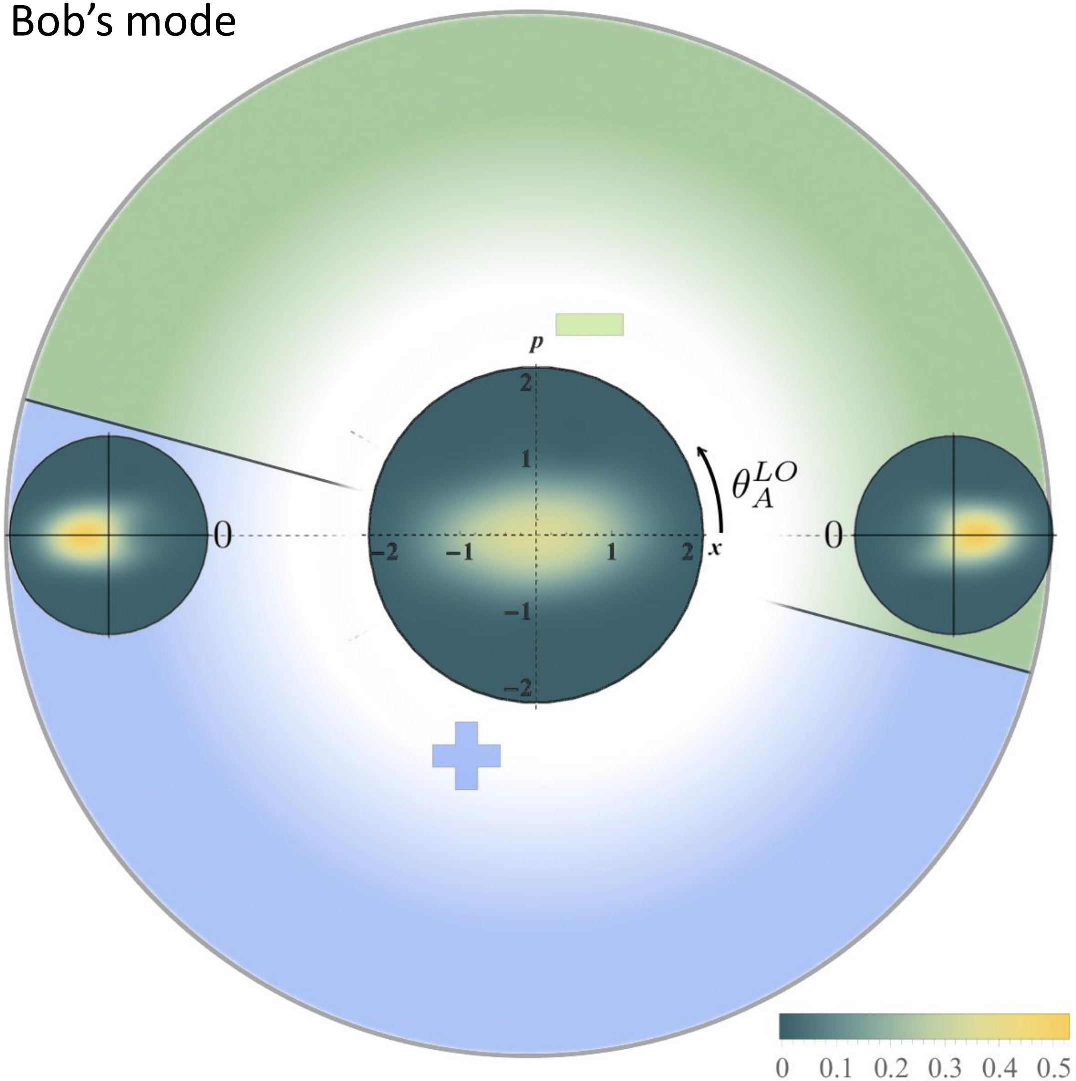

Einstein-Podolsky-Rosen Steering: Results

State measured on Bob's mode

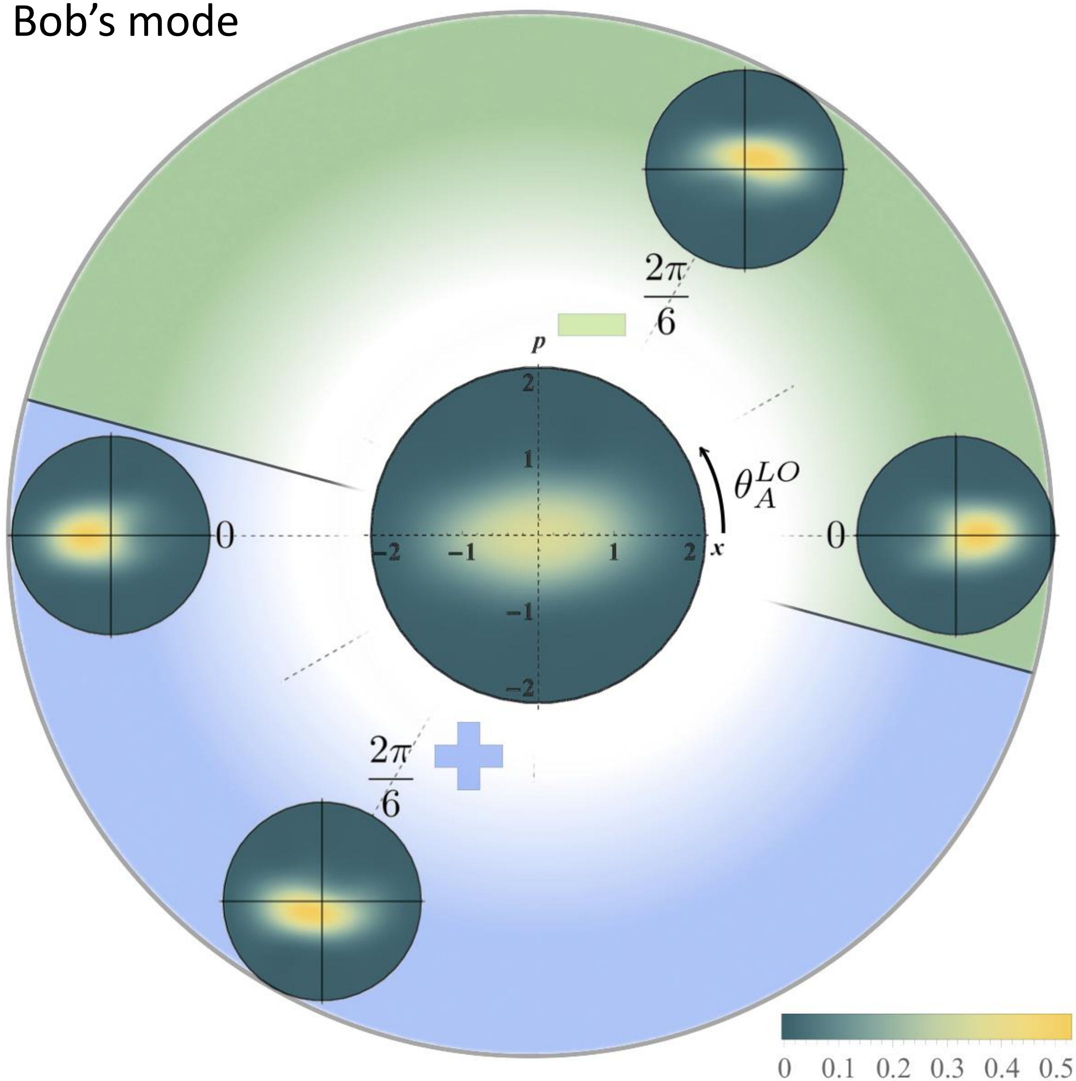

Einstein-Podolsky-Rosen Steering: Results

State measured on Bob's mode

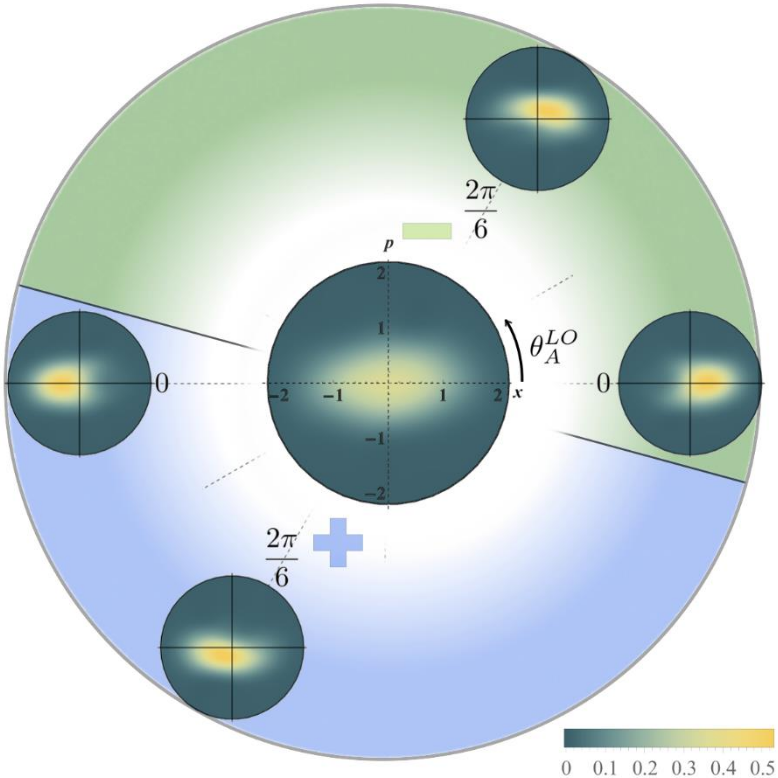

- How many measurements to see a violation?

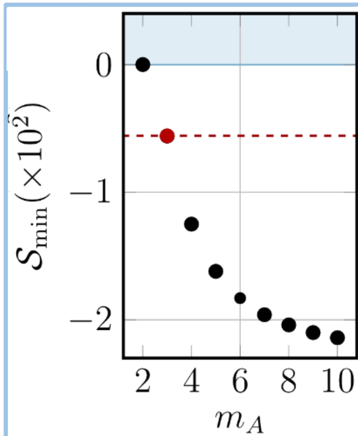

Einstein-Podolsky-Rosen Steering: Results

- How many measurements to see a violation?

State measured on Bob's mode

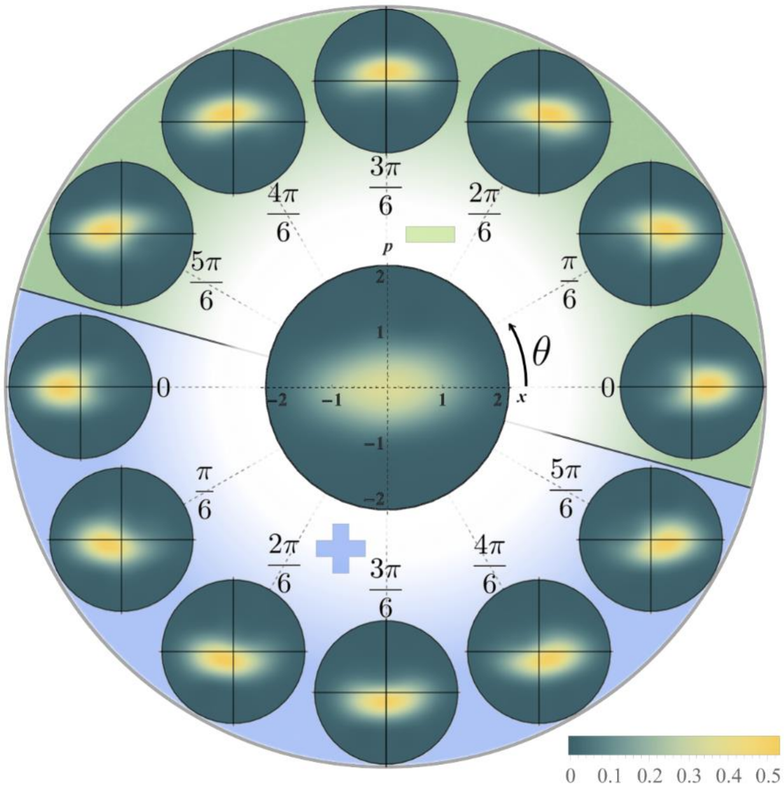

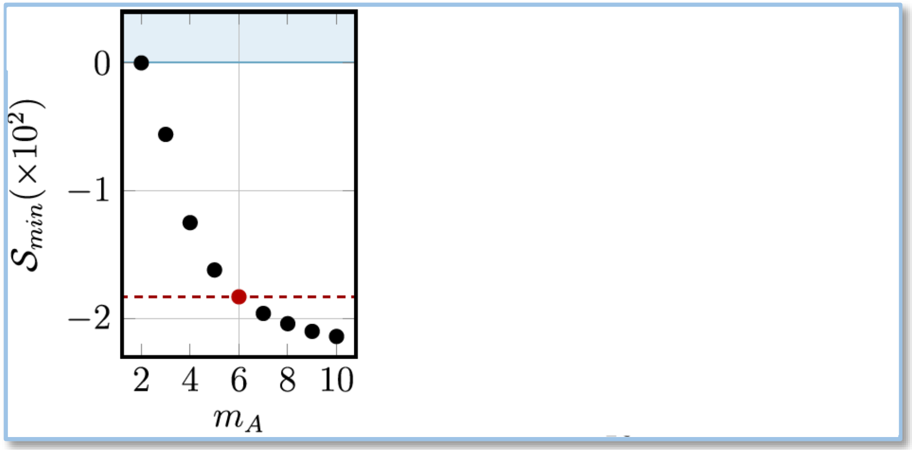

Einstein-Podolsky-Rosen Steering: Results

- How many measurements to see a violation?
- Adjusting the heralding ratio compensates for homodyne losses

State measured on Bob's mode

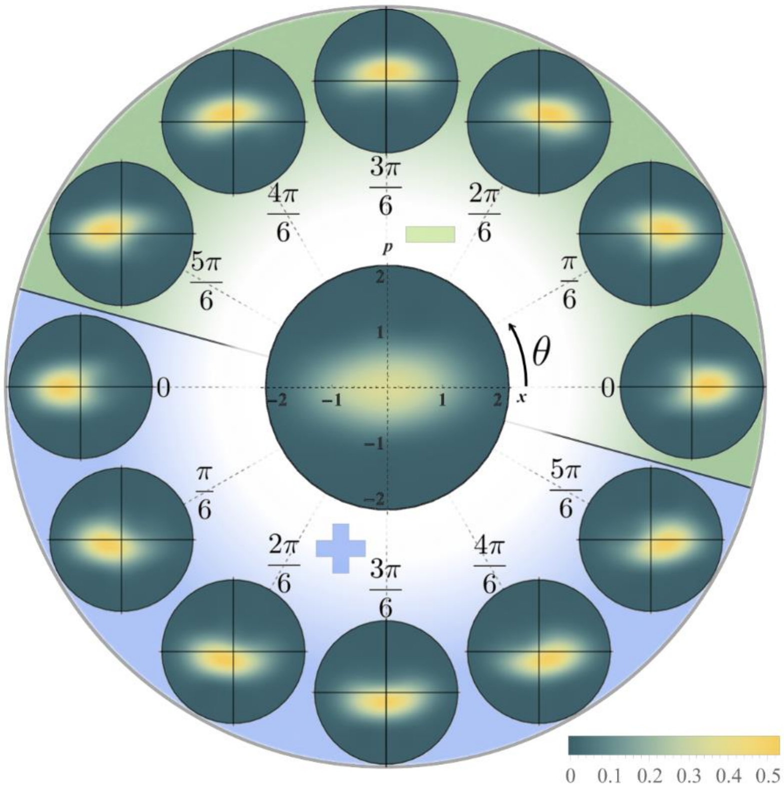

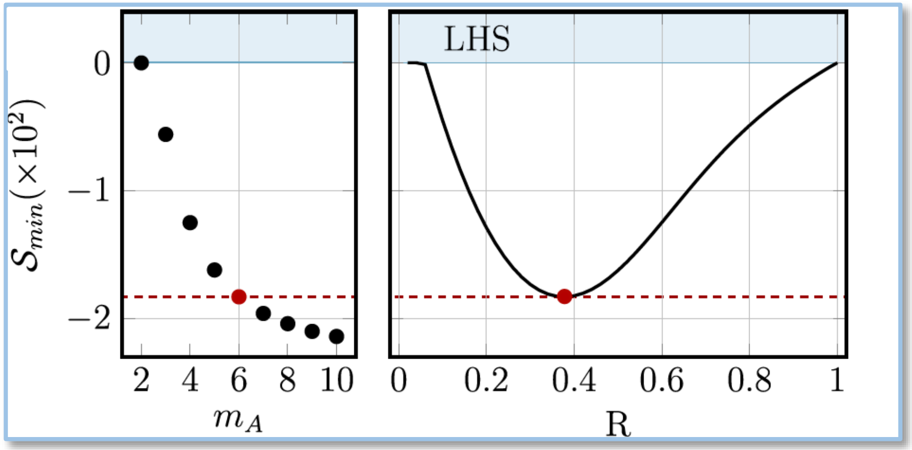

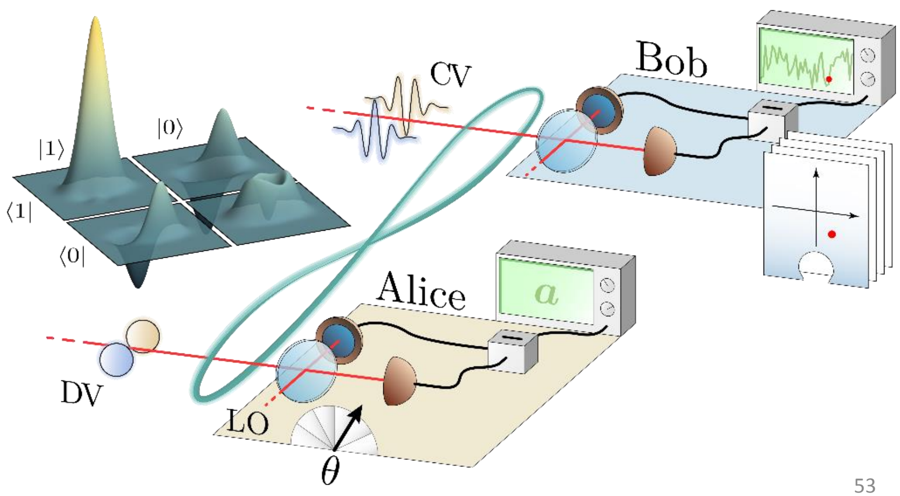

Einstein-Podolsky-Rosen Steering: Results

Laboratoire Kastler Brossel
Physique quantique et applications

State measured on Bob's mode

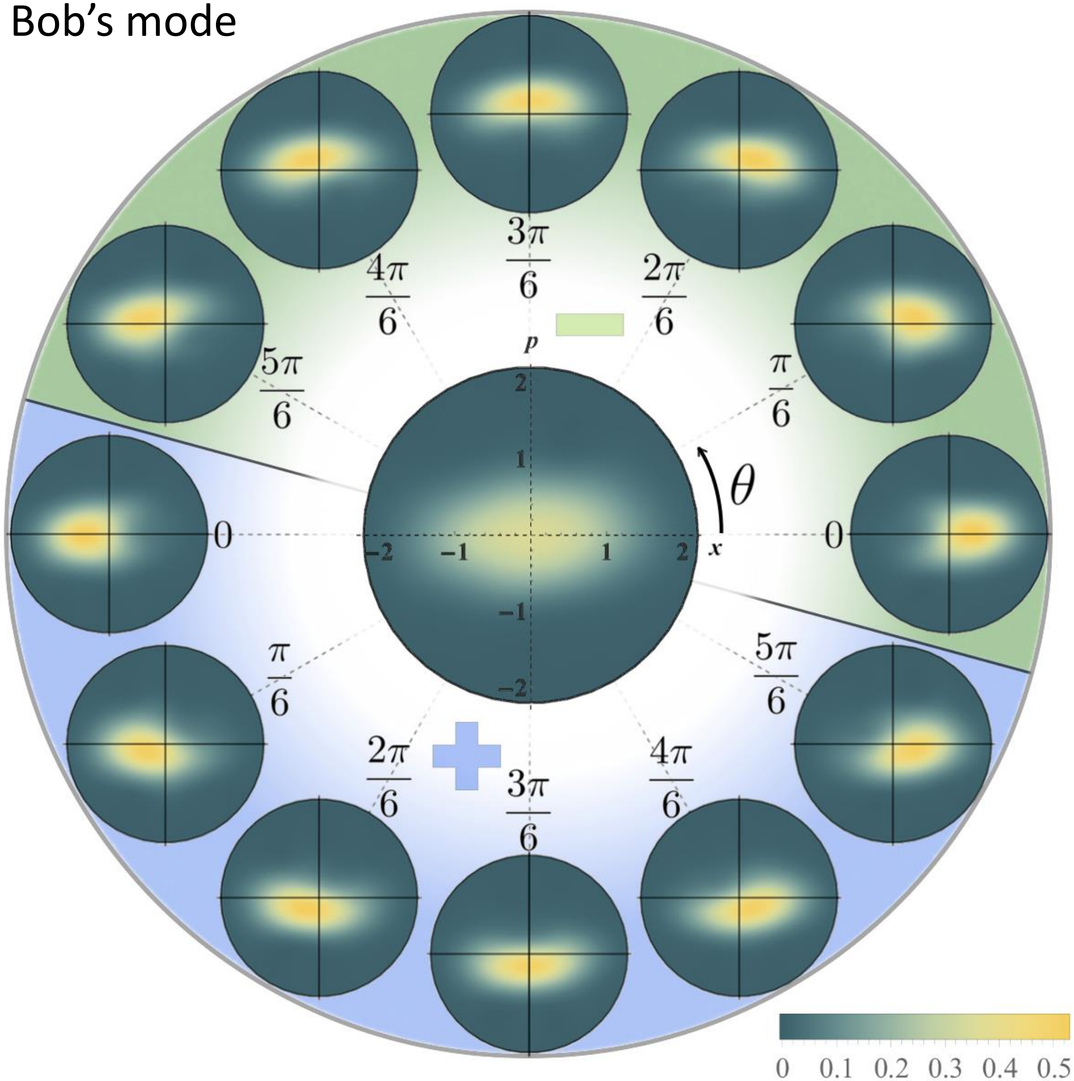

Demonstrating EPR Steering

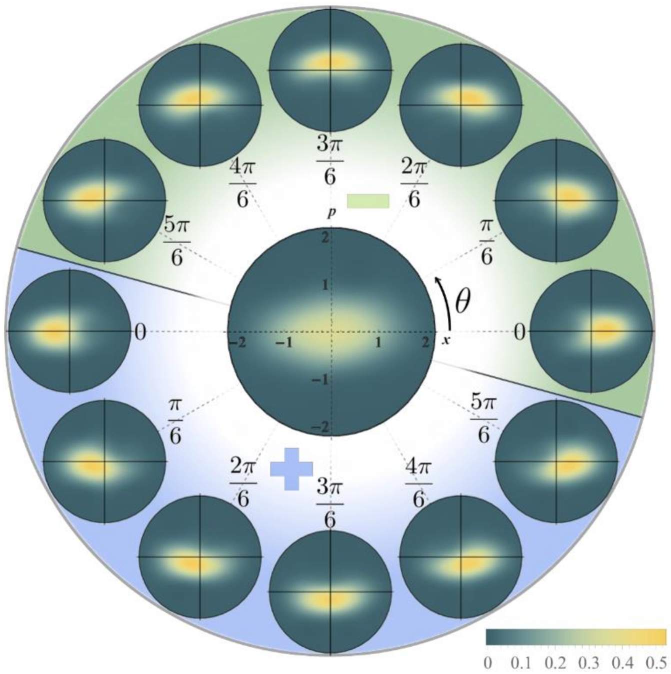

$$\{\rho_{\pm|\theta}\}$$

- Steerability ensured through EPR-steering inequality violation:

$$\sum_{\pm,\theta} Tr(F_{\pm|\theta}\rho_{\pm|\theta}) \geq 0$$

Demonstrating EPR Steering

Laboratoire Kastler Brossel
Physique quantique et applications

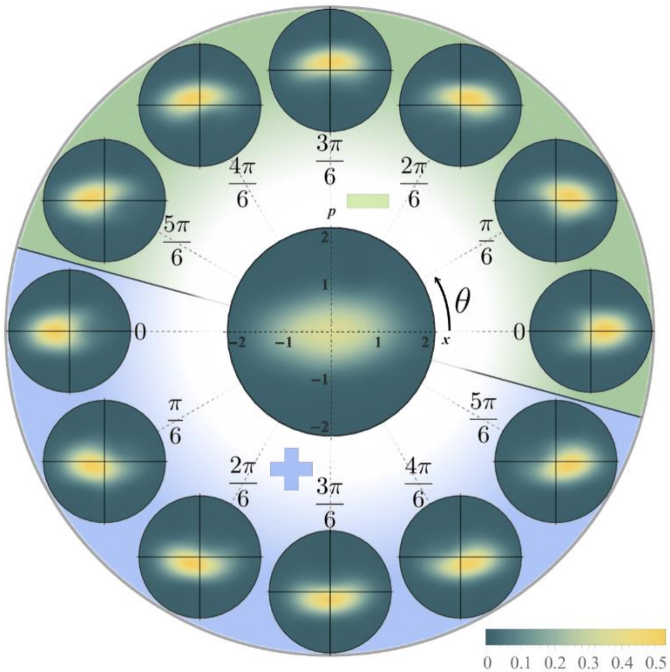

$$\{\rho_{\pm|\theta}\}$$

- Steerability ensured through EPR-steering inequality violation:

$$\sum_{\pm,\theta} Tr(F_{\pm|\theta}\rho_{\pm|\theta}) \geq 0$$

- Operators found through Semi-Definite-Programming.

Cavalcanti et. al. Rep.Prog.Phys. 80 (2017) 024001

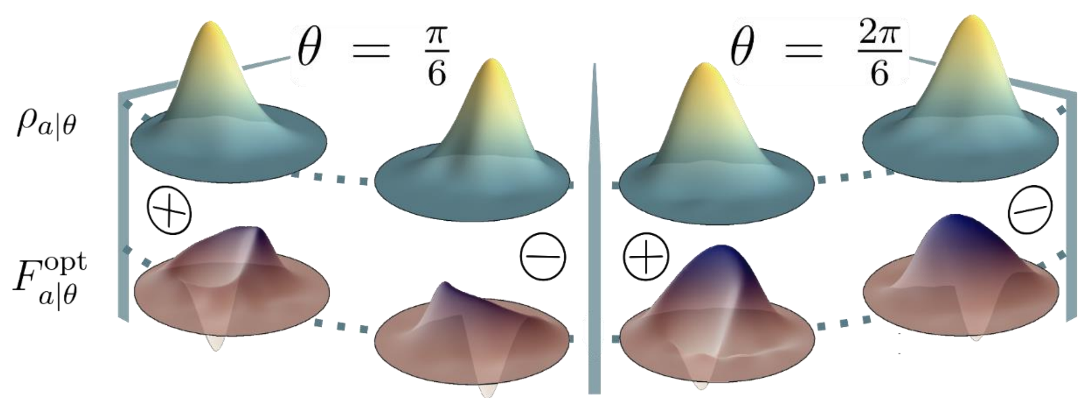

Demonstrating EPR Steering

Laboratoire Kastler Brossel
Physique quantique et applications

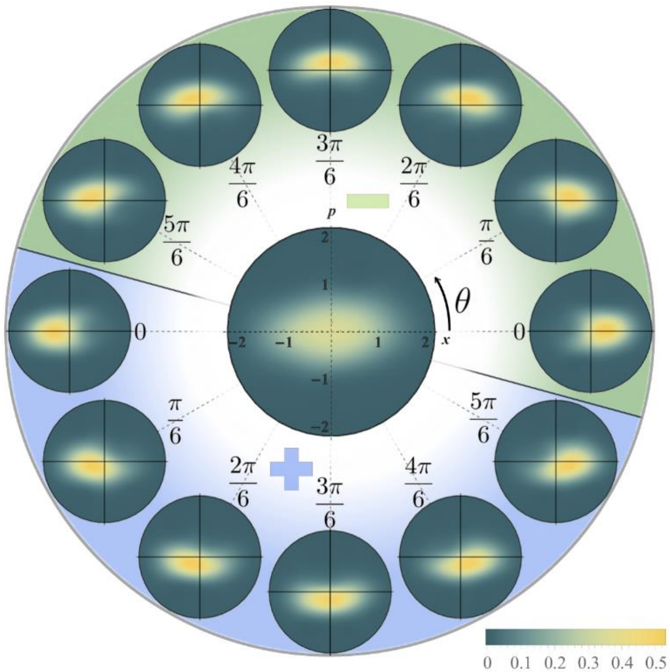

$$\{\rho_{\pm|\theta}\}$$

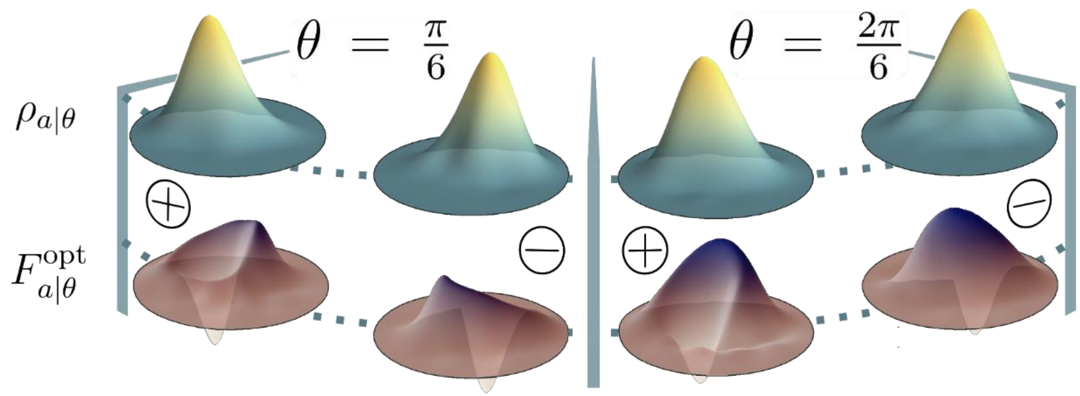

Access to the full assemblage through quantum tomography, operators are applied numerically

→ Any inequality violation proves EPR steering

→ Uncertainties introduced by tomography need to be carefully evaluated

$$\sum_{\pm,\theta} Tr(F_{\pm|\theta}\rho_{\pm|\theta}) \geq 0$$

Evaluating tomographic uncertainties

- Only tomographic error are considered as Alice is untrusted and the operators are applied numerically.

- Typically: Bootstrap method

$$\{x_N,\theta_N\}_N \longrightarrow \rho^{ML} \longrightarrow \left\{ \begin{array}{lllll} \{x_N^{(1)},\theta_N^{(1)}\}_N & \xrightarrow{ML} & \rho^{(1)} & \longrightarrow & Tr(\hat{F}\rho^{(1)}) \\ \{x_N^{(2)},\theta_N^{(2)}\}_N & \longrightarrow & \rho^{(2)} & \longrightarrow & Tr(\hat{F}\rho^{(2)}) \\ \vdots & & \vdots & & \vdots \\ \{x_N^{(M)},\theta_N^{(M)}\}_N & \longrightarrow & \rho^{(M)} & \longrightarrow & Tr(\hat{F}\rho^{(M)}) \end{array} \right.$$

$$\{Tr(\hat{F}\rho_N^{(M)})\}_M \longrightarrow < f >, Var(f), \ldots$$

Evaluating tomographic uncertainties

Laboratoire Kastler Brossel
Physique quantique et applications

- Only tomographic error are considered as Alice is untrusted and the operators are applied numerically.

- Typically: Bootstrap method

$$\{x_N,\theta_N\}_N \longrightarrow \rho^{ML} \longrightarrow \left\{ \begin{array}{lll} \{x_N^{(1)},\theta_N^{(1)}\}_N & \xrightarrow{ML} \rho^{(1)} & \longrightarrow Tr(\hat{F}\rho^{(1)}) \\ \{x_N^{(2)},\theta_N^{(2)}\}_N & \longrightarrow \rho^{(2)} & \longrightarrow Tr(\hat{F}\rho^{(2)}) \\ \vdots & \vdots & \vdots \\ \{x_N^{(M)},\theta_N^{(M)}\}_N & \longrightarrow \rho^{(M)} & \longrightarrow Tr(\hat{F}\rho^{(M)}) \end{array} \right.$$

$$\{Tr(\hat{F}\rho_N^{(M)})\}_M \longrightarrow < f >, Var(f), \ldots$$

$$\mathcal{S} = \sum_{\pm,\theta} Tr(F_{\pm|\theta}\rho_{\pm|\theta})$$

Repeat process 12 times

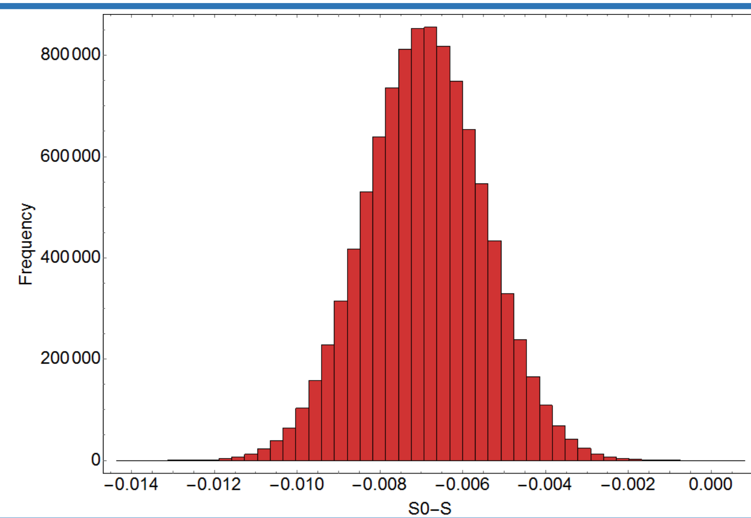

Evaluating tomographic uncertainties

- Only tomographic error are considered as Alice is untrusted and the operators are applied numerically.

- Typically: Bootstrap method

$$\{x_N, \theta_N\}_N \longrightarrow \rho^{ML} \longrightarrow \begin{cases} \{x_N^{(1)}, \theta_N^{(1)}\}_N \xrightarrow{ML} \rho^{(1)} \longrightarrow Tr(\hat{F}\rho^{(1)}) \\ \{x_N^{(2)}, \theta_N^{(2)}\}_N \longrightarrow \rho^{(2)} \longrightarrow Tr(\hat{F}\rho^{(2)}) \\ \vdots \qquad\qquad \vdots \qquad\qquad \vdots \\ \{x_N^{(M)}, \theta_N^{(M)}\}_N \longrightarrow \rho^{(M)} \longrightarrow Tr(\hat{F}\rho^{(M)}) \end{cases}$$

Assumption

$$\{Tr(\hat{F}\rho_N^{(M)})\}_M \longrightarrow < f >, Var(f), \ldots$$

- Unreliable results because finite number of measurements
- Can give negative eigenvalues
- Estimated state can be on the border of physical states

R. Blume-Kohout, **New Journal of Physics**, vol. 12, no. 4, p. 043034, 2010.
B. Jungnitsch, et.al.**,** **Physical Review Letters**, vol. 104, no. 21, p. 210401, 2010.
R. Blume-Kohout, **arXiv e-prints**: 1202.5270[quant-ph], 2012.

Evaluating tomographic uncertainties

- Only tomographic error are considered as Alice is untrusted and the operators are applied numerically.

- Typically: Bootstrap method

$$\{x_N,\theta_N\}_N \longrightarrow \rho^{ML} \longrightarrow \left\{ \begin{array}{lll} \{x_N^{(1)},\theta_N^{(1)}\}_N \xrightarrow{ML} \rho^{(1)} & \longrightarrow & Tr(\hat{F}\rho^{(1)}) \\ \{x_N^{(2)},\theta_N^{(2)}\}_N \longrightarrow \rho^{(2)} & \longrightarrow & Tr(\hat{F}\rho^{(2)}) \\ \vdots \qquad\qquad \vdots & & \vdots \\ \{x_N^{(M)},\theta_N^{(M)}\}_N \longrightarrow \rho^{(M)} & \longrightarrow & Tr(\hat{F}\rho^{(M)}) \end{array} \right.$$

Assumption

$$\{Tr(\hat{F}\rho_N^{(M)})\}_M \longrightarrow \; < f >,\, Var(f),\, \ldots$$

- Alternatively: Use only the likelihood function $\mathcal{L}(\rho) = \prod_N tr(\{x_N,\theta_N\}_N|\rho)$

Find the probability distribution $\mu(\mathcal{S}) = \frac{1}{c}\int \mathcal{L}(\rho)\delta(\mathcal{S}(\rho)-\mathcal{S})d\rho$

Metropolis-Hastings algorithm: Random walk biased on $\mathcal{L}(\rho)$

$$\{x_N,\theta_N\}_N \longrightarrow \mathcal{L}(\rho) \xrightarrow{MH} \mu(\mathcal{S}) \longrightarrow \; < \mathcal{S} >,\, Var(\mathcal{S}),\, \ldots$$

P. Faist and R. Renner, **Physical Review Letters**, vol. 117, July 2016.

Evaluating tomographic uncertainties

Laboratoire Kastler Brossel
Physique quantique et applications

$$\{x_N, \theta_N\}_N \longrightarrow \mathcal{L}(\rho) \xrightarrow{MH} \mu(\mathcal{S}) \longrightarrow <\mathcal{S}>, Var(\mathcal{S}), \ldots$$

Time-Consuming, especially for 12 iterations -> 1 month for 12*10000 points

Is it worth it?

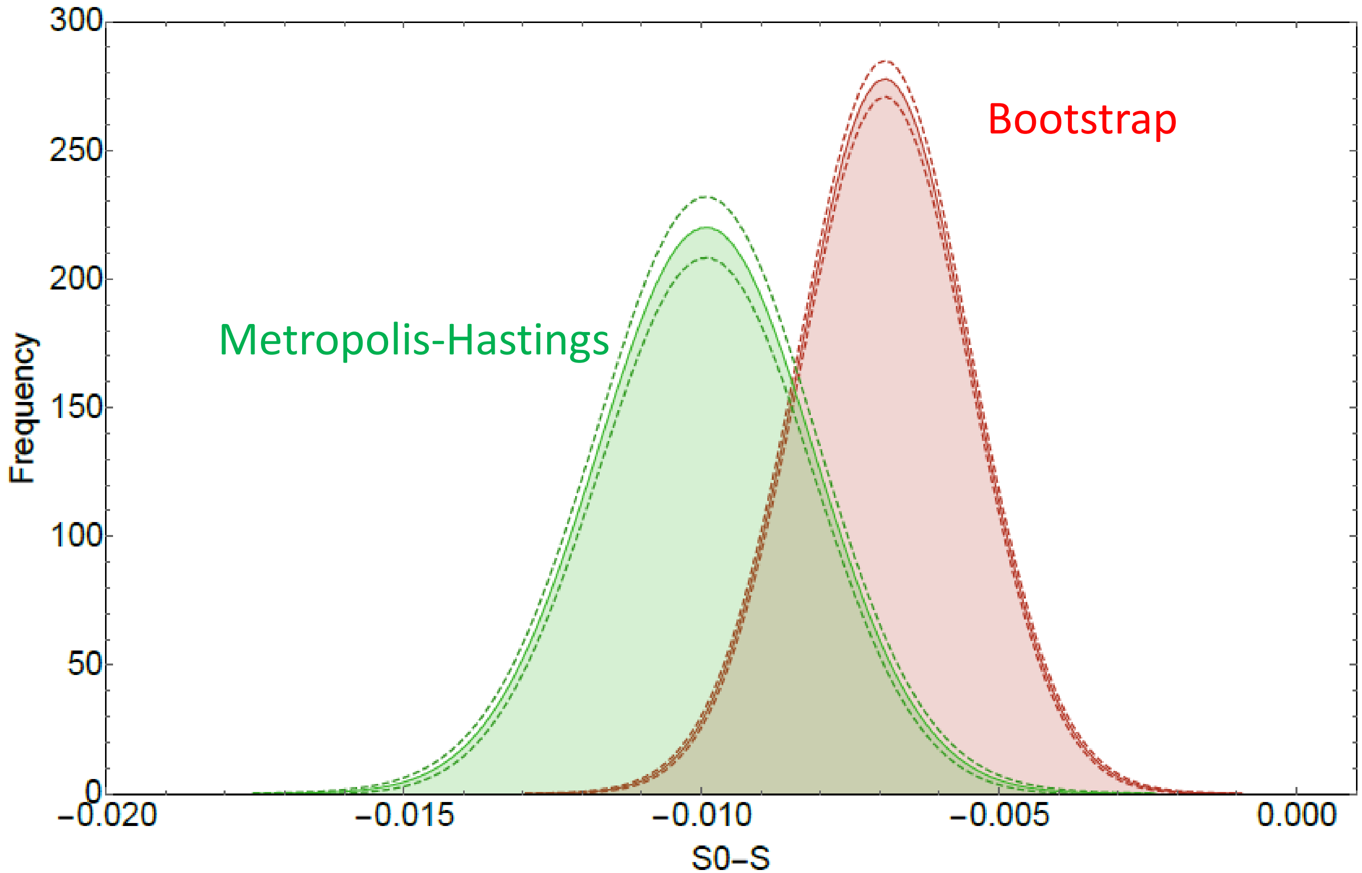

Demonstrating EPR Steering

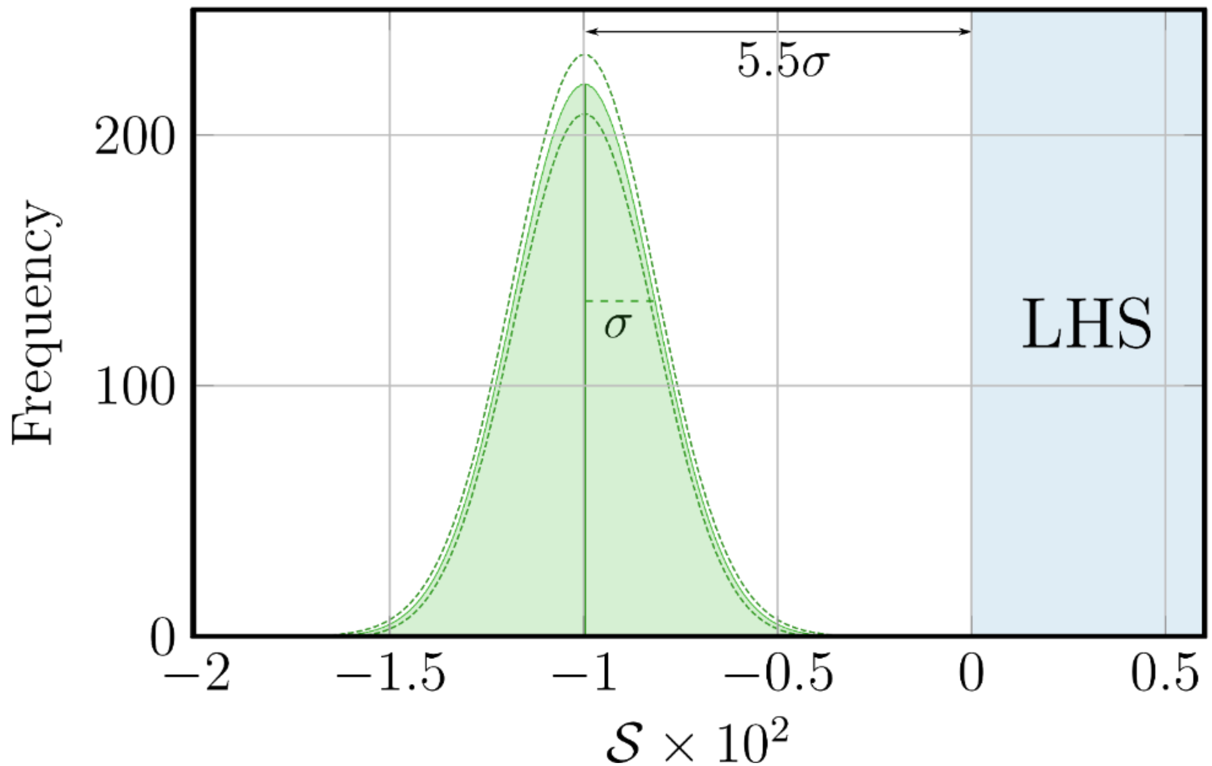

- Distance to the local bound > 5 std. Deviation for optimal steering inequality.

Outline

I	Optical quantum state engineering	☑
II	Hybrid entanglement of light	☑
III	Remote state preparation of arbitrary CV qu-modes	☑
IV	Experimental demonstration of EPR steering	☑
V	Towards quantum teleportation from DV to CV	

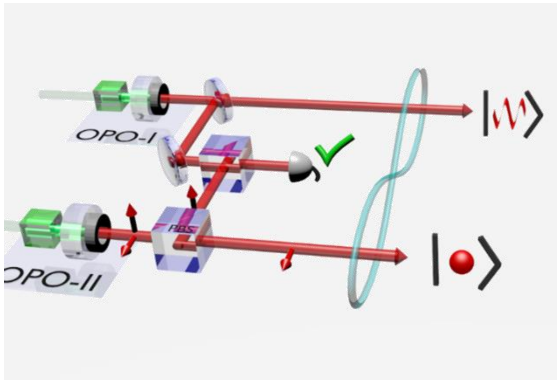

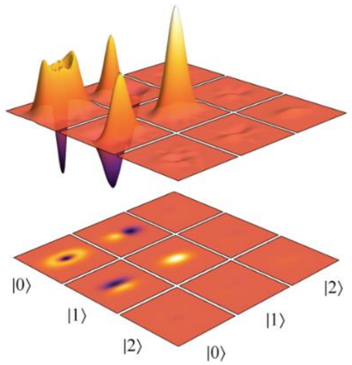

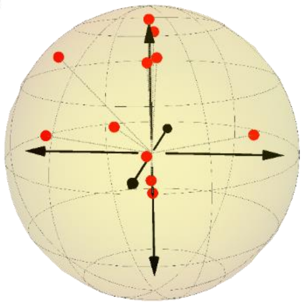

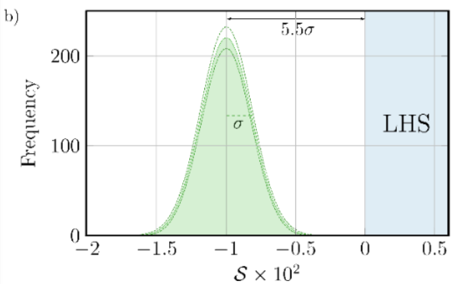

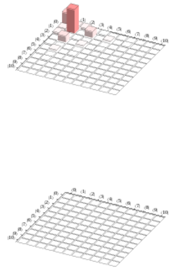

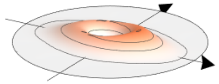

Quantum teleportation

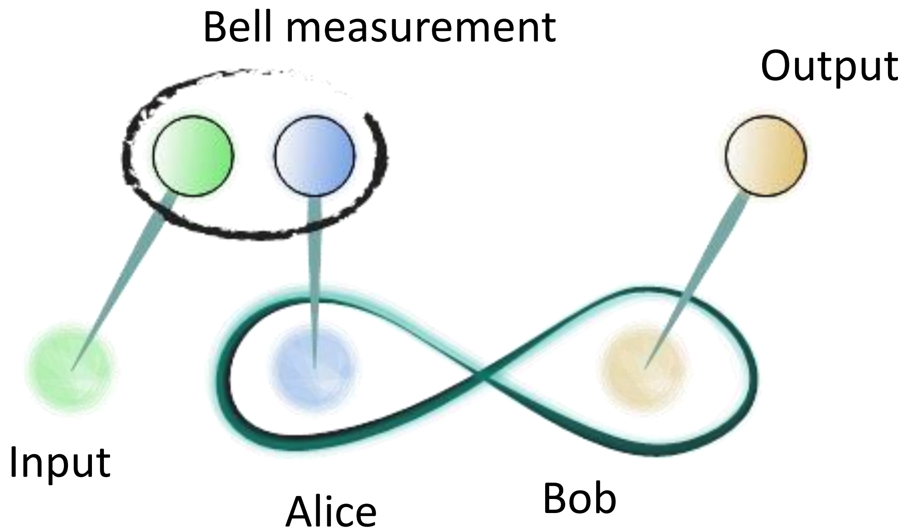

Applications:

- Local quantum computing
- Quantum repeaters (via entanglement swapping)
- Quantum signal converter (via hybrid entanglement)

Quantum teleportation: DV vs CV

	Efficiency	**Fidelity**
Discrete-variable	• Limited to 50% for single-mode systems because of undistinguishability of Bell states. • Different degrees of freedom, ancillary qubits or hybrid schemes are possible solutions.	• Up to 100% Record in passive protocols: 95% Record for active protocols: 90%
Continuous-variable	• Asymptotically 100% using homodyne tomography. • Non orthogonality of coherent states bounds the success probability of the protocol.	• In principle 100% However strongly limited by the amount of squeezing available in practice.

Quantum teleportation: DV vs CV

	Efficiency	Fidelity
Discrete-variable	• Limited to 50% for single-mode systems because of undistinguishability of Bell states. • Different degrees of freedom, ancillary qubits or hybrid schemes are possible solutions.	• Up to 100% Record in passive protocols: 95% Record for active protocols: 90%
Continuous-variable	• Asymptotically 100% using homodyne tomography. • Non orthogonality of coherent states bounds the success probability of the protocol.	• In principle 100% However strongly limited by the amount of squeezing available in practice.

Examples of hybrid approach:

- High-fidelity teleportation of continuous-variable quantum states using delocalized single photons. U. L. Andersen *et.al.* Physical Review Letters **111**, 050504 (2013)

- Deterministic quantum teleportation of photonic quantum bits by a hybrid technique. S. Takeda *et.al.* Nature **500,** 315-318 (2013).

DV to CV converter

Transfer information from DV to CV encoding

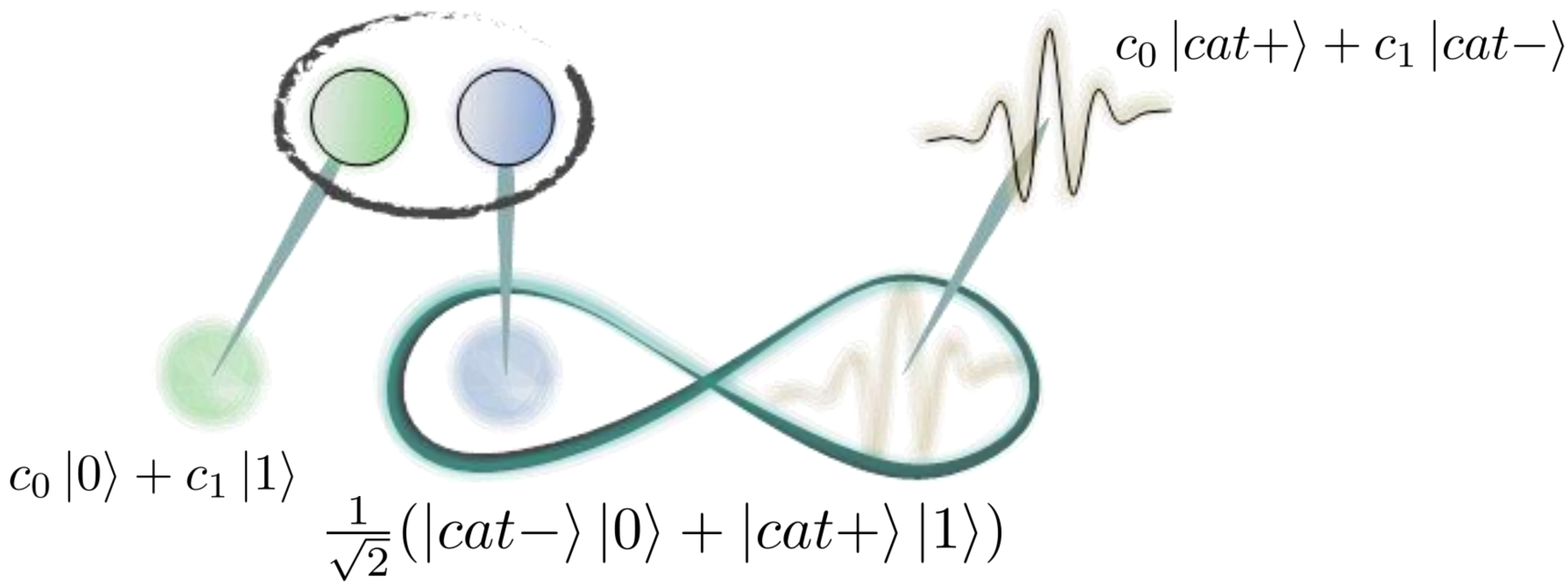

DV to CV converter

After mixing Input with Alice's mode on a 50/50 beam splitter:

$$
\begin{aligned}
|0\rangle_I |0\rangle_A \tfrac{c_0}{\sqrt{2}} |cat-\rangle_B &+ |0\rangle_I |1\rangle_A \left(\tfrac{c_1}{2} |cat-\rangle_B + \tfrac{c_0}{2} |cat+\rangle_B\right) \\
&+ |1\rangle_I |0\rangle_A \left(\tfrac{c_1}{2} |cat-\rangle_B - \tfrac{c_0}{2} |cat+\rangle_B\right) \\
&- |0\rangle_I |2\rangle_A \tfrac{c_1}{2} |cat+\rangle_B \\
&+ |2\rangle_I |0\rangle_A \tfrac{c_1}{2} |cat+\rangle_B
\end{aligned}
$$

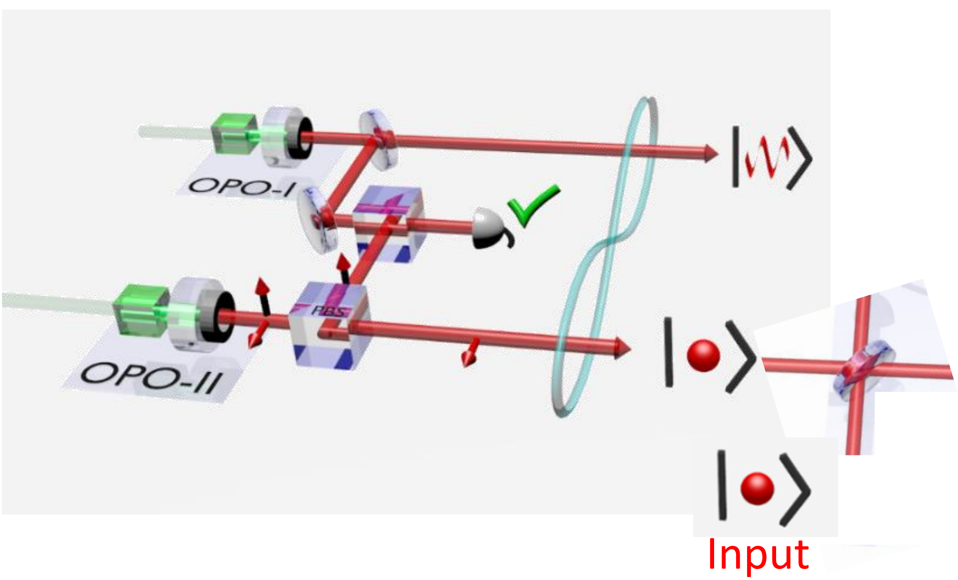

DV to CV converter

After mixing Input with Alice's mode on a 50/50 beam splitter:

$$
\begin{aligned}
&|0\rangle_I |0\rangle_A \tfrac{c_0}{\sqrt{2}} |cat-\rangle_B + |0\rangle_I |1\rangle_A \left(\boxed{\tfrac{c_1}{2} |cat-\rangle_B + \tfrac{c_0}{2} |cat+\rangle_B}\right) \quad \text{Qu-bit \#1} \\
&+ |1\rangle_I |0\rangle_A \left(\boxed{\tfrac{c_1}{2} |cat-\rangle_B - \tfrac{c_0}{2} |cat+\rangle_B}\right) \quad \text{Qu-bit \#2} \\
&- |0\rangle_I |2\rangle_A \tfrac{c_1}{2} |cat+\rangle_B \\
&+ |2\rangle_I |0\rangle_A \tfrac{c_1}{2} |cat+\rangle_B
\end{aligned}
$$

Measurement needed: $|1\rangle\langle 1|_{A/I}$

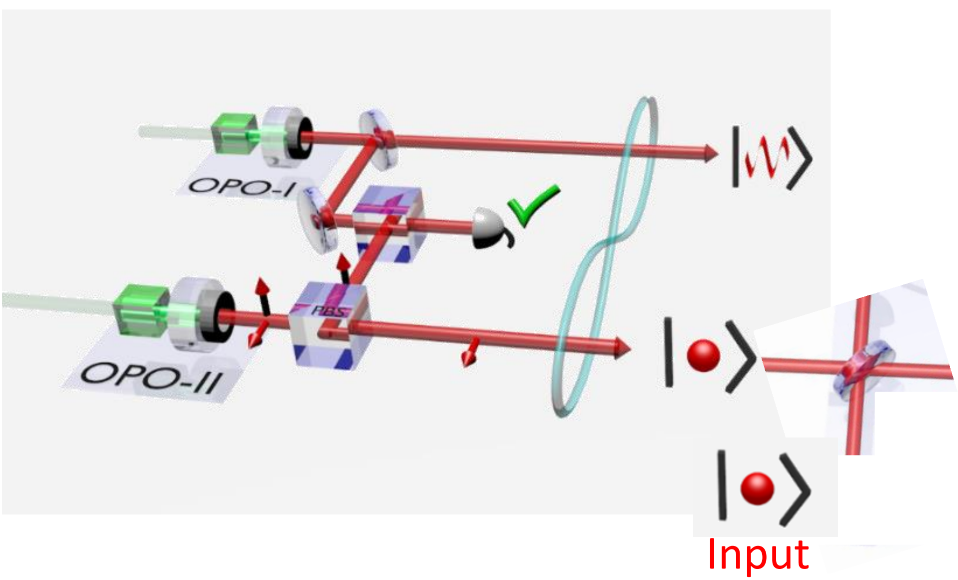

DV to CV converter

Laboratoire Kastler Brossel
Physique quantique et applications

After mixing Input with Alice's mode on a 50/50 beam splitter:

$$\cancel{|0\rangle_I |0\rangle_A \frac{c_0}{\sqrt{2}} |cat-\rangle_B} + |0\rangle_I |1\rangle_A \left(\boxed{\frac{c_1}{2} |cat-\rangle_B + \frac{c_0}{2} |cat+\rangle_B}\right) \text{ Qu-bit \#1}$$

$$+ |1\rangle_I |0\rangle_A \left(\boxed{\frac{c_1}{2} \cancel{|cat-\rangle_B - \frac{c_0}{2} |cat+\rangle_B}}\right) \text{ Qu-bit \#2}$$

$$\cancel{- |0\rangle_I |2\rangle_A \frac{c_1}{2} |cat+\rangle_B}$$

$$\cancel{+ |2\rangle_I |0\rangle_A \frac{c_1}{2} |cat+\rangle_B}$$

Measurement implemented: $|1\rangle \langle 1|_A$

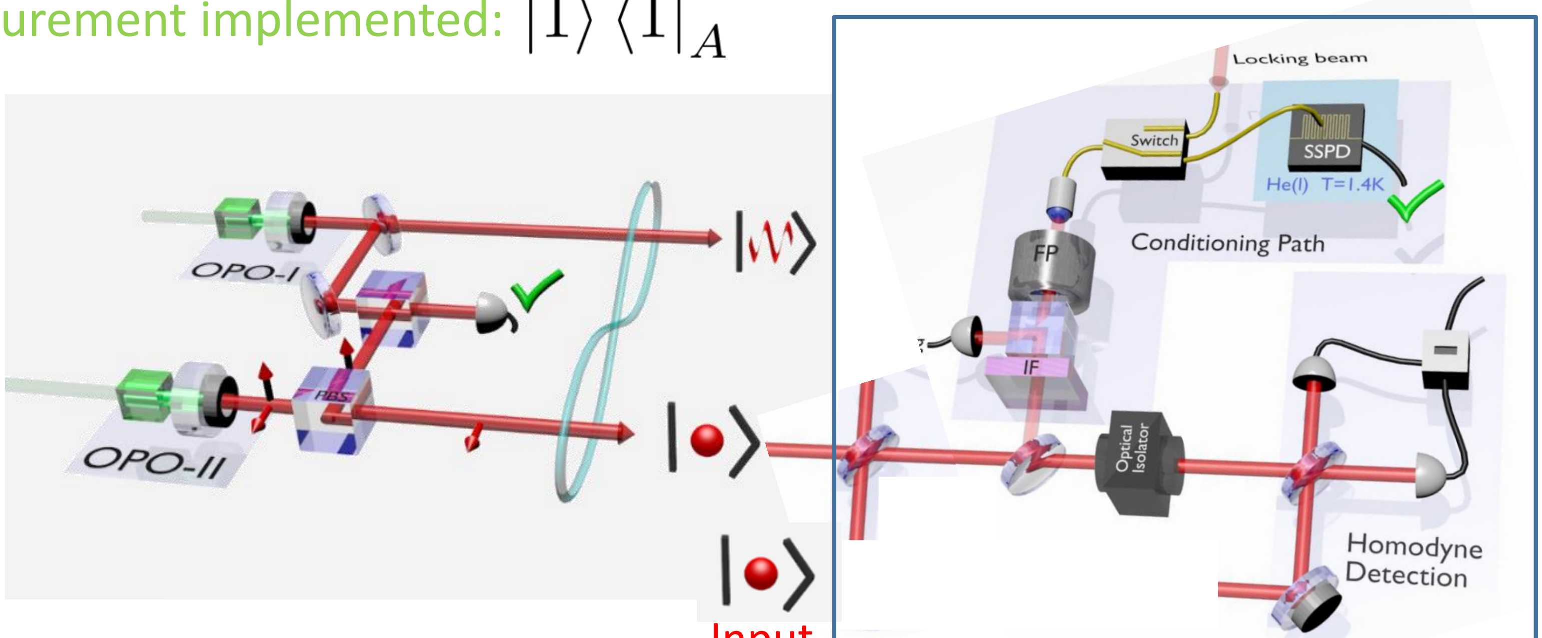

Bell measurement

DV to CV converter

Our implementation:

- Passive teleportation
- A single Bell measurement is implemented: < 25% efficiency
- Quantum signal converter (via hybrid entanglement)
- Use of attenuated coherent state as input

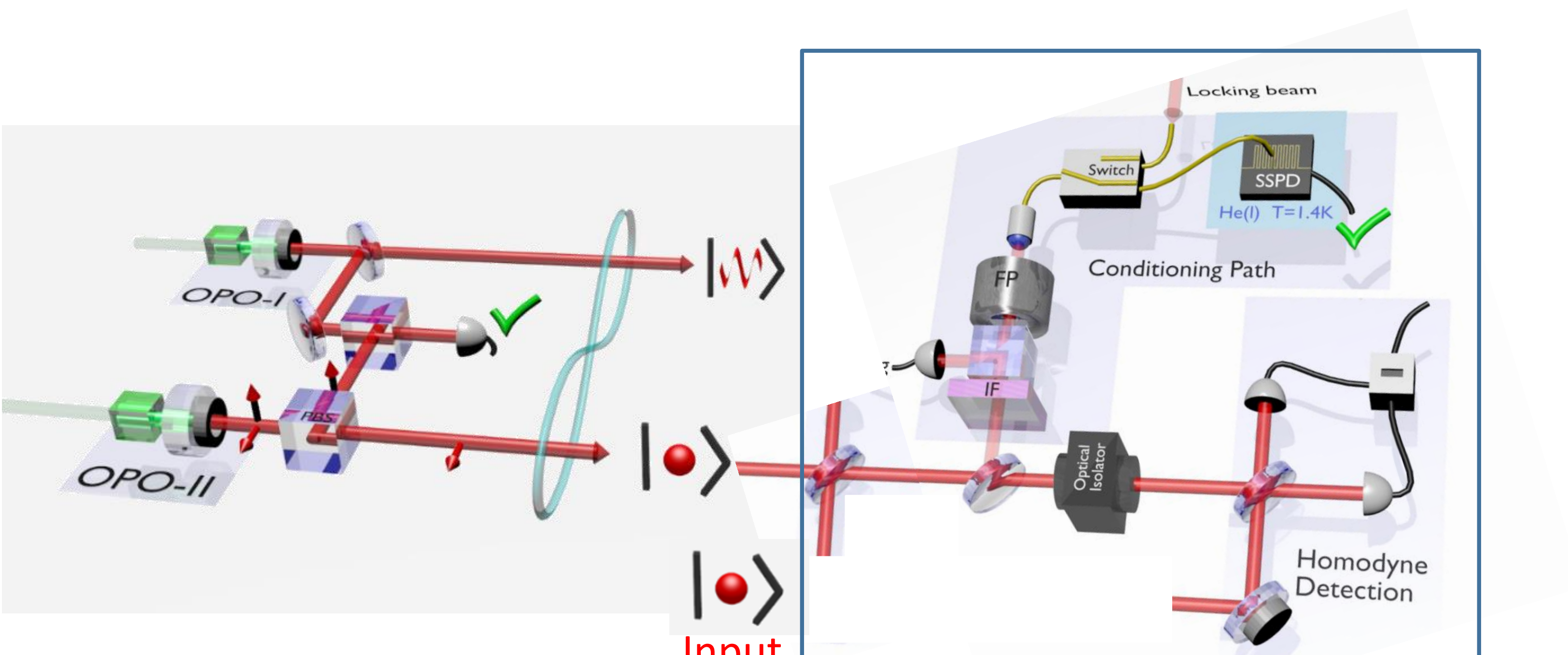

Bell measurement

DV to CV converter: Expected performance

Laboratoire Kastler Brossel
Physique quantique et applications

Fidelity of teleported state with target state: $c_0 \left|cat+\right\rangle + c_1 \left|cat-\right\rangle$

Ideal case

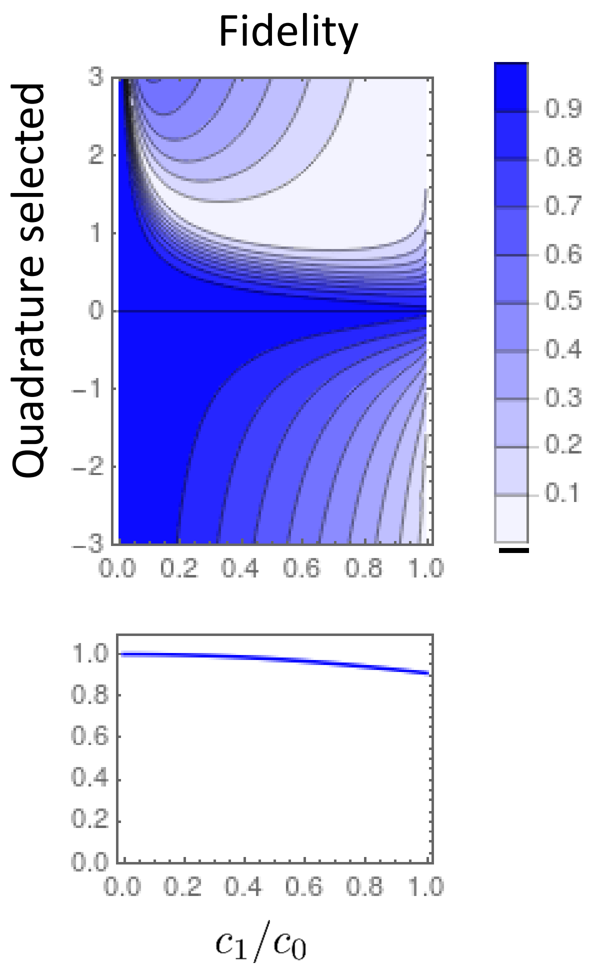

With (pessimistic) losses

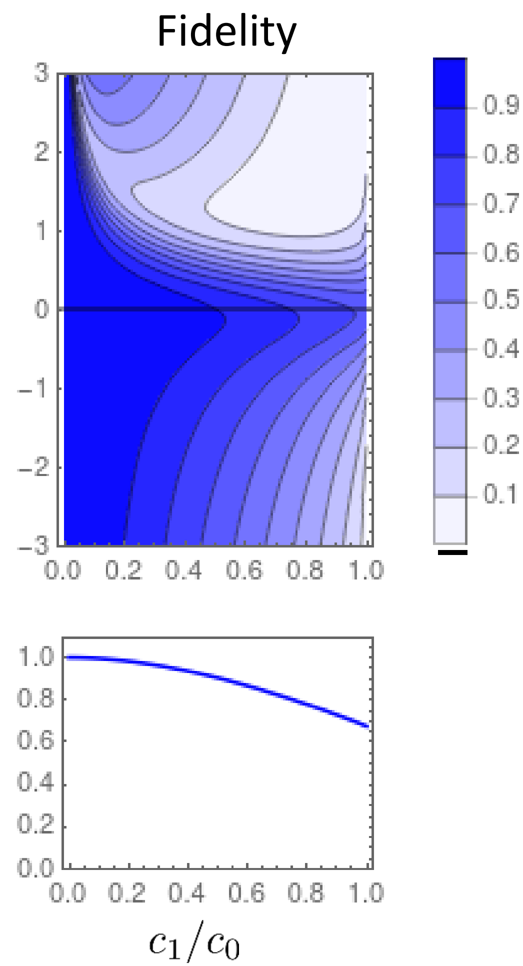

DV to CV converter: Teleported states

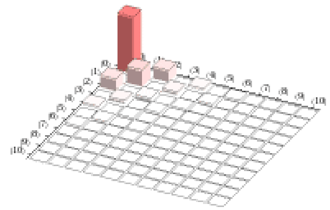

Teleported Qu-mode with pessimistic losses

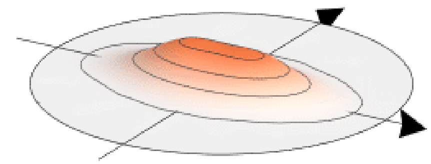

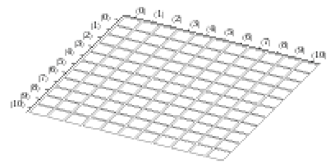

DV to CV converter: Teleported states

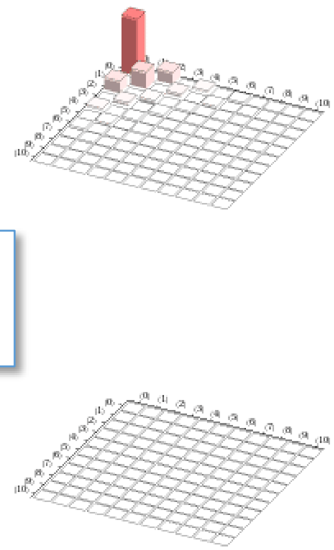

Teleported Qu-mode with pessimistic losses

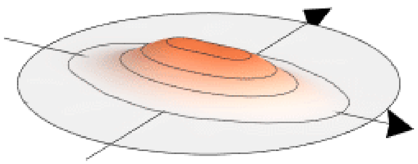

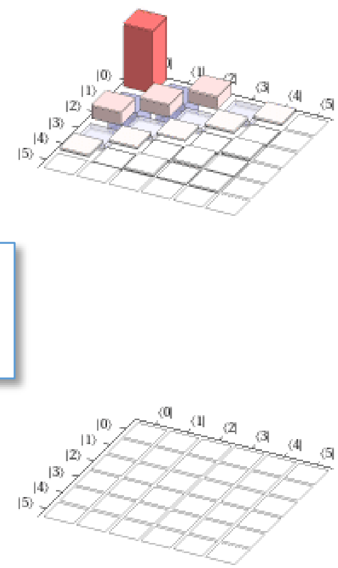

Teleported Qu-mode with pessimistic losses + Coherent state as input

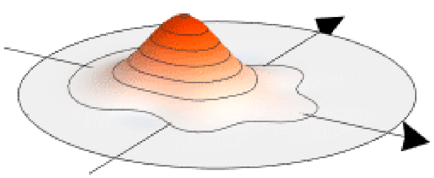

DV to CV converter: preliminary results

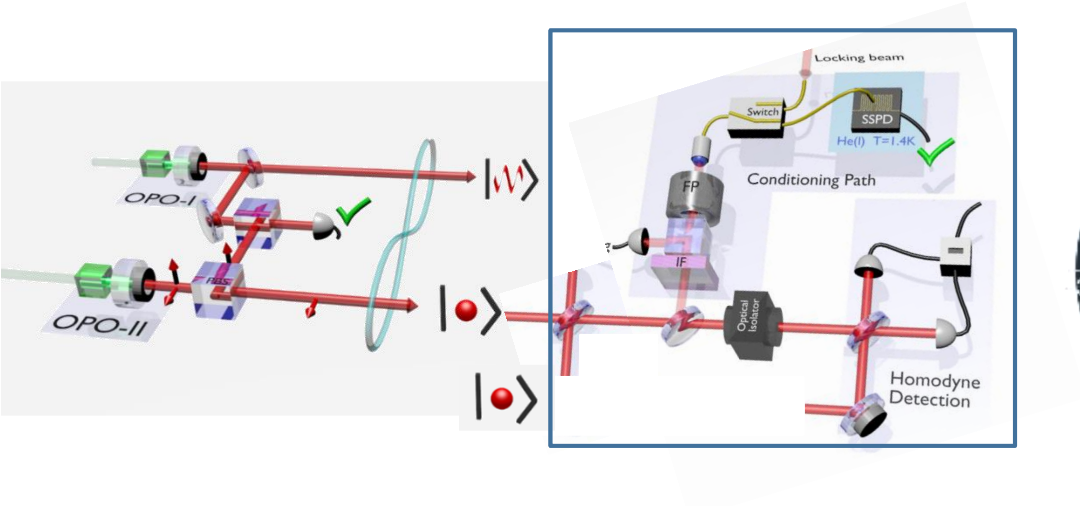

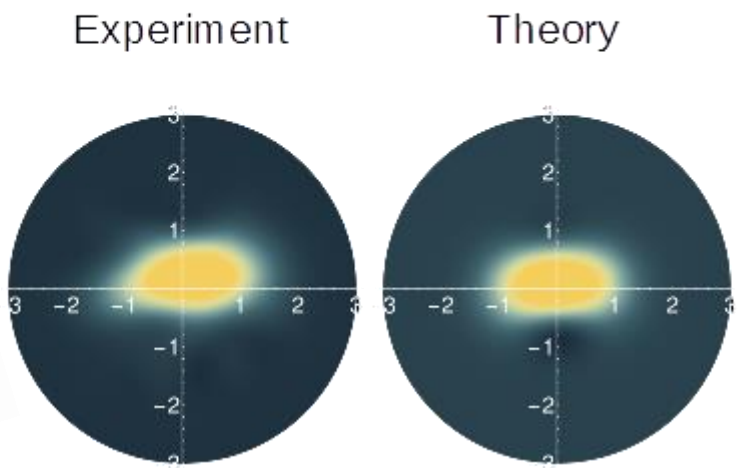

$$c_0\,|cat+\rangle + c_1 e^{i\pi/2}\,|cat-\rangle$$

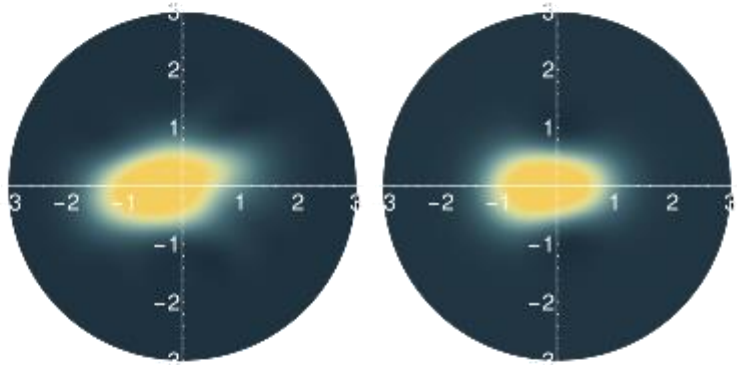

$$c_0\,|cat+\rangle + c_1 e^{i\pi}\,|cat-\rangle$$

$$c_1 \approx 15\%$$

Possible improvements:

- Quadrature selection band can be recuded further with more data
- Increasing c1 up to 20%
- Working on new protocol using a qubit as input

Summary and outlook

- New **hybrid CV-DV** resource for quantum information processing

- Applications:
  - Remote state preparation
  - EPR Steering demonstration
  - Towards hybrid teleportation




Jérémy Raskop **Olivier Morin** **Tom Darras** **Giovanni Guccione**

Optimal Steering inequality

$$\mathcal{S} = Tr(\sum_{a,\theta} F_{a|\theta}\sigma_{a|\theta}) \geq 0$$

Optimal steering inequality means optimal operators $\{F_{a|\theta}\}$

We use the program in *Cavalcanti et. al. Rep.Prog.Phys. 80 (2017) 024001*

$$|\psi\rangle = \sqrt{R}\,|0\rangle_A\,|cat-\rangle_B + \sqrt{1-R}\,|1\rangle_A\,|cat+\rangle_B$$

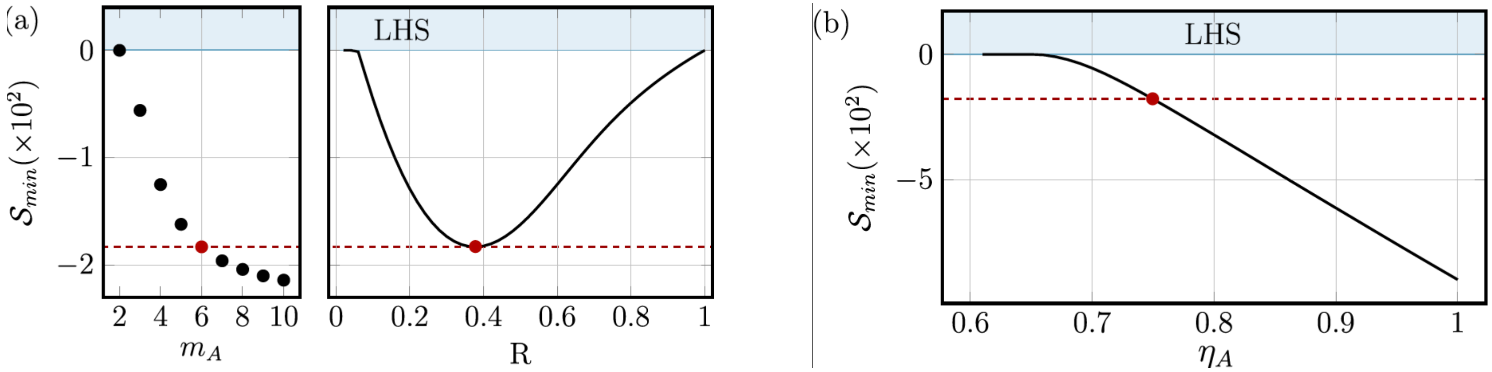

Max-Lik Error bar computation

Problems of Bootstrapping:

- Unreliable results because quantum state inferred through finite number of measurements
- Can give negative eigenvalues
- Estimated state can be on the border of physical states

R. Blume-Kohout, *Optimal, reliable estimation of quantum states*, **New Journal of Physics**, vol. 12, no. 4, p. 043034, 2010.
B. Jungnitsch, S. Niekamp, M. Kleinmann, O. Gühne, H. Lu, W.-B. Gao, Y.-A. Chen, Z.-B. Chen and J.-W. Pan, *Increasing the Statistical Signicance of Entanglement Detection in Experiments*, **Physical Review Letters**, vol. 104, no. 21, p. 210401, 2010.
R. Blume-Kohout, *Robust Error Bars for Quantum Tomography*, **arXiv e-prints**: 1202.5270[quant-ph], 2012.

Other method: exploration of Likelihood space through Metropolis-Hastings algorithm

P. Faist and R. Renner, *Practical, Reliable Error Bars in Quantum Tomography*, **Physical Review Letters**, vol. 117, July 2016.

Instead of considering ρ_{ML}, the likelihood function $\mathcal{L}(\rho) = \prod tr(\{x,\theta\}|\rho)$ is studied as a distribution $\frac{1}{c}\int \mathcal{L}(\rho)d\rho$

Any parameter f can be computed using $\mu(f) = \frac{1}{c}\int \mathcal{L}(\rho)\delta(f(\rho)-f)d\rho$

Idea: Random walk biased by the likelihood function in the space of possible density matrices to find $\mu(f)$

Max-Lik Error bar computation

Idea: Random walk biased by the likelihood function in the space of possible density matrices to find $\mu(f)$

- Choose a new ρ' following $Q(\rho'|\rho_n)$.
- Compute $a = \mathcal{L}(\rho')/\mathcal{L}(\rho)$. If $a > 1$ set $\rho_{n+1} = \rho'$, if $a < 1$ decide randomly to set $\rho_{n+1} = \rho'$ with probability a, or else set $\rho_{n+1} = \rho_n$.

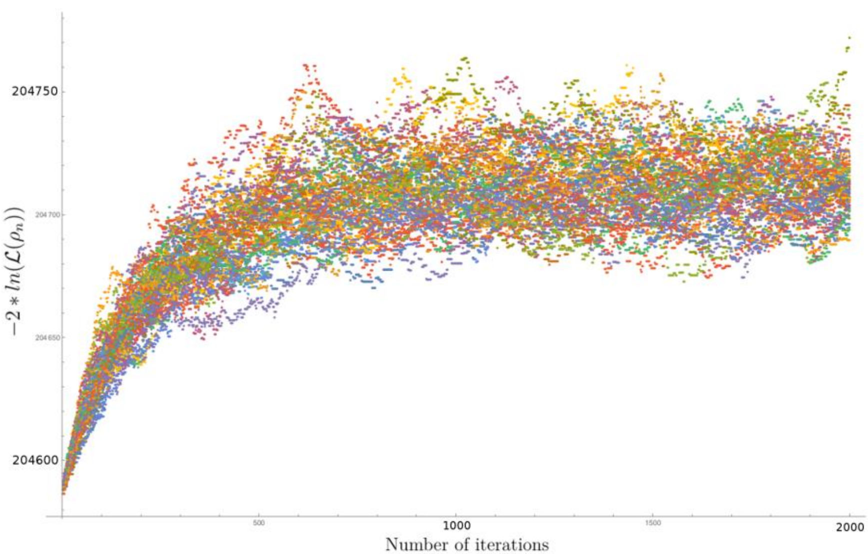

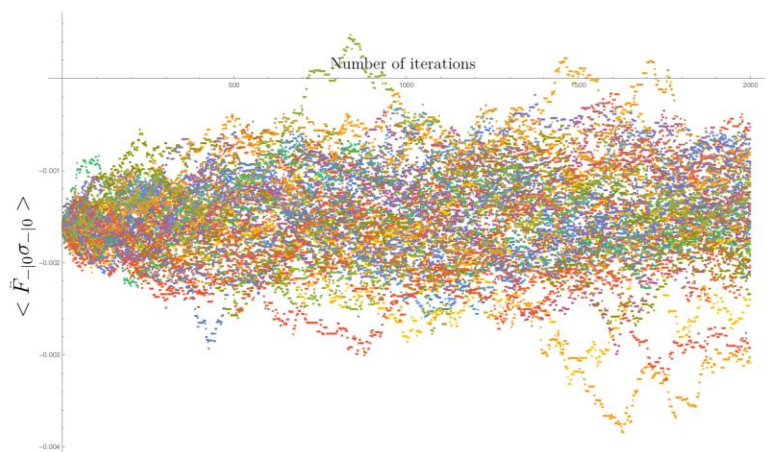

Max-Lik Error bar computation

Parameters to set: Keep only some of the values of the algorithm to avoid correlations between events

Integrated autocorrelation time can be computed through binning analysis

$$A_{a|x}^{(0)} = (f_{a|\theta}(\rho_i))_{i\leq M}$$

$$A_{a|x}^{(l)} = \frac{1}{2}(A_{a|x,2i-1}^{(l-1)} + A_{a|x,2i}^{(l-1)})_{i\leq M/2^l}.$$

$$\Delta_{a|x}^{(l)} = \sqrt{Var(A_{a|x}^{(l)}) * 2^l/M}.$$

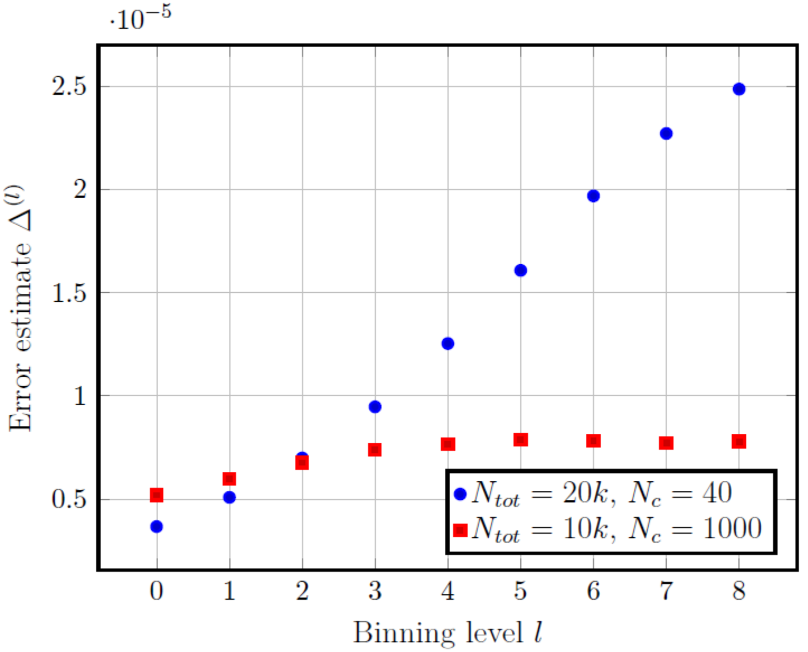

Max-Lik Error bar computation

We consider only errors on the reconstruction as Alice is untrusted and the operators are applied numerically

Typically error bar computation by BootStrapping methods:

From N measurement events $\{x,\theta\}$ the experimental density matrix is considered to be the one most likely to have lead to these N measurements.

Typically for 1-mode states such as Schrödinger cat states, N = 50k points.
Here, each $\rho_{a|\theta}$ is reconstructed from 65k events.

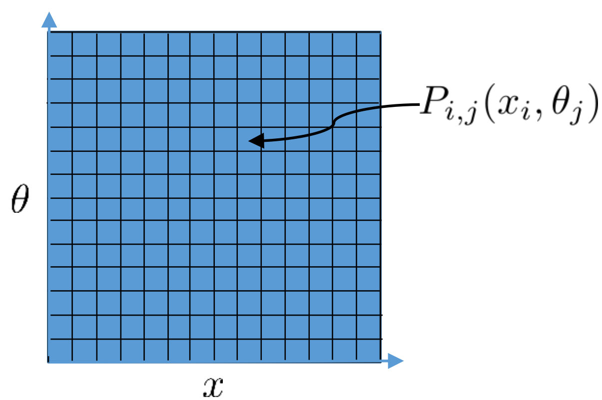

- We compute each $P_{i,j}(x_i,\theta_j)$ using $\rho_{a|\theta}$ reconstructed from experimental data.
- We then randomly select N events in the boxes with bias $P_{i,j}(x_i,\theta_j)$.
- Then we reconstruct the corresponding matrix N_{it} times.
- We compute the steering violation from a number (out of N_{it}^{12}) assemblages.

Max-Lik Error bar computation

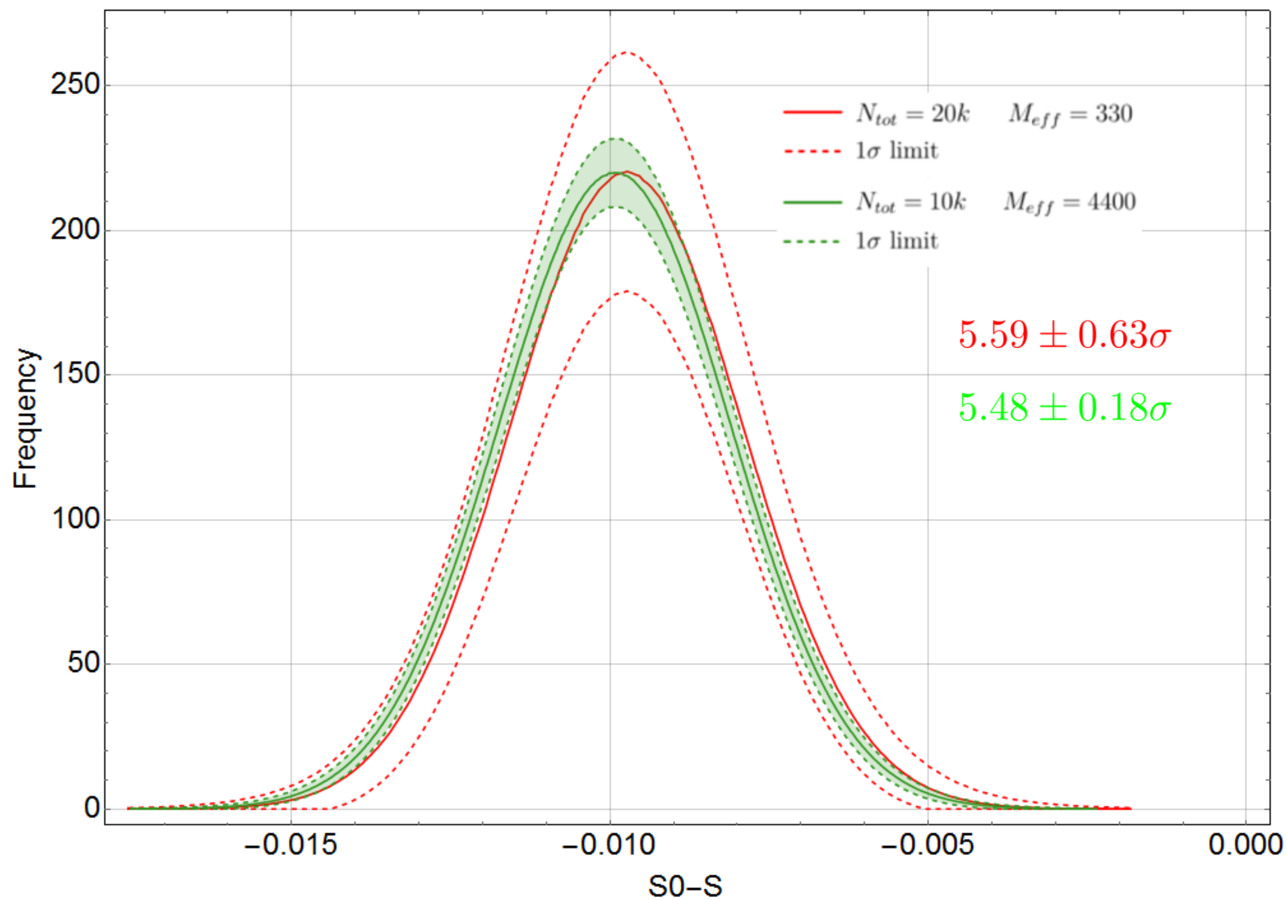

Max-Lik Error bar computation: Skewing of the histogram

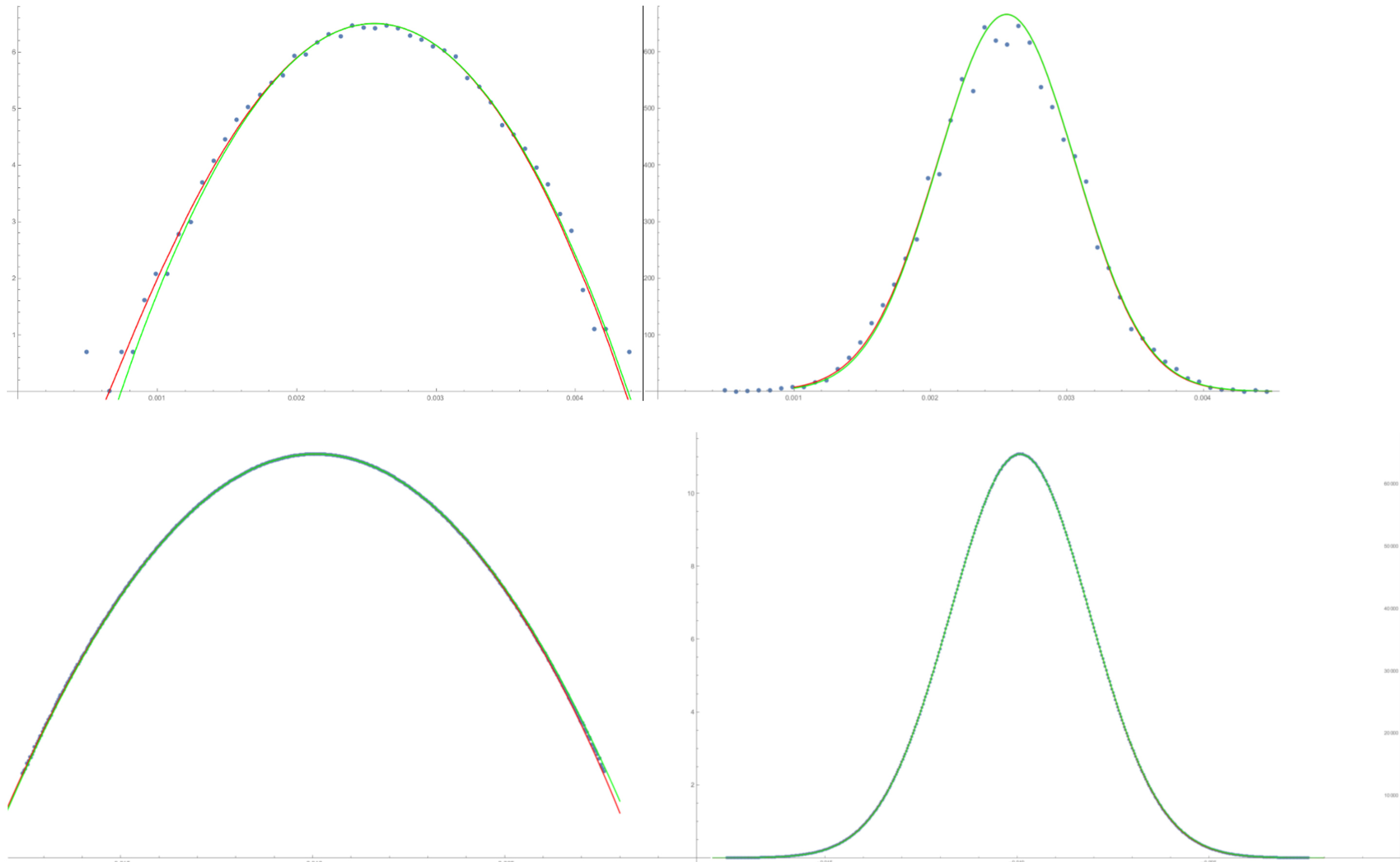

Second Scheme